UNIVERSITY OF BIRMINGHAM

A DIGITAL RECONSTRUCTION OF THE TRIASSIC APEX PREDATOR *SAUROSUCHUS GALILEI* (PSEUDOSUCHIA: LORICATA)

by

MOLLY J. FAWCETT

A thesis submitted to the University of Birmingham for the degree of

MSC BY RESEARCH EARTH SCIENCE

Institute of Earth Science
School of Geography, Earth, and Environmental Sciences
College of Life and Environmental Sciences
University of Birmingham
April 2023

ABSTRACT

During the Triassic Period, pseudosuchian reptiles diverged and dominated the terrestrial and semi-aquatic ecosystems. A very successful paraphyletic pseudosuchian grade were a group commonly referred to as ‘rauisuchians’. *Saurosuchus galilei*, first described by Osvaldo Reig over six decades ago, was a hypercarnivorous, quadrupedal rauisuchian that dominated the terrestrial ecosystems in the Late Triassic, about 237 - 208.5 million years ago. Here, the first digital reconstruction of a juvenile, three dimensionally, well-preserved *Saurosuchus* cranium (PVSJ 32), from the Ischigualasto Formation in Argentina, was carried out. Using finite element analysis (FEA), the morphological function of the *Saurosuchus* cranium was biomechanically explored, comparing the stress magnitudes and distributions to theropod dinosaurs, including *Allosaurus fragilis*, in order to assess the functional convergence between Triassic and post-Triassic carnivores. With their large size and morphological similarities to post-Triassic theropods, including dorsoventrally deep skulls and ziphodont (serrated) dentitions, *Saurosuchus* is suggested to have been a key apex predator and therefore would show analogous stress and bite magnitudes to similarly sized apex theropods. However, this hypothesis disregards functional behaviours that can influence more refined predatory roles. Similar stress magnitudes and distributions between *Saurosuchus* and *Allosaurus* were displayed under the same functional simulations, which indicates a somewhat strong skull and functional convergence with theropods to a certain extent. However, higher stresses and a weak bite for its size were also shown (1015–1885 N). This indicates that *Saurosuchus* potentially consumed softer parts of carcasses, which would mean that it was quite wasteful with its prey, differing to theropods and other pseudosuchians. This analysis increases our knowledge of the functional diversity of pseudosuchians and also highlights the key functional differences between Triassic and post-Triassic apex predators.

ACKNOWLEDGEMENTS

I would like to thank all the following people who helped me in some way during the process of completing this thesis.

Firstly, my two supervisors in the Earth Science department of the University of Birmingham, Richard J. Butler and Stephan Lautenschlager, whose discussions and guidance helped me learn new palaeontological methodologies and technical skills required to complete my thesis. I could not have asked for two better supervisors, they were extremely supportive and inspiring, allowing my MSc degree to be such an enjoyable experience that I will never forget.

To Jordan Bestwick, who taught me many valuable lab skills and whose passion for palaeontology inspired me to want to explore the subject even further.

I would also like to thank Martin D. Ezcurra & Julia Desojo for the photos of the *Saurosuchus galilei* specimen PVSJ 32. Richard Ketcham and Matthew Colbert for the CT-scans of the specimen, allowing me to create the reconstructed digital model.

I would also like to mention my many wonderful friends from the University of Birmingham that helped shape me into the confidant, enthusiastic person I am today, Ellen Hill, Azara Blackwood, Lucy Rabjohn, Chara Chatzistefanou, Caitlin Butler, and Dom Biasi.

And of course, a big thanks to my family members whose support gave me the courage to attempt and finish this piece of work, my parents – Carole and Nick, and my siblings – Vicky and Jack.

TABLE OF CONTENTS

LIST OF FIGURES

LIST OF TABLES

LIST OF ABBREVIATIONS

Institutional Abbreviations:

AL	Alligator specimens from Rockefeller Wildlife Refuge, Grand Chenier, LA, USA
BMRP	Burpee Museum of Natural History, Rockford, IL
CV	Municipal Museum of Chongqing, Yuzhong, Chongqing, China
IVPP	Institute of Vertebrate Paleontology and Paleoanthropology, Academia Sinica, Beijing, People's Republic of China
LACM	Natural History Museum of Los Angeles County, Los Angeles, CA
MCN	Museu de Ciências Naturais, Fundação Zoobotânica do Rio Grande do Sul, Porto Alegre, Brazil
PVL	Instituto Miguel Lillo, Tucuman, Argentina
PVSJ	Division of Vertebrate Paleontology of the Museo de Ciencias Naturales de la Universidad Nacional de San Juan, Argentina
TMP	Royal Tyrrell Museum of Palaeontology, Drumheller; UA, University of Alberta, Edmonton
TTUP	Museum of Texas Tech, Lubbock, Texas
UCMP	University of California Museum of Paleontology, Berkeley, California, USA
UFSM	Universidade Federal de Santa Maria, Santa Maria, Brazil.
UFRGS-PV	Paleoverte brate Collection of the Laboratório de Paleovertebrados of the Universidade Federal do Rio Grande do Sul, Porto Alegre, Brazil

USNM	National Museum of Natural History, Smithsonian Institute, Washington D.C., USA
UUVP	University of Utah, Vertebrate Paleontology Collections, Utah, USA.
YPM VP	Division of Vertebrate Paleontology Collection,

Osteological Abbreviations:

an	angular
aof	antorbital fenestra
d	dentary
en	external naris
f	frontal
j	jugal
la	lacrimal
ltf	lower temporal fenestra
mx	maxilla
mf	mandibular fenestra
n	nasal
o	orbit
pf	prefrontal

po	postorbital
pof	postfrontal
pmx	premaxilla
qj	quadratojugal
qu	quadrate
sq	squamosal
su	surangular

Myologic Abbreviations:

m. AMEM	m. adductor mandibulae externus medialis
m. AMEP	m. adductor mandibulae externus profundus
m. AMES	m. adductor mandibulae externus superficialis
m. AMP	m. adductor mandibulae posterior
m. PSTp	m. pseudotemporalis profundus
m. PSTs	m. pseudotemporalis superficialis
m. PTd	m. pterygoideus dorsalis
m. PTv	m. pterygoideus ventralis.

Other Abbreviations:

FBS	front bite scenario
BBS	back bite scenario
FEA	finite element analysis
MDA	multibody dynamic analysis
MYA	million years ago

CHAPTER I
INTRODUCTION

Around 252 million years ago (MYA), the Triassic period and the Mesozoic era began, following the Earth's worst-ever extinction event, also known as the Great Dying (Huang *et al.*, 2011; Zhongming *et al.*, 2021). However, the Triassic is also marked by one of the greatest changes in vertebrate evolutionary history, with the emergence and radiation of archosaurian reptiles, which came to dominate terrestrial and semi-aquatic ecosystems throughout the Triassic Period (Huene, 1938a; Bonaparte, 1967; Chatterjee, 1986; Long & Padian, 1986; Parrish & Carpenter, 1986; Benton & Clark, 1988; Sereno, 1991; Lucas, 1998; Gower & Sennikov, 2000; Langer, 2005; Irmis *et al.*, 2007; Nesbitt *et al.*, 2010; Sues & Fraser, 2010; Butler *et al.*, 2011; Nesbitt, 2011). The archosaur clade comprises two lineages: Pseudosuchia (the lineage leading to crocodiles) and Avemetatarsalia (the lineage leading to birds) (Gower & Sennikov, 2000). Pseudosuchians were initially able to diversify at a quicker rate compared to the avemetatarsalians and therefore dominated the Triassic Period (Nesbitt, 2005a, b, 2011; Butler *et al*., 2009, 2011). Crocodylomorpha is a group of pseudosuchians that includes all extant crocodilians and their extinct crocodilian-like relatives, and includes the only pseudosuchians to survive the end-Triassic mass extinction (Benton & Clark, 1988). The clade Paracrocodylomorpha is composed of the group Crocodylomorpha and their closest relatives (Nesbitt, 2011). Rauisuchia is a group of large non-crocodylomorph archosaurs that belong to this clade (Gauthier and Padian, 1985; Gower, 2000; Nesbitt, 2011). The name “Rauisuchia” is derived from the genus name *Rauisuchus*, created in honour of the fossil collector Dr. Wilhelm Rau, who discovered the holotype of the genus in 1928/29, and meaning ‘Rau's crocodile’ (Huene, 1942). “Rauisuchia”, hereafter referred to as

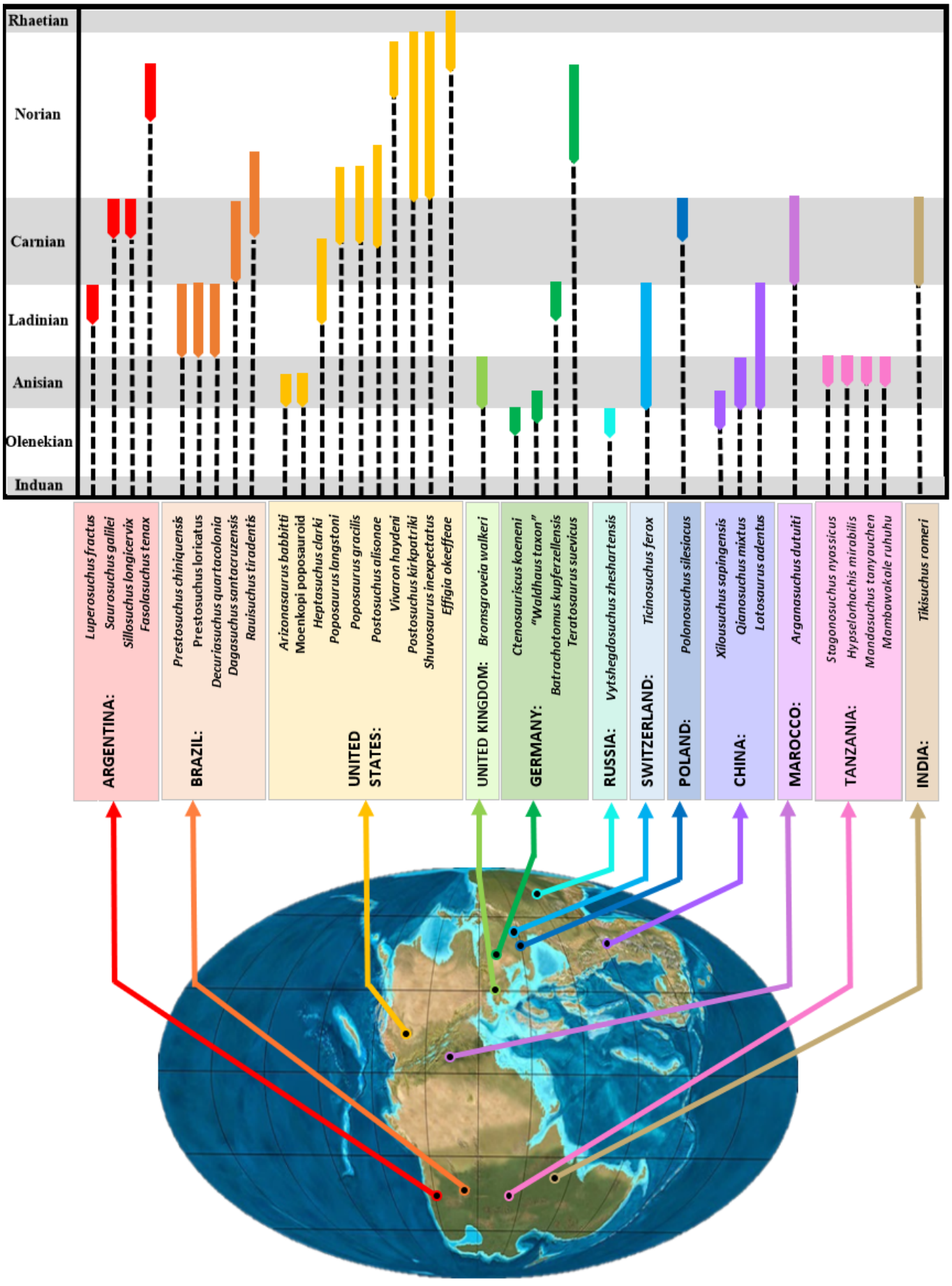
Rhaetian
Norian
Carnian
Ladinian
Anisian
Olenekian
Induan
ARGENTINA:
Luperosuchus fractus
Saurosuchus galilei
Sillosuchus longicervix
Fasolasuchus tenax
BRAZIL:
Prestosuchus chiniquensis
Prestosuchus loricatus
Decuriasuchus quartacolonia
Dagasuchus santacruzensis
Rauisuchus tiradentis
UNITED STATES:
Arizonasaurus babbitti
Moenkopi poposauroid
Heptasuchus clarki
Poposaurus langstoni
Poposaurus gracilis
Postosuchus alisonae
Vivaron haydeni
Postosuchus kirkpatriki
Shuvosaurus inexpectatus
Effigia okeeffeae
UNITED KINGDOM:
Bromsgroveia walkeri
GERMANY:
Ctenosauriscus koeneni
"Waldhaus taxon"
Batrachotomus kupferzellensis
Teratosaurus suevicus
RUSSIA:
Vytshegdosuchus zheshartensis
SWITZERLAND:
Ticinosuchus ferox
POLAND:
Polonosuchus silesiacus
CHINA:
Xilousuchus sapingensis
Qianosuchus mixtus
Lotosaurus adentus
MAROCCO:
Arganasuchus dutuiti
TANZANIA:
Stagonosuchus nyassicus
Hypselorhachis mirabilis
Mandasuchus tanyauchen
Mambawakale ruhuhu
INDIA:
Tikisuchus romeri

Fig. 1. The distribution of all rauisuchians discovered in time (Triassic period) and space (the Earth when all continents were joined within the landmass Pangea). Note that the stratigraphic ranges contain age error for all the individual taxa listed (modified from França, 2011; Nesbitt *et al.*, 2013).

rauisuchians (*sensu* Nesbitt & Desojo, 2017), were very large hypercarnivores often measuring 4-6 m in length but could reach to sizes of 8-10 m, e.g., species such as *Fasolasuchus tenax* and the shuvosaurid *Sillosuchus longicervex* (Nesbitt, 2011; Nesbitt *et al.*, 2013). They were widespread across the supercontinent – Pangea during the Triassic, with previous research identifying rauisuchian fossils on all continents except Australia and Antarctica (Fig. 1) (Gower, 2000).

Previous research has suggested that rauisuchians are typically characterised by relatively long hind limbs compared to the forelimbs, which were directly positioned underneath their bodies (referred to as a pillar-erect posture) (Krebs, 1976; Benton & Clark, 1988). Many rauisuchians also had large, deep skulls relative to their body, with recurved, serrated teeth (Nesbitt *et al.*, 2013). However, these characters are not seen in all rauisuchians, for example the shuvosaurids (e.g., *Sillosuchus, Shuvosaurus* and *Effigia*) were toothless and likely beaked herbivores (Nesbitt, 2011; Bestwick *et al.*, 2021). Furthermore, most of these characters are plesiomorphic among many of the Early Triassic archosaurs (Nesbitt *et al.*, 2013). Despite this, the evolution of these characters allowed rauisuchians to become apex predators on the terrestrial landscape during the Mid to Late Triassic. Rauisuchians preyed upon the very first dinosaurs, including dinosauromorphs, sauropodomorphs, theropods, and therapsids (Tolchard *et al.*, 2019). However, their reign unexpectedly ended when they became extinct at the end of the Triassic, which is thought to be due to the global end-Triassic mass extinction event (201.3 MYA) (Benton, 2004).

In the past, there has been great confusion over the phylogenetic relationships and diagnosis of Rauisuchia, and, despite the increased research done in the late 20th century on rauisuchians, there is still little consensus on the matter (Nesbitt *et al.*, 2013). Due to this, the phylogenetic relationships between rauisuchian taxa and whether they form a single clade are still widely debated (Gower, 2000; Brusatte *et al.*, 2010; Nesbitt, 2011; Nesbitt *et al.*, 2013; Nesbitt and Desojo, 2017). The debate concerns whether rauisuchians are monophyletic (a natural group), paraphyletic (with respect to other pseudosuchian clades), or polyphyletic (spread throughout the well-recognised pseudosuchian groups) (Gower, 2000). Many researchers have used the term 'Rauisuchia' in a paraphyletic sense with respect to Crocodylomorpha (e.g., Nesbitt, 2005*a*; Gower and Nesbitt, 2006; Weinbaum and Hungerbühler, 2007; Nesbitt, 2011). However, some other researchers have recovered a monophyletic Rauisuchia in their analyses (e.g., Nesbitt, 2007; Lautenschlager, 2008; Desojo and Rauhut, 2009; Brusatte *et al.*, 2010). Due to this uncertainty, in this thesis I refer to this group as a paraphyletic assemblage, which includes non-crocodylomorph Loricata, Poposauroidea and *Ticinosuchus ferox* (Fig. 2) (Butler *et al.*, 2011; Nesbitt, 2011; Nesbitt *et al.*, 2013; Butler *et al.*, 2017; Roberto-Da-Silva *et al.*, 2018).

The focus of this thesis is *Saurosuchus galilei*, the genus meaning 'lizard crocodile' in Greek and the species name in honour to Galileo J. Scaglia, who prepared the holotype. which was discovered and named by Osvaldo Reig in 1959. *Saurosuchus* was a large quadrupedal rauisuchian within the clade Loricata, which was on average 6–7 m in length but could reach to possibly 9 m in length, making it one of the largest rauisuchians in the fossil record (Reig, 1959; Sill, 1974; Alcober, 2000; Trotteyn *et al.*, 2011). Fossils of *Saurosuchus* are known from the Late Triassic (late Carnian) Ischigualasto Formation in Argentina (Fig. 1) (Sill, 1974).

1.1 Rauisuchian Phylogenetics

Rauisuchian taxonomy and evolution have long been poorly understood, and, because of this, debates regarding the phylogenetic placement of *Saurosuchus galilei* and other rauisuchians still occur (Gower, 2000; Brusatte *et al.*, 2010; Nesbitt, 2011; Nesbitt *et al.*, 2013; Nesbitt and Desojo, 2017; Tolchard *et al.*, 2019; Butler *et al.*, 2022; Damke *et al.*, 2022). The reasons for this misunderstanding are a combination of a fragmentary fossil record, poor specimen preservation, insufficient 'primary' research, confusion in alpha-level taxonomy, and the lack of understanding of wider Triassic pseudosuchian relationships (Gower, 2000; Nesbitt *et al.*, 2013). However, our understanding has greatly increased due to the advances in phylogenetic methodologies such as character construction (Sereno, 2007) and taxon inclusion (Brusatte, 2010). Along with an increased number of recently discovered near-to-complete specimens and the introduction of quantitative methodologies, such as integrated biomechanical modelling, we now have a better understanding of rauisuchians than ever before.

Although Meyer (1861) and Mehl (1915) described specimens that have subsequently been referred to as rauisuchians, the person that could be considered to have first recognised this group was Huene (1942). He described the fossil reptiles *Rauisuchus tiradentes, Prestosuchus chiniquensis* and *Prestosuchus loricatus*, all from the Middle Triassic of Brazil (Fig. 1) (Huene, 1942). *Saurosuchus* was originally placed within the family Rauisuchidae, along with *Rauisuchus, Prestosuchus,* and *Stagonosuchus nyassicus* in a review written by Reig (1961). Later, Romer (1966) proceeded to place *Saurosuchus* and *Rauisuchus* within Erythrosuchidae, whilst placing *Prestosuchus, Procerosuchus, Stagonosuchus,* and *Mandasuchus tanyauchen* (Charig, 1956) into Prestosuchidae. Many different compositions of Prestosuchidae and Rauisuchidae were suggested

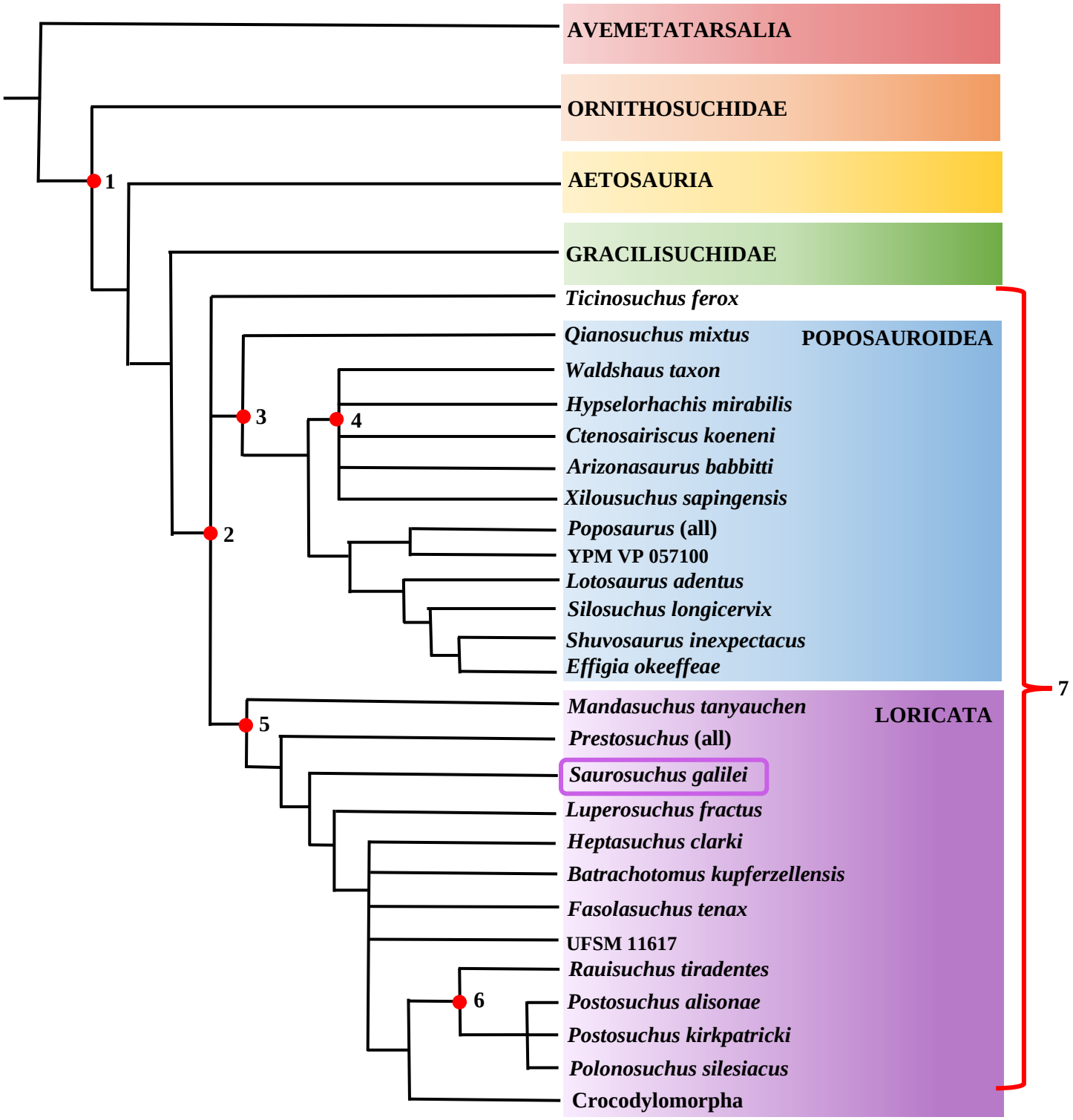

Fig. 2. Phylogenetic relationships of rauisuchians among Pseudosuchia. Pseudosuchia (**1**), Paracrocodylomorpha (**2**), Poposauroidea (**3**), Ctenosauriscidae (**4**), Loricata (**5**), Rauisuchidae (**6**), Rauisuchians (**7**) (adapted from Tolchard *et al.*, 2019; Butler *et al.*, 2022; Damke *et al.*, 2022).

over the years, although some without support from diagnostic characters (e.g., Charig, 1967). Many early archosaur phylogenies that included rauisuchians used composite scoring for suprageneric taxa, assuming monophyly of groups such as Prestosuchidae (e.g., Juul, 1994). However, more recent phylogenies do not assume monophyly of rauisuchians and use species-/genus-level terminal taxa (Brusatte *et al.*, 2010; Butler *et al.*, 2011; Nesbitt, 2011). For more on the taxonomic history of rauisuchian classification see Gower (2000), Brusatte *et al.* (2010) and Nesbitt (2011).

Rauisuchians currently comprise the monophyletic group Poposauroidea Nopsca 1923 (including subclade Ctenosauriscidae Kuhn 1964) and non-crocodylomorph members of the clade Loricata Merrem, 1820 (including the subclade Rauisuchidae Huene 1942), plus *Ticinosuchus ferox* Krebs 1965 (Fig. 2) (*sensu* Tolchard *et al.*, 2019). The clade Poposauroidea (first referred to as 'group X' in Nesbitt, 2007) includes: sail-backed quadrupedal species such as *Arizonasaurus babbitti* Welles 1947, *Ctenosauriscus koeneni* von Huene 1902, *Xilousuchus sapingensis* Wu 1981, *Bromsgroveia walkeri* Galton 1985, *Hypselorhachis mirabilis* Butler et al. 2009, and the 'Waldhaus taxon' Butler et al. 2011 (Nesbitt, 2005; Butler *et al.*, 2011; Nesbitt, 2011); gracile bipedal species such as *Effigia okeeffeae* Nesbitt & Norell 2006, *Poposaurus langstoni* Long & Murry (1995) *sensu* Weinbaum & Hungerbühler 2007 (='*Lythrosuchus' langstoni*), Lotosaurus adentus Zhang 1975, *Poposaurus gracilis* Mehl 1915 *sensu* Weinbaum & Hungerbühler 2007, and *Sillosuchus longicervix* Alcober & Parrish 1997 (Nesbitt and Norell, 2006; Schoch *et al.*, 2010; Gauthier *et al.*, 2011); herbivorous species such as *Lotosaurus adentus* Zhang 1975 and *Shuvosaurus inexpectacus* Long & Murry 1995 sensu Nesbitt 2007 (Nesbitt *et al*., 2013); and the semi-aquatic species *Qianosuchus mixtus* Li *et al.*, 2006. Loricata currently includes: *Arganasuchus dutuiti* Jalil & Peyer 2007, *Polonosuchus silesiacus* Sulej (2005) *sensu* Brusatte et al. 2009

(=‘*Teratosaurus*’ *silesiacus*), *Postosuchus kirkpatricki* Chatterjee 1985, *Postosuchus alisonae* Peyer et al. 2008 and *Rauisuchus triradentes* Huene 1938b, *Teratosaurus suevicus* Meyer 1861, *Tikisuchus romeri* Chatterjee & Majumdar 1987, *Vivaron haydeni* Lessner et al, 2016; *Batrachotomus kuperfurzellensis* Gower 1999, *Dagasuchus santacruzensis* Lacerda et al. 2015, *Decuriasuchus quartacolonia* França et al. 2011, *Fasolasuchus tenax* Bonaparte 1981, *Heptasuchus clarki* Dawley et al. 1979, *Luperosuchus fractus* Romer 1971, *Mambawakale ruhuhu*, *Mandasuchus tanyauchen* Charig 1956, *Prestosuchus chiniquensis* Huene 1938b, *Prestosuchus loricatus* Huene 1938b, *Stagonosuchus nyassicus* Huene 1938a, and *Saurosuchus galilei* Reig 1959 (Fig. 1) (Lacerda *et al.*, 2015; Lacerda *et al.*, 2016; Lessner *et al.*, 2016; Roberto-da-Silva *et al.*, 2018; Desojo *et al.*, 2020; Damke *et al.*, 2022).

1.2 Fossil Record

As previously stated, the rauisuchian fossil record is fragmented and generally quite poor, and this, with the addition of an unresolved taxonomy, has led to a lack of rauisuchian research in the past (Nesbitt *et al.*, 2013). However, due to an influx of recent discoveries of material from new and previously known taxa (Fig. 3), rauisuchians are now gaining increased attention from palaeontologists (e.g. Gower, 2000; Sen, 2005; Sulej, 2005; Li *et al.*, 2006; Nesbitt & Norell, 2006; Jalil & Peyer, 2007; Desojo & Arcucci, 2009; Brusatte *et al.*, 2010; Butler *et al.*, 2011; França *et al.*, 2011; Gauthier *et al.*, 2011; Trotteyn *et al.*, 2011; Nesbitt *et al.*, 2013; Tolchard *et al.*, 2019; Damke *et al.*, 2022). Rauisuchians have been discovered in most terrestrial vertebrate-producing Triassic formations globally (Nesbitt *et al.*, 2013). However, there are many previously published

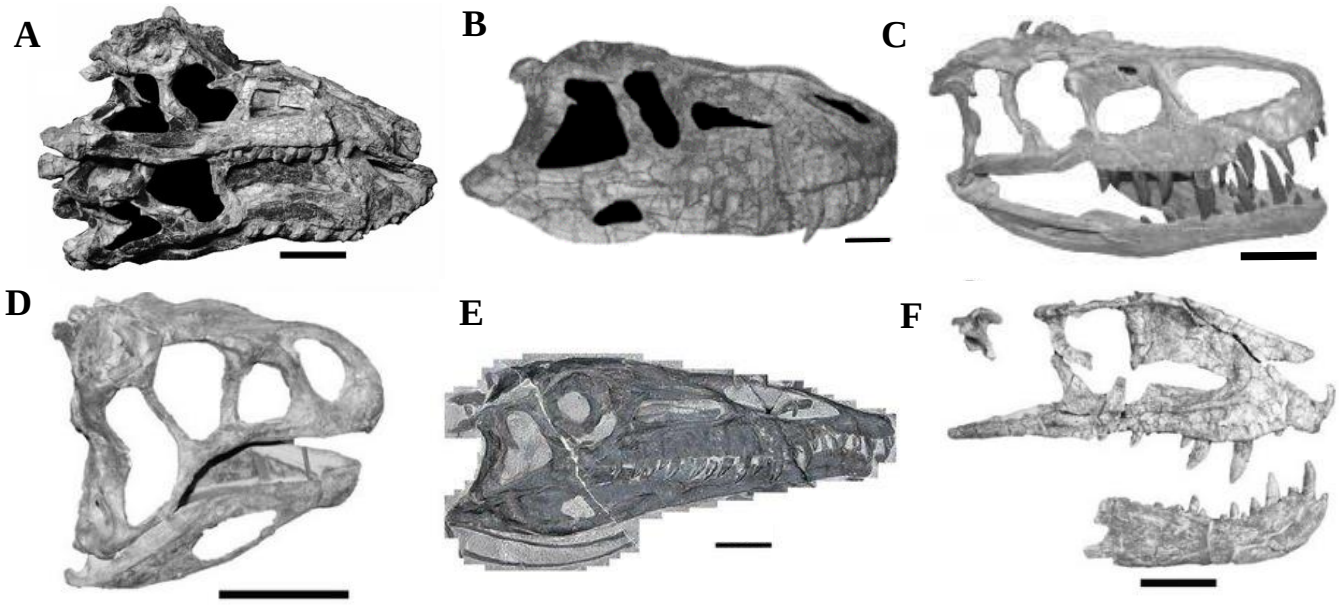

Fig. 3. Photographs of rauisuchian skulls in right lateral view: (**A**) *Decuriasuchus quartacolonia* skull (MCN PV10105c, above; MCN PV10105d, below), (França *et al.*, 2011); (**B**) reversed image of *Prestosuchus chiniquensis* (UFRGS 0156-T) (Nesbitt *et al.*, 2013) (**C**) *Batrachotomus kupferzellensis* (Brusatte, 2008) (**D**) *Lotosaurus adentus* (Brusatte *et al.*, 2010); (**E**) *Qianosuchus mixtus* gen. et sp. nov (IVPP V14300) (Li *et al*., 2006); (**F**) reversed image of *Postosuchus kirkpatricki* (TTUP 9000) (Brusatte *et al.*, 2010). Scale bars = 5 cm (**A**, **B**, **E**), 10cm (**C**, **D**, **F**).

records that report Triassic vertebrate faunas/assemblages to include rauisuchians which are based exclusively on teeth (e.g., Renesto, et al., 2003; Heckert, 2004; Heckert et al., 2012). Teeth are now considered a non-diagnostic feature for any rauisuchian/rauisuchian subgroup, because recurved, serrated teeth are present in the most groups of amniotes (Nesbitt *et al.*, 2013). Nonetheless, rauisuchians were able to cover a large morphospace spanning across all modern continents except Australia and Antarctica (Gower, 2000; Brusatte *et al.*, 2008). Although rauisuchians were widespread, they are mainly known from 3 formations: the Chinle Formation of North America (Stewart *et al.*, 1972), the Ischigualasto Formation of Argentina (the location of *Saurosuchus*) (Alcober, 2000; Currie *et al.*, 2008), and the Santa Maria Formation of Brazil (Schultz *et al.*, 2000).

All specimens of *Saurosuchus* have been found in the Ischigualasto Formation, San Juan province, Argentina (Alcober, 2000). The holotype of *Saurosuchus* (PVL 2062) was first described by Reig (1959) in a preliminary report. The specimen PVL 2062 was found in the upper third of the strata within the formation and included a nearly complete skull with the most posterior portion missing (Reig, 1959). The next specimen discovered was PVL 2198, found in the middle part of the formation, which included a laterally deformed skull that is complete from the anterior most tip to the temporal fenestrae, and postcranial material including parts of dermal armour, some dorsal scutes, eleven dorsal vertebrae, left ilium, both ischia, and associated ribs (Reig, 1959). In 1974, Sill described three referred specimens: PVL 2557, PVL 2472 and PVL 2267, as well as redescribing the previously discovered material (Sill, 1974). The specimen PVL 2557 was also found in the middle part of the formation, and included nine caudals, chevrons, two dorsal vertebrae, parts of the right femur, fibula, right ilium, ischium, partial pubis, some associated ribs, both sacrals, tibia, and complete right tarsus and foot (Sill, 1974). The specimen PVL 2472 was found in the lower third of

the formation, and included an astragalus, tibia, and one poorly preserved cervical vertebra (Sill, 1974). Lastly, the specimen PVL 2267 was also found in the lower third of the formation, and included a partial femur, fibula, poorly preserved partial ilium, tibia, and a well-preserved tarsus and partial foot (Sill, 1974). In 1981, Bonaparte mentioned two recent discoveries in the collections of the San Juan Museum. The discovery included two new skeletons; Bonaparte also made a preliminary description of the specimen PVSJ 74, comprising a pelvis (Bonaparte, 1984).

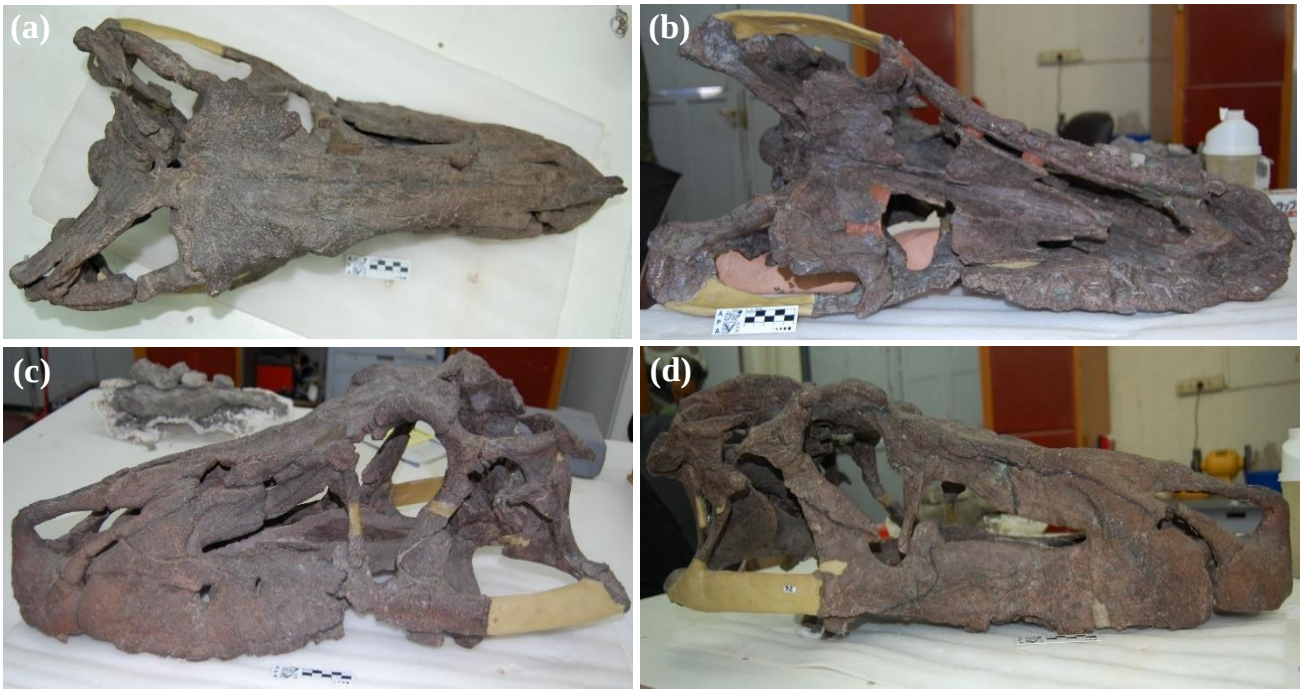

Fig. 4. Pictures of the fossil specimen PVSJ 32 in the Ischigualasto Formation of San Juan Province, Argentina. (**a**) dorsal view; (**b**) ventral view; (**c**) left lateral view; (**d**) right lateral view. Scale bar = 5 cm (Photos taken by Martin D. Ezcurra & Julia Desojo).

The most recently reported specimen, PVSJ 32, was found in the base of the Upper Triassic Ischigualasto Formation, located about 15m above a 228 MYA layer of tuff in a silty abandoned channel deposit (Rogers *et al.*, 1993). This specimen included an almost complete skull of *Saurosuchus galilei* (Fig. 4). The main parts that can be observed to be missing include the

anteroposterior rami of the quadratojugal and ventral articular surfaces of the quadrates (Alcober, 2000). This specimen was found by Alfred Romer and his team during the late 1950s (Reig, 1959).

Out of the seven known specimens discovered three include cranial material, PVSJ 32 being the latest, most complete and well-preserved skull (Alcober, 2000). This specimen has the entire posterior region of the braincase preserved, showing anatomical features that cannot be seen in the holotype PVL 2062 (Sill, 1974). Although, preservation of the fossilised skull is generally quite good. There is some damage on the external surfaces of the premaxilla and maxilla (Alcober, 2000). There is also observable deformation on the left side of the skull due to lateral shearing stress (Fig. 4). The erosion due to fossilisation affected the left paraoccipital process (almost all of it), the anterior part of the palate, the posterior part of both mandibular rami, and most of the teeth on the premaxilla and maxilla (Alcober, 2000).

1.3.1 Rauisuchian Anatomy

After the discovery of *Saurosuchus galilei* (Reig, 1959) and *Ticinosuchus ferox* (Krebs, 1965), it was proposed by both Reig (1961) and Krebs (1965) that rauisuchians were a widespread group of Triassic archosaurs (Fig. 1) with affinities that lay with pseudosuchians rather than with non-crown-group early archosauriforms, also known as proterosuchians, an alternative hypothesis first suggested in 1963 by Hughes (Hughes, 1963; Romer, 1966, 1972; Bonaparte, 1982; Paul, 1984). Rauisuchians have many similarities to theropod dinosaurs (Nesbitt and Norell, 2006; Brusatte *et al.*, 2008). However, they also have some traits that distinguish them from theropods and other archosaurs. The key characteristics that rauisuchians share can be seen in the cranial material (Alcober, 2000), linked to their largely carnivorous diet. One of these is an extra slit-like antorbital fenestra (which has been previously named as a subnarial/accessory/supplementary fenestra) (labelled *sf* in Fig. 5) which lies between the premaxilla and maxilla in juvenile stages (Krebs, 1976; Alcober, 2000). This gap varies among different taxa in its relative size and position and can even vary from alternate sides of the same skull (Gower, 2000 Fig. 3; Nesbitt and Desojo, 2017). This variation notwithstanding, this character is used as a key diagnostic synapomorphy for rauisuchians in many phylogenetic analyses (Benton, 1984; Benton and Clark, 1988; Parrish, 1993; Brusatte *et al*., 2010; Nesbitt, 2011; Butler *et al.*, 2014; Nesbitt and Desojo, 2017). The function of this trait is still widely debated with Gower (2000) suggesting two main hypotheses. The first states that the function is related to the air sinus system, whereas the second is related to nerve transmission or blood vessels (Gower, 2000). This aperture can be seen in many rauisuchians (e.g., Chatterjee, 1985; Benton, 1986a; Long and Murry, 1995; Alcober, 2000; Gower, 2000). However, in some taxa this aperture is smaller and more circular, which is thought to be a homologous feature (e.g., in *Batrachotomus*; Gower, 2000). *Prestosuchus chiniquensis*, a well-known traditional rauisuchian,

has been considered quite problematic in the past, as it appears to lack this aperture (Gower, 2000). However, recent work has demonstrated that this antorbital fenestra is present in *Prestosuchus* and must have closed in the specimen UFGRS PV 0156 during ontogeny (Fig. 3) (Alcober, 2000; Mastrantônio *et al*., 2013). However, due to a supposed movable premaxilla-maxilla joint, the position and shape of this subnarial fenestra has been open to interpretation (Mastrantônio, 2010). These moveable joints in the cranium are thought to be another common feature that can be found in rauisuchians (Benton, 1984). The function is hypothesized to be for a wide bite extension, allowing for more tough and crunchy foods to be consumed (Erickson *et al*., 2003). This would have been useful for rauisuchian as apex predators in the Triassic, with hypercarnivorous diets which potentially required a lot of bone crushing. This can still be seen today in extant crocodilians which have similar carnivorous diets, allowing them to have a stronger bite in order to kill their prey (Erickson *et al.*, 2003).

1.3.2 *Saurosuchus* Cranial Anatomy

Both Sill (1974) and Alcober (2000) have identified diagnostic features of *Saurosuchus* based on the skull of the specimens PVL 2062 (holotype) and PVSJ 32. It is clear that *Saurosuchus* has a highly sculptured skull, especially when it comes to the maxilla and skull roof (Sill, 1974; Alcober, 2000). The thickening of the frontal lateral margins forms a raised margin at the level of the orbital

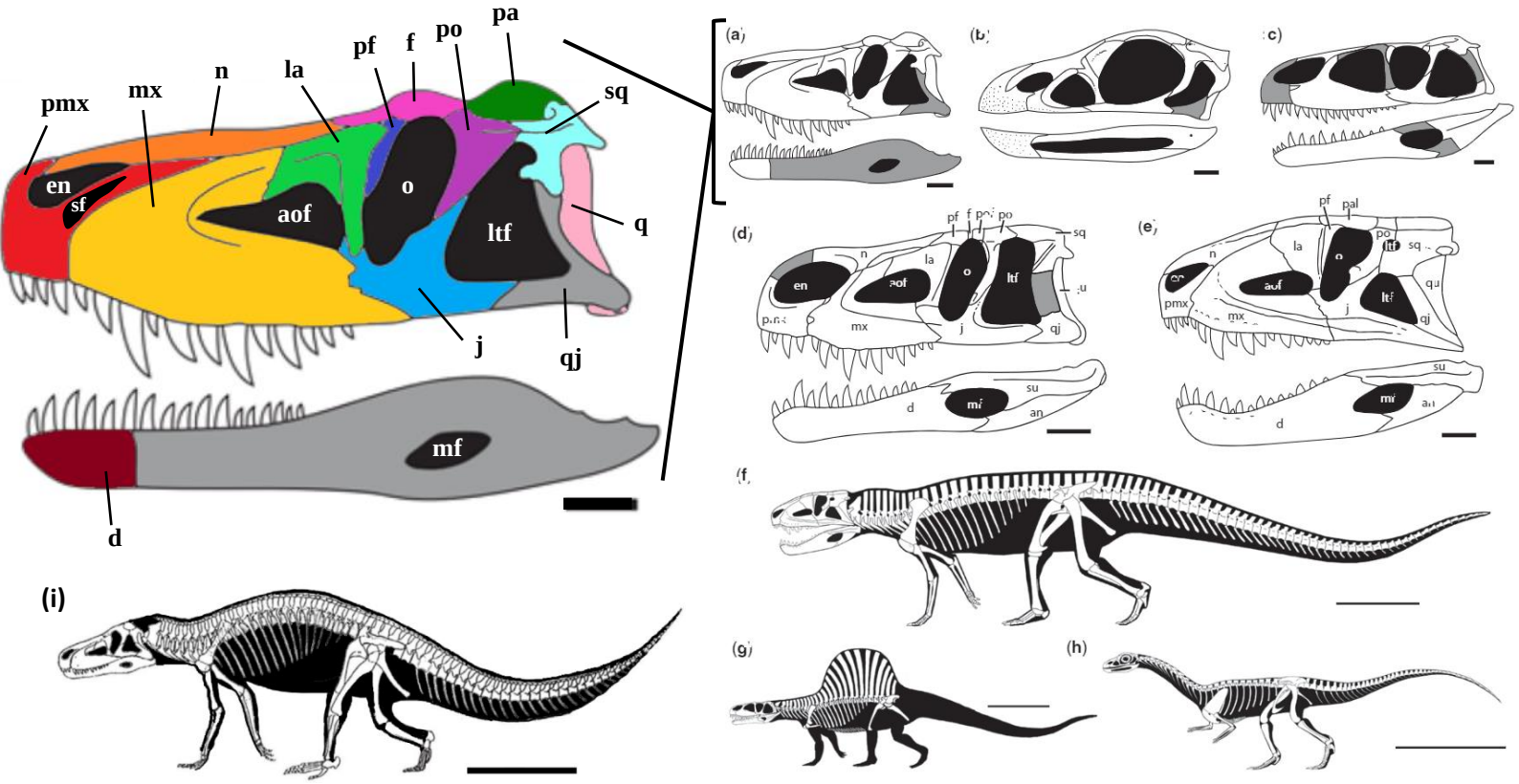

Fig. 5. Skulls and skeletons of rauisuchians in left lateral view: (**a**) Juvenile *Saurosuchus galilei* skull with labelled version on the left and the addition of the cranial opening behind the naris (adapted from Nesbitt *et al.*, 2013 and Alcober, 2000) (**b**) *Effigia okeeffeae* skull; (**c**) *Arizonasaurus babbitti* skull; (**d**) *Batrachotomus kupferzellensis* skull (Gower, 1999); (**e**) *Postosuchus kirkpatricki* skull; (**f**) *Postosuchus kirkpatricki* skeleton; (**g**) *Arizonasaurus babbitti* skeleton (Nesbitt, 2005a); (**h**) *Effigia okeeffeae* skeleton; (**i**) *Saurosuchus galilei* skeleton (adapted from Benton, 1984). Indication of unknown portions of skulls from missing fossils are shown in grey. Labels: an, angular; aof, antorbital fenestra; d, dentary (dark red); en, external naris; f, frontal (dark pink); j, jugal (blue); la, lacrimal (light green); ltf, lower temporal fenestra; mx, maxilla (yellow); mf, mandibular fenestra; n, nasal (orange); o, orbit; pf, prefrontal (dark blue); po, postorbital (purple); pof, postfrontal; pmx, premaxilla (red); qj, quadratojugal; qu, quadrate (light pink); sf, subnarial fenestra; sq, squamosal (light blue); su, surangular. Scale bars: 1 cm (**b**, **c**); 5 cm (**a**, **d**, **e**); 50 cm (**f**–**h**); 1 m (**i**). (Adapted from Nesbitt *et al.*, 2013 and Benton, 1984).

fenestra, resulting in a unique dorsal margin of the orbit (Fig. 5) (Alcober, 2000). This unique dorsal margin of the orbit was referred to as the "orbital arch" by Sill (1974) and has not yet been observed in any other pseudosuchian (Alcober, 2000). The lateral process (laterally projected above the dorsal border of the orbit) of the frontal forms a posterolateral corner (Alcober, 2000). Both previous diagnoses primarily focused on this frontal thickening as characteristic of *Saurosuchus*. However, Alcober (2000) also mentioned some other derived traits such as the loss of the dorsally exposed frontal suture due to the development of the dermal sculpturing, causing the dorsal view of the postfrontal to become reduced. Another derived character that can be found in the skull of *Saurosuchus* is the robust, laterally orientated capitate process of the laterosphenoid (Alcober, 2000). The ventral process of the lacrimal causes it to be adjacent to the jugal laterally. Lastly, on the dorsal part of the supraoccipital a development of the crista can be observed (Fig. 5) (Alcober, 2000). These characters form a structured dorsoventrally deep skull with a relatively tall and narrow snout, often called "hatchet-shaped" (Holtz Jr, 1998). This skull shape is very similar to carnivorous theropods, in which the skull is adapted to be resistant to vertical compressive loads and functions most effectively as a slicer or slasher (Busbey, 1995). These morphological similarities to theropods, along with evidence of their bite marks on numerous herbivore and mesopredator fossil bones, have led to the suggestion that *Saurosuchus* and other rauisuchians were the apex predators of Middle and Late Triassic food webs, performing the same ecological role as later evolving post-Triassic theropods (Chatterjee, 1985; Alcober, 2000; Gower, 2000; Nesbitt *et al.*, 2013; Roberto-Da-Silva *et al.*, 2018; Mastrantônio *et al.*, 2019).

1.4 Diet and Ecology

It is agreed by most palaeontologists that rauisuchians were massive, quadrupedal carnivorous predators (e.g., *Batrachotomus kuperferzellensis, Postosuchus kirkpatricki, Prestosuchus chiniquensis,* and *Saurosuchus galilei*) due to fossil evidence showing morphological similarities to carnivorous theropods (Chatterjee, 1985; Alcober, 2000; Brusatte *et al.*, 2009; Weinbaum, 2011, 2013). These traits include large, pointed, labiolingually compressed, recurved and serrated (known as ziphodont) teeth, typically observed in predators that need to tear through meat (D´Amore, 2009; Nesbitt *et al.*, 2013; Brink *et al*., 2015). Their carnivorous diet can also be inferred based on their relatively tall and narrow skulls, similar to the well-known carnivorous theropod dinosaurs such as allosaurids and tyrannosaurids (Chatterjee, 1985). Indeed, in 1985, Chatterjee described the rauisuchian *Postosuchus,* and believed that this Triassic predator exhibited traits, including bipedalism, that foreshadowed and therefore was close to the ancestry of the Jurassic/Cretaceous apex predator *Tyrannosaurus*. However, this was erroneous and rauisuchians were revealed to be a unique group of archosaurs that were more closely related to crocodilians and which overlapped in time with early dinosaurs in the Triassic Period (Peyer *et al.*, 2008). In Triassic strata rauisuchians have often been found together with common medium–large herbivorous tetrapods which were suggested to likely be their prey (Nesbitt *et al.*, 2013). This can particularly be seen in the case of *Saurosuchus galilei* and *Prestosuchus chiniquensis,* which were considerably larger in size compared to other carnivorous tetrapods and consequently were likely the apex predators in the Triassic faunas they inhabited in South America (Argentina and Brazil respectively) (Nesbitt *et al.*, 2013). These two species have been shown to be sympatric with many herbivorous therapsids, rhynchosaurs, dinosauromorphs and dicynodonts (Zerfass *et al.*, 2004; Langer *et al.*, 2007). Rauisuchians were able to become these apex predators due to not only an extremely structured, competent cranium (Fig. 5), but also postcranial traits such as an erect gait (with a vertical, rather

than curved, femur and acetabulum like in monitor lizards) which allowed them to have quick, agile, terrestrial locomotion that was superior to the rhynchosaurs and dicynodonts that they preyed on (Nesbitt *et al.*, 2013). Benton (1984) and Bonaparte (1984) suggested that this trait was convergently evolved in different ways by the rauisuchians and theropod dinosaurs: in rauisuchians the hip socket faces downward, whereas in dinosaurs the hip socket faces outward connecting the femur to the side of the hip (Bonaparte, 1984).

Due to these derived carnivorous cranial and postcranial adaptations, rauisuchians were able to fill many ecological roles and were very successful up until the end of the Triassic period. They all went extinct along with many other archosaur lineages in the end-Triassic mass extinction event. The causes of this extinction are still not completely understood, but the current consensus is massive volcanic activity known as the Central Atlantic Magmatic Province (CAMP) on the Atlantic Oceans (Blackburn et al., 2013). It is thought that these eruptions led to huge climatic upheavals due to the immense amount of carbon dioxide and sulphur dioxide it released. This theory was initially rejected by some authors, due to the lack of ash-fall horizons on the rock (Newark Supergroup) in eastern North America that records the Triassic–Jurassic boundary (Fowell & Olsen, 1995). However, wider sampling confirmed that the CAMP eruptions started a few thousand years before the extinction event in Nova Scotia and Morocco and then continued for the next 600,000 years after the initial event (Blackburn et al., 2013). This mass extinction resulted in the rise of theropod dinosaurs with the footprint record showing an increase in size following the Triassic-Jurassic boundary (Griffin & Nesbitt, 2020). With the absence of rauisuchians and other large-bodied reptilian lineages, theropod dinosaurs were the sole large terrestrial predators and could fill the now empty niches in the Jurassic (Olsen *et al.*, 2002). Although most rauisuchians were mainly carnivorous their skull morphology and dentition indicate the possibility of a more diverse diet. For example, the semi-aquatic *Qianosuchus mixtus* had a crocodilian-like skull and

teeth, indicating a diet of aquatic vertebrates such as sauropterygians, protorosaurs, ichthyosaurs and fish (Li *et al.*, 2006). On the other hand, beaked rauisuchians such as *Lotosaurus adentus*, *Effigia okeeffeae* and *Shuvosaurus inexpectatus* have skull morphologies that suggest a diet of plants, invertebrates, vertebrate eggs, and meat, similar to extant avian species (Gower, 2000; Nesbitt, 2007; Lautenschlager & Desojo, 2011; Bestwick *et al.*, 2021).

Many often assume that since Pangea is one giant landmass that the environment across it would be very similar throughout the whole land. However, on the contrary there were many differences from the northern to the southern parts such as weather, temperature, humidity, and therefore variation in flora (Damuth *et al.*, 1992). As previously stated, rauisuchians were a very widespread group of archosaurs, and taxa from the major rauisuchian clades, such as *Ticinosuchus ferox*, *Effigia okeeffeae* and *Rauisuchus tiradentes* are known to have inhabited strongly seasonal environments (Golonka & Ford, 2000; Pires *et al.*, 2005; Nützel *et al.*, 2010). The areas where many rauisuchians have been discovered were fluvial environments; continental terrestrial deposits laid down in floodplains and river channels (Nesbitt *et al.*, 2013). This is the case for some terrestrial rauisuchians which were fossilised after being washed into a brackish lagoon/lake (e.g., *Batrachotomus kupferzellensis*; Schoch, 2002; Hagdorn & Mutter, 2011). *Ticinosuchus ferox* was found in a marine intraplatform basin, one of the most diverse Triassic Lagerstätten environments (Krebs, 1965; Lautenschlager & Desojo, 2011). Specimens of *Qianosuchus mixtus* were found preserved in coastal limestones, which further indicates to a semi-aquatic lifestyle (Li *et al*., 2006; Nesbitt, 2011). The specimen of *Saurosuchus* studied here (PVSJ 32) was found in a silty abandoned channel deposit, at the base of the Ischigualasto Formation (Alcober, 2000). Very much like the Jurassic dinosaurs that succeeded them, the rauisuchians were likely to be warm-blooded, which allowed them to evolve their advantageous pillar-erect posture and lead a successful niche as

the apex predators (Benton, 2021). Their warm-blooded metabolisms are also indicated by the state of their bone histology, which is more similar to mammals, birds and dinosaurs than to that of other reptiles (Benton, 2021).

Due to their large size, morphological similarities and bite mark evidence on herbivorous/meso predator fossil bones, it suggests that rauisuchians were apex predators and performed the same ecological role as the later evolving theropods (Chatterjee, 1985; Alcober, 2000; Gower, 2000; Nesbitt *et al.*, 2013; Roberto-Da-Silva *et al*., 2018). However, the ecological classification of an apex predator is quite broad and disregards the functional behaviour of predators, which can have subtly different impacts on the environments in which they live (DeVault et al., 2003, Wallach et al., 2015, Wilkenros et al., 2013). For example, based on predicted high bite forces and heavily worn teeth, tyrannosaurids are hypothesised to consume a large quantities of bones (i.e., osteophagy) relative to other theropods (Rayfield, 2004, 2005; Sakamoto, 2010; Gignac and Erickson, 2017). Whereas, Allosaurids, are suggested to have had weaker bite and instead employed a "strike-and-tear" technique with relatively fewer tooth-bone interactions (Rayfield *et al.*, 2001, 2005; Montefeltro *et al.*, 2020). Therefore, without quantitative investigation into the functional morphology, the hypothesis that rauisuchians are the direct Triassic analogues of theropods is a rather simplistic statement.

1.5 Biomechanical Modelling Methodologies

An important area when it comes to studying extinct fossils is understanding the diet - feeding habits, skull strength/bite force and possible cranial kinesis – and ecology of the individual or species (Nesbitt *et al.*, 2013). This is especially important when studying rauisuchians (*Saurosuchus* in this case), since they have varied well-adapted sculptured crania (Alcober, 2000). Although many studies have investigated the potential feeding behaviours and diets of Triassic pseudosuchians, few studies have used biomechanical modelling methods, including finite element analysis (FEA), to explore the functional morphology (Bestwick *et al*., 2021). These methods have allowed a better understanding of the broader morphological evolution of pseudosuchians and how taxa may have partitioned and competed for resources (Desojo & Vizcaíno, 2009; Von Baczko *et al.*, 2014; Von Baczko, 2018; Taborda *et al.*, 2021). Computed tomography (CT) now allows the identification and visualisation of fossils and is usually the first step in these quantitative methodologies (Sutton, 2008). These CT-scans of fossil specimens are used in order to create digital reconstructions. Sometimes fossil specimens may have taphonomic deformation and disarticulation, and therefore further processing of the digital model in software like Avizo and Blender is required before any computational analysis can be done (Lautenschlager, 2016*a*, 2017). Avizo is an image analysis platform which allows CT data to be visualised, processed, and quantified (Kakuturu, 2017). It has developed two primary capacities in particular that has really aided digital reconstructions of fossil specimens (Garwood & Dunlop, 2014). One of these capacities of Blender is the production of high-quality figures of CT-scanned data to be displayed in publications (Garwood and Sutton, 2010, 2012; Garwood *et al*., 2011, 2012; Spencer *et al*., 2012; Zamora *et al.*, 2012; Giles and Friedman, 2013). However, recently the major palaeontological use of Blender is to manually model meshes and create raytraced reconstructions of fossil organisms (Garwood & Dunlop, 2014). Many

publications have been released using this technique in Blender (e.g., Stein, 2010; Haug *et al.*, 2011, 2012; Stein & Selden, 2012; Haug & Haug, 2012; Garwood & Dunlop, 2014; Lautenschlager, 2016*a*, 2017; Butler *et al.*, 2022). Soft tissues are unfortunately not well preserved and are very rarely seen (Lautenschlager, 2016*b*). Although current reconstructions are limited in conveying information such as the extent, orientation or arrangement of the muscles due to the cranial muscular system complexity, with the introduction of computer-aided imaging (e.g., CT), many of these limitations can be resolved (Snively & Russell, 2007; Werneburg, 2011; Lautenschlager, 2016*b*). These digital techniques help restore the hard-tissue morphology and remove the taphonomic and preservational artifacts that exist on the fossil specimens, and recently these techniques have also been used for soft tissue reconstructions, like in this Thesis (Lautenschlager, 2012; Cunningham *et al.*, 2014; Lautenschlager *et al.*, 2014).

Feeding, respiration and fighting are some key functional behaviours of many archosaurs, and all these behaviours impart loads (forces) upon the vertebrate cranium in different ways (Rayfield, 2005). These loads induce stress and strain on the bones and soft tissues of the cranium, however, there has been research that suggests that the cranial bones have structural characteristics that modify the stress and strain environment of the skull (strain transmission, resistance and dissipation) (Rayfield, 2005). Some of these features include bone thickenings or reduction, sutures, trabeculation, and the distribution of material property in the cranium (Thomason & Russell, 1986; Jaslow, 1990; Jaslow & Biewener, 1995; Herring & Teng, 2000; Rayfield *et al.*, 2001; Rafferty *et al.*, 2003). Such features can serve as indicators of loading patterns, and furthermore the functional behaviour of the fossil specimen (Rafferty & Herring, 1999; Rayfield *et al.*, 2001; Jenkins *et al.*, 2002; Bestwick *et al*., 2021). One of these newly advanced biomechanical modelling methodologies that allows for a better understanding on the possible cranial kinesis of extinct fossil groups is

integrated biomechanical modelling, e.g., in this case Finite Element Analysis (FEA). FEA is an engineering computer-based technique which is capable of calculating the stress and strain within cranium structures in response to applied loads from different functional behaviours (Rayfield, 2005). Functional analyses, such as FEA, that are based on digital models of fossil specimens provide the means for biomechanical studies and allows the quantifying of the fossil cranial function (Rayfield, 2007; Curtis, 2011; Rahman *et al.*, 2015). There are many skeletal features exhibited by pseudosuchians that have been described as convergent with distantly related theropod dinosaurs from the Jurassic and Cretaceous Period (Stocker et al., 2016). *Saurosuchus* has an orbital shape that is dorsoventrally high and smaller in width, which is also seen in other theropods like the Tyrannosaurids. This structural adaptation means that it is likely able to resist high muscle forces generated with prey capture and dismemberment in order to keep up with the requirements of the posterior half of the skull (Henderson, 2003). The structured skull roof of *Saurosuchus* indicates a high level of robustness, therefore, it is expected to display low levels of stress and deformation, similar to theropods. However, the general shape of the skull is rectangular which may cause the anterior section to experience slightly higher stresses than theropods with a dorsoventrally shallower snout. The quadrate and vomer display less thickness than other bones in the posterior section, indicating that this could also be a mechanical weakness for *Saurosuchus*. Overall, it is hypothesised that *Saurosuchus* will display analogous FEA results to that of theropods, with low stress and deformation and a high bite force, due to the morphological similarities. In this study, I use FEA to explore the cranial mechanics of *Saurosuchus* and a comparative theropod analogue, *Allosaurus fragilis*, to therefore investigate the degree of the convergence hypothesised between apex pseudosuchians (rauisuchians) and avemetatarsalians (theropods).

1.6 Aims

Here, I employ a biomechanical modelling approach in a comparative investigation of the functional morphology of a rauisuchian: the Triassic apex predator *Saurosuchus galilei*. The aim of this project was to characterise the functional morphology of *Saurosuchus* and the implications for the feeding behaviour and ecology. This required (i) the reconstruction and retrodeformation of the cranial skeleton using CT scans of the fossil specimen PVSJ 32 in two software programs (AVIZO and BLENDER) (ii) the reconstruction of the jaw musculature and quantification of the muscle force using editing and measurement tools in BLENDER in order to carry out the FEA (iii) the creation of biomechanical models using FEA to create von Mises contour plots of the digital model for two intrinsic bite simulations (iv) the estimation of the bite force for the *Saurosuchus* model from constrained nodes at the tips of the teeth which measures the reaction force caused by the modelled adductor muscles (v) the comparison of the results to other rauisuchians, theropod dinosaurs, extant crocodilians using previous FEA research, including a similarly sized 3D model from the theropod *Allosaurus fragilis* (Rayfield et al., 2001, Lautenschlager, 2015, Montefeltro et al., 2020). This characterised the *Saurosuchus* cranium biomechanically and quantified the functional similarities and differences between Triassic and post-Triassic predators.

CHAPTER II
MATERIAL AND METHODS

2.1 CT-Scans

The computed tomography (CT) scans of the juvenile *Saurosuchus galilei* specimen PVSJ 32 that were used for this digital reconstruction were from the University of Texas High-Resolution X-ray CT Facility Archive 0169 (original scan data) and 0216 (as available on Digimorph.org: http://digimorph.org/specimens/Saurosuchus_galilei/). Scans of the *Saurosuchus* skull were scanned by Richard Ketcham and Matthew Colbert on 11/09/1999. Scan settings include: 420 kV (energy), 4.7 mA (current), 2 brass filters, an air wedge, a translate-rotate scan, an integration time of 16 ms, a slice thickness of 2.0 mm, 661 mm S.O.D., 2 views, 1 ray per view, 2 samples per view, interslice spacing of 1.8 mm, 400 mm field of reconstruction, a reconstruction offset of 500, and a reconstruction scale of 150. Slices were in 8bit mode. Scans were mirrored so the right and left lateral view were the opposite of the fossilised specimen.

2.2 AVIZO

The CT image files (396 in total) were then subsequently imported into AVIZO Lite (Version 9.3.0, Visualization Science Group). The individual elements of the skull were highlighted and separately labelled using the AVIZO segmentation editor to produce surface models and volumes. This allowed the individual elements (cranial bones) in the skull to be exported separately into the software BLENDER, in order to restore any damaged and/or deformed areas.

2.3.1 BLENDER – Skull Reconstruction

Blender (BLENDER.ORG) was developed by The Blender Foundation and is a cross-platform 3-D computer graphics application. It allows 3D objects to be imported, created, modified (e.g., the light, colour, and texture), and the ray tracing of the resulting model. After the Avizo files had been imported into the software BLENDER 2.80, visualisation and editing steps were carried out to retrodeform the skull to its hypothesised non-deformed original morphology (Fig. 6). These restoration steps followed the same method of Lautenschlager (2016*a*), with deformation, cracks

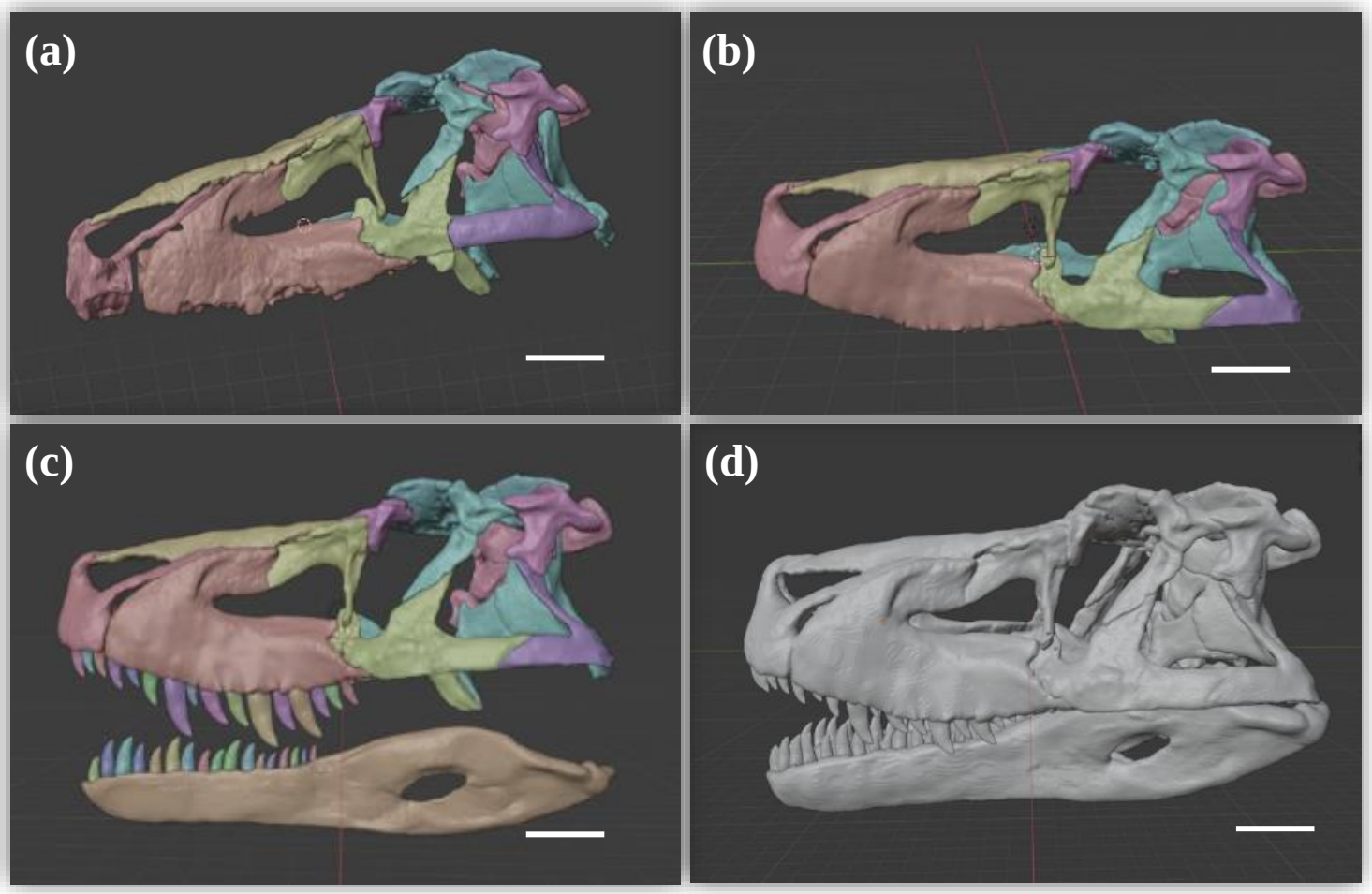

Fig. 6. Process of digitally restoring the skull of *Saurosuchus galilei* (PVSJ 32) and reconstruction of the mandible, using an adjusted *Allosaurus fragilis* digital mandible, on the software BLENDER 2.8x: (**a**) left lateral view of skull before any editing steps performed (premaxilla from the right side); (**b**) left lateral view of skull after editing steps completed; (**c**) left lateral view of skull including the lower mandible and teeth; (**d**) left lateral view of finished reconstructed skull. Scale bars = 10 cm

and holes repaired using the *Saurosuchus* 2D restoration by Alcober (2000) and osteological comparisons with closely related rauisuchians (e.g., *Batrachotomus kupferzellensis*, *Prestosuchus* spp.; (Roberto-Da-Silva *et al*., 2018; Desojo *et al*., 2020). A full reconstruction was created using reflection and superimposition of complete/more complete elements to restore breaks or missing portions. Due to the considerable deformation on the right side of the skull, the left side was therefore used as a template for the reconstruction, except for the premaxilla which was better preserved on the right side. Assuming bilateral symmetry, the duplication and mirror command was used, and a mirror-image was created in order to complete the overall digital skull. Despite the unexpectedly large size of PVSJ 32, the *Saurosuchus* specimen is a juvenile, which can clearly be observed from several features that were included in the final restored model to increase the accuracy. These features included the subnarial fenestrae between the premaxillae and maxillae and an open suture between the exoccipitals and basioccipitals (Alcober, 2000) (Fig. 5 & 6).

Finally, the final model was reconstructed using a model of a generic carnivorous archosaur tooth and the mandible of a *Allosaurus fragilis* specimen, as unfortunately these were not persevered on the PVSJ 32 specimen. The generic archosaur teeth were box-modelled (see Rahman and Lautenchlager (2016)), then were sized and positioned accordingly to the alveoli morphology of PVSJ 32. The mandible of *Allosaurus fragilis* (MOR 693, see Rayfield et al. (2001) for scanning details) was chosen as the initial template for the hypothetical mandible because most Triassic theropod and rauisuchian mandibles are also poorly preserved. *Allosaurus* mandibles, on the other hand, are preserved in great detail with high-quality three-dimensional scans available (Rayfield et al., 2001). Furthermore, previous preserved fragments of *Saurosuchus* mandibles show several features that are superficially more similar to theropod dinosaurs like *Allosaurus*, such as an anterior process of the coronoid, than to more closely related rauisuchians (Sill, 1974, Alcober, 2000). The *Allosaurus* mandible and carnivorous archosaur tooth served as a basis for the digital

model, with the use of the Alcober (2000) reconstruction as a template and the sculpting tools in Blender, the reconstruction of the teeth and a mandible was carried out and added to the skull model (Fig. 6). The digital skull model was reconstructed to serve as a foundation and guide for the reconstruction of the cranial musculature. This allows the reduction/avoidance of measurement and scaling errors, commonly caused by deformed anatomy of the skull, since the measurements will be taken straight from the muscles rather than from the original specimen.

2.3.2 BLENDER – Muscle Reconstruction

Some of the earliest muscle reconstructions date back to more than a century ago (Lull, 1908). Previously, soft-tissue/muscle reconstruction methods had a theoretical framework in the form of general attachment site identification (Barghusen, 1973) or two dimensional (2-D) drawings and schematics (Adams, 1918; Anderson, 1936; Haas, 1955, 1963, 1969). However, recently the use of computational techniques has advanced these reconstructions and drastically changed the study of fossils (Cunningham *et al.*, 2014). Here, the digital approach used was similar to the traditional muscle reconstruction methodologies that have been previously carried out (e.g., Dilkes, 1999; Holliday, 2009; Lautenschlager, 2016*b*, Bestwick et al., 2021). First, the muscle attachment sites were identified on the reconstructed digital model of the *Saurosuchus* skull and adjusted mandible (Fig. 7). The muscles identified were m. AMEM, m. adductor mandibulae externus profundus; m. AMES, m. adductor mandibulae externus superficialis; m. AMP, m. adductor mandibulae posterior; m. PSTp, m. pseudotemporalis profundus; m. PSTs, m. pseudotemporalis superficialis; m. PTd, m. pterygoideus dorsalis; m. PTv, m. pterygoideus ventralis. Since most muscles follow the same structure of suspension between their origin and insertion (Lautenschlager, 2016*b*), this allowed a point-to-point connection to be made and the 3D muscle arrangements to be reconstructed (Fig. 8).

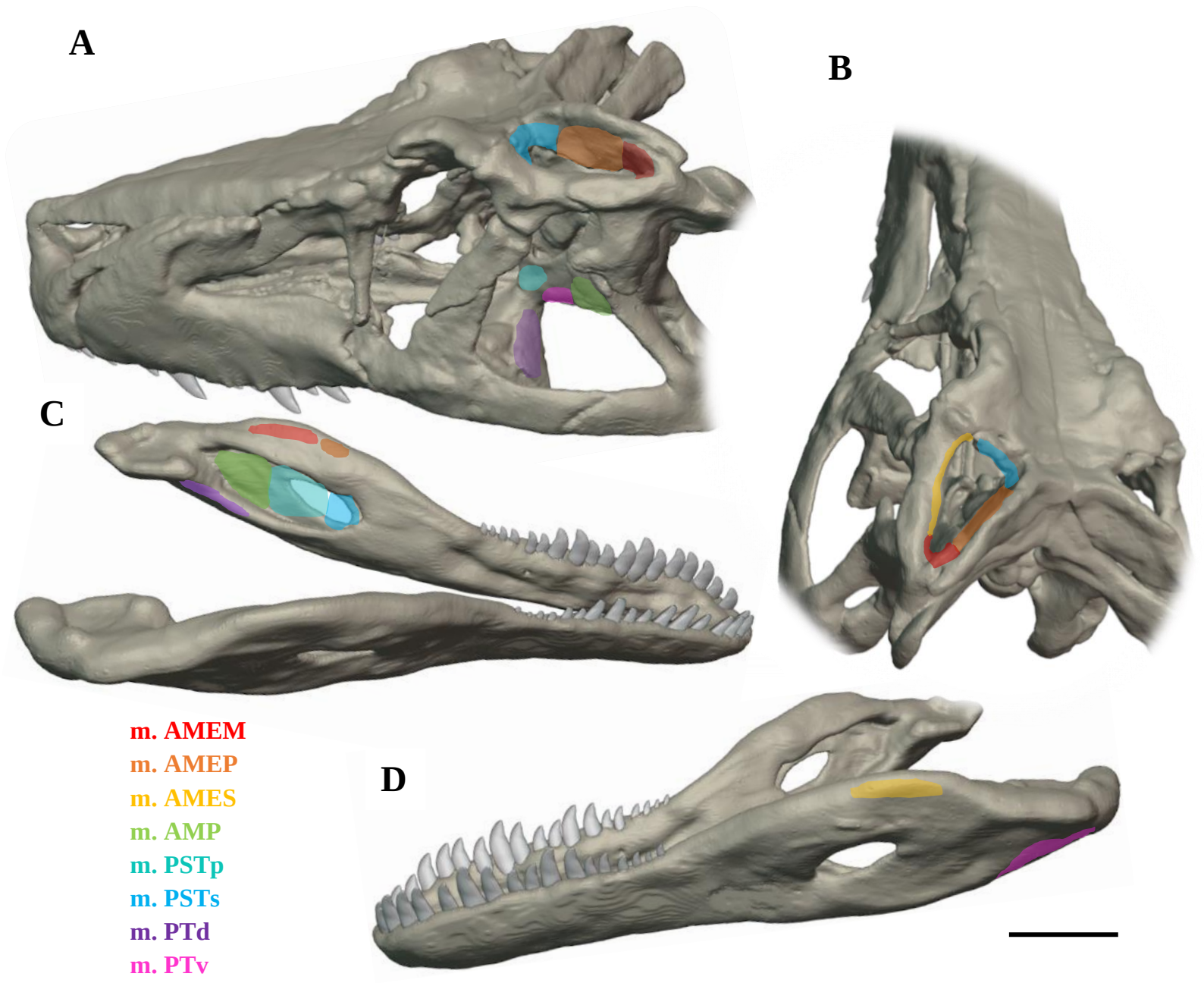

Fig. 7. Muscle attachment locations in the skull of *Saurosuchus galilei*. (PVSJ 32) and reconstructed mandible, using an adjusted *Allosaurus fragilis* digital mandible. Muscle origin sites in (**A**) left dorsolateral and (**B**) dorsal view (slight lateral tilt). Muscle insertions in (**C**) right medial and (**D**) left lateral view. Abbreviations: m. AMEM, m. adductor mandibulae externus medialis (red); m. AMEP, m. adductor mandibulae externus profundus (orange); m. AMES, m. adductor mandibulae externus superficialis (yellow); m. AMP, m. adductor mandibulae posterior (green); m. PSTp, m. pseudotemporalis profundus (turquoise); m. PSTs, m. pseudotemporalis superficialis (blue); m. PTd, m. pterygoideus dorsalis (purple); m. PTv, m. pterygoideus ventralis (pink). Scale bar = 10 cm. (Inspired by Lautenschlager, 2013)

The full muscle bodies were created in Blender using the combination of box-modelling and the sculpting tools. The reconstructed muscle models provide a clear picture of the muscle origins and insertions and their three-dimensional position (Lautenschlager, 2016*b*). However, it is key to note that they only approximate the full muscle anatomy, which limits their accuracy and usefulness for measurements. The knowledge of the position, orientation, and qualitative/quantitative details for biomechanical questions and inferences on functional morphology is essential.

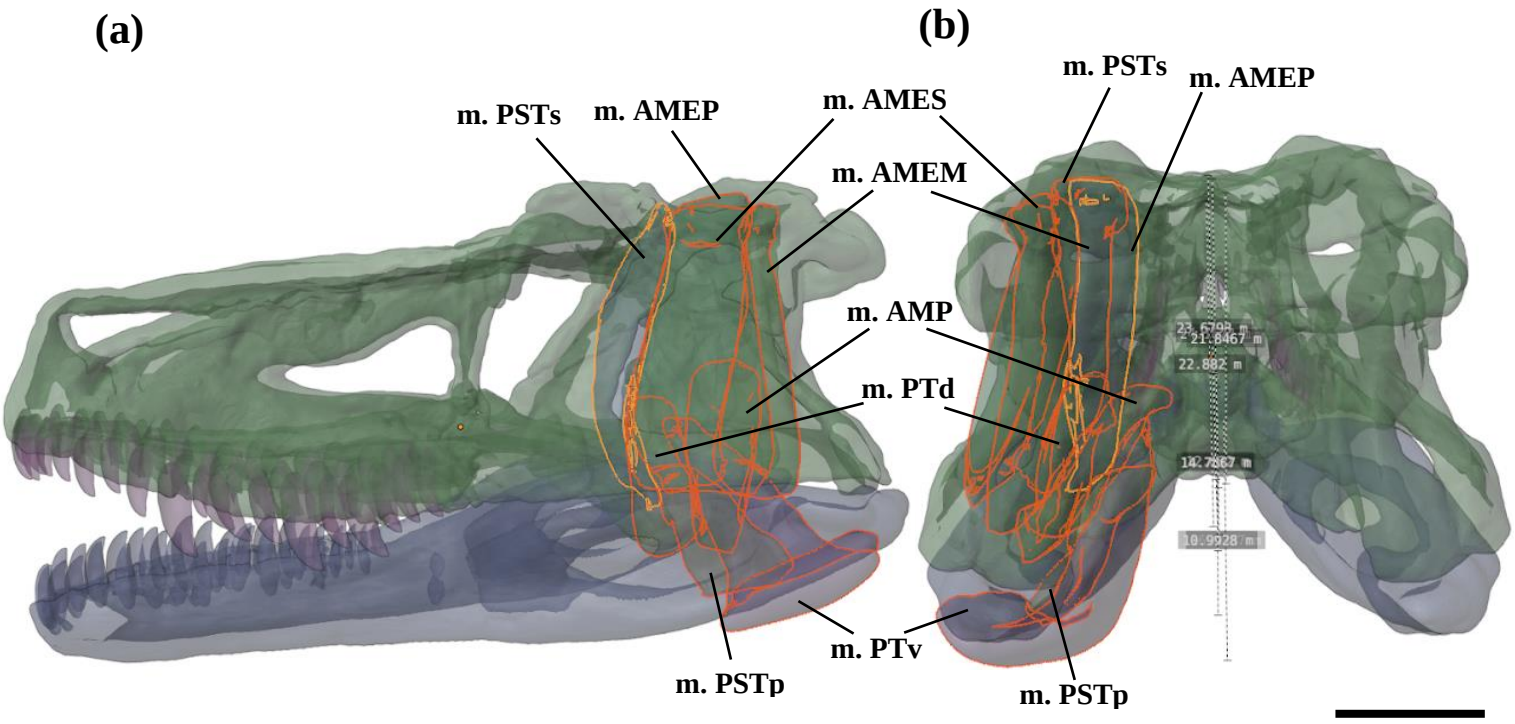

Fig. 8. BLENDER digital cranium model of *Saurosuchus galilei* (PVSJ 32) with reconstructed muscles outlined in orange. Digital model in transparent view with muscle lengths labelled in cm (ignore BLENDER units): m. AMEM, 22.882; m. AMEP, 23.6798; m. AMES, 21.8467; m. AMP, 14.7867; m. PSTp, 12.032; m. PSTs, 24.1672; m. PTd, 10.9928; m. PTv, 16.9357. (**a**) left lateral view of digital model; (**b**) posterior view of digital model. Abbreviations: as for Fig. 7. Scale bar = 10 cm

After the 3D cranial muscles had been reconstructed in Blender, measurements were made in order to calculate the muscle forces. These measurements included the vertical muscle lengths (cm) (Fig. 8). The muscle lengths measured from the *Saurosuchus* digital model were used as a proxy for

calculations of the physiological cross-sectional area (cm^2), which was then multiplied by an isometric muscle stress value of 30.0 N cm^{-2}. Table 1. displays the cross-sectional area value and calculated total muscle force inferred for each muscle.

Table 1. Cross-sectional area in cm^2 and muscle force estimates in N calculated for the individual muscles reconstructed on the *Saurosuchus galilei* digital model in the software BLENDER.

Muscle	Cross-sectional area (cm^2)	Muscle force (N)
m. AMEM	10.358	310.734
m. AMEP	16.736	502.078
m. AMES	19.495	584.845
m. AMP	12.065	361.946
m. PSTp	13.791	413.733
m. PSTs	11.195	335.839
m. PTd	12.098	362.943
m. PTv	23.811	714.342

2.4 Finite Element Analysis

The 3D model of *Saurosuchus*, including the skull and adjusted mandible, was imported into the software HyperMesh 13.0.110 (Altair Engineering) for the generation of solid tetrahedral meshes (model consisting of 3,741,217 elements). All material properties in the model were assigned and treated as isotropic and homogeneous. Material properties used: bone E = 15 MPa, v = 0.29; teeth E = 60.4 MPa, v = 0.31 as in Montefeltro *et al.*, (2020). Intrinsic scenarios for *Saurosuchus* were simulated for the skull and mandible models, using a simplified jaw adductor muscle-driven bite. Two intrinsic scenarios were carried out on the digital model, and were analysed to indicate the

distribution and magnitude of the von Mises stress and to estimate the muscle-driven biting force:

- a bilateral front bite scenario (FBS) at the first premaxillary and first dentary tooth,
- a bilateral back bite scenario (BBS) at the 14th maxillary and 16th dentary tooth.

For each intrinsic scenario, constraints were placed on nodes at the craniomandibular articular surfaces, similar to previous studies (Montefeltro *et al.*, 2020). Each node was constrained in all directions (x, y, z). For the skull model, five nodes were constrained on each quadrate articular surface and two nodes on the occipital condyle. Furthermore, for the mandible model, five nodes were constrained on each glenoid. To estimate the biting force of the *Saurosuchus* model, nodes were constrained at the tips of the teeth to measure the reaction force caused by the modelled adductor muscles. In both the bilateral scenarios, the tips of the teeth on both sides of the skull and mandible models were constrained. For bilateral bite scenarios the PM1 and D1 teeth (front bite) and M14 and D16 (back bite) were constrained. The FEA was performed in the software ABAQUS/CAE 6.14-1. ABAQUS is a general-purpose finite element program which is designed for advanced structural and heat transfer analysis specifically (Garwood & Dunlop, 2014). It is designed for the use of nonlinear/linear stress analysis of many structures, ranging from extremely small to very large structures (Garwood & Dunlop, 2014). The *Saurosuchus* model, for both intrinsic bite scenarios, was processed and analysed in ABAQUS. Contour plots of von Mises stress (a measure of overall structure strength under loading conditions) distribution were used to display and assess the finalised FEA models (Fig. 9-12 & 15), including the comparative theropod analogue *Allosaurus fragilis* model MOR 693 (Fig. 16). The blue/green colours indicating the lowest magnitudes of stress experienced and red/grey indicating the highest. Stresses were also measured at ten equally spaced locations along the dorsal and ventral surfaces of the cranium (Fig.13-14). Measurement locations across the surfaces of all crania are shown in Appendices 1 & 2.

CHAPTER III
RESULTS

During the bilateral front bite scenario (hereafter, FBS), the bite force estimate for the *Saurosuchus galilei* digital model was 1,015 N for the skull and 1,087 N for the mandible (Fig. 9A). During the bilateral back bite scenario (hereafter, BBS), the bite force estimate was 1,885 N for the skull and 1,920 N for the mandible (Fig. 9B). Although variable in magnitude, a general pattern was discernible for the von Mises stress distribution in the skull and mandible of *Saurosuchus* (Fig. 9-13). The areas that displayed the highest magnitude of stress/the stress hotspots, indicated by the red and grey colours, on the skull model for the two simulated scenarios include: the dorsoposterior margin of the frontal; jugal; the posterior margin of the quadratojugal; quadrate body; pterygoid; parietal; lacrimal; dorsal margin of the squamosal and postorbital; vomer; ectopterygoid; and the braincase (specifically the basioccipital and exoccipital). Regions that displayed moderate stresses,

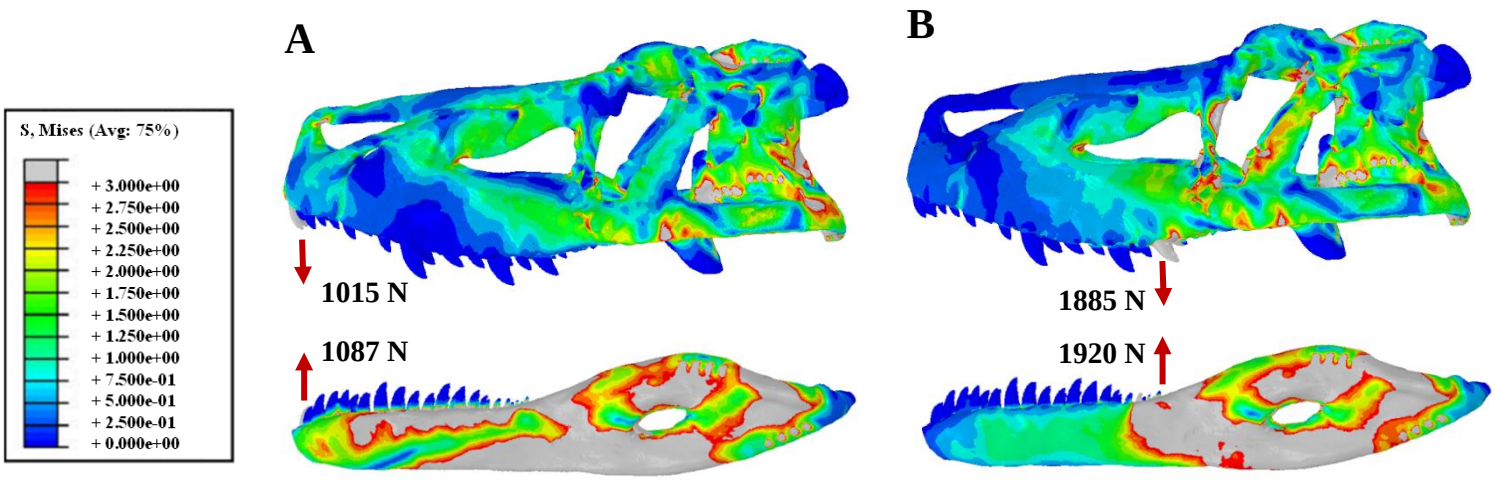

Fig. 9. Von Mises stress contour plots from finite elements analysis (FEA) of the *Saurosuchus galilei* digital model (PVSJ 32) in left lateral view for two intrinsic bite scenarios, with blue denoting the lowest magnitude of stress experienced and grey displaying the highest. The location and respective estimated values of muscle-driven bite forces are indicated on the models during each scenario: (**A**) bilateral front bite (FBS) of skull and mandible; (**B**) bilateral back bite (BBS) of skull and mandible. Units for von Mises stress = MPa.

indicated by the yellow and green colours, on the skull for both scenarios include: the posterior margin of the maxilla and nasal; the ventral margin of the squamosal and postorbital; jugal; and the anterior margin of the quadratojugal and frontal. The areas that displayed low stress levels, indicated in the different shades of blue, for both scenarios include: the anterior margin of the maxilla; the posterior margin of the paraoccipital process; the ventricular projection of the ectopterygoid and pterygoid; nasal; and the dorsal projection of the frontal and lacrimal (Fig. 9).

3.1 Von Mises Stress Distribution

The distribution and magnitude of the von Mises stress displayed many differences between the two intrinsic bite scenarios for the *Saurosuchus* model. It was clear to see that overall, there was a higher amount of stress experienced during the FBS compared to the BBS for the skull model (Fig. 9). The key differences that were observed between the two bite simulations were located at the anterior and median sections of the skull. During the FBS, there was a major increase in stress experienced by the premaxilla body, especially at the anterior corner of the external naris, nasal and the anterior margin of the lacrimal (Fig. 9A). Whereas during the BBS, it displayed mainly low stress levels for the premaxilla and nasal, with only the posterior end of the nasal experiencing moderate stresses (Fig. 9B). During the BBS, it indicated higher levels of stress, compared to the FBS, in the regions around the orbital fenestra (orbit/eye socket) such as the ventricular projection of the lacrimal, ventral margin of the frontal, prefrontal, and the anterior margin of the postorbital and jugal body. Overall, during the FBS the anterior portion of the skull (dorsal rostrum: premaxilla and nasal) displayed higher stresses, whereas for the BBS the stresses experienced were more concentrated in the median portion (orbital region: jugal, lacrimal, prefrontal, and postorbital) of the skull.

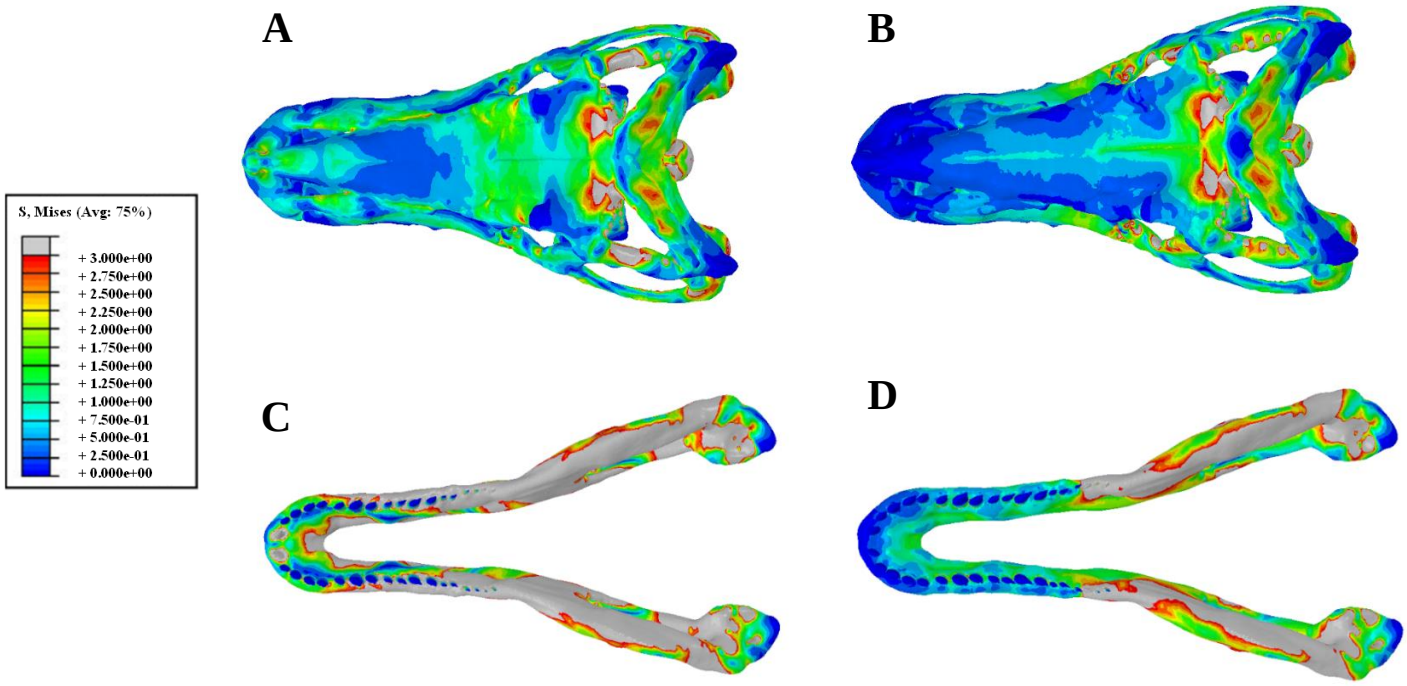

Fig. 10. Von Mises stress contour plots from finite elements analysis (FEA) of the *Saurosuchus galilei* digital model (PVSJ 32) in left dorsal view for two intrinsic bite scenarios, with blue denoting the lowest magnitude of stress experienced and grey displaying the highest. The muscle-driven bite scenarios: (**A**) skull bilateral front bite; (**B**) skull bilateral back bite; (**C**) mandible bilateral front bite; (**D**) mandible bilateral back bite. Units for von Mises stress = MPa.

The major differences in the von Mises stress distribution for the two intrinsic bite scenarios were more visible when analysing the skull model in dorsal view (Fig. 10). As seen in the lateral view (Fig. 9), The most obvious difference was the higher stresses experienced by the premaxilla and nasal body during the FBS (Fig. 10A). On the other hand, the BBS displayed low to no stresses experienced by the premaxilla and only some moderate stresses for the posterior margin of the nasal body (Fig. 10B). When in dorsal view, a large stress hotspot was observed on the postorbital and squamosal during the FBS, especially the section where the postorbital is articular to the squamosal. A stress hotspot was also observed in the median margin of the dorsal prefrontal for the FBS. During the BBS, lower stresses were indicated where the two parietal bones are articular to one another, compared to for the FBS.

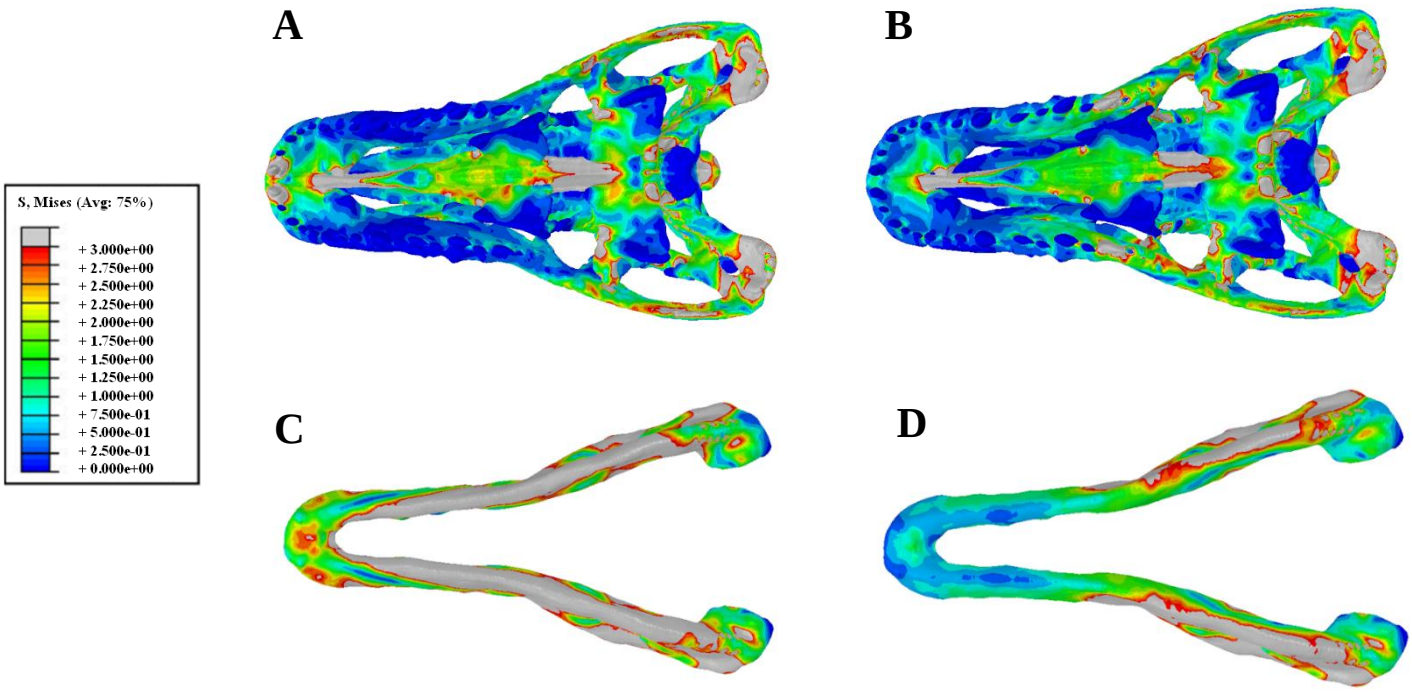

Fig. 11. Von Mises stress contour plots from finite elements analysis (FEA) of the *Saurosuchus galilei* digital model (PVSJ 32) in left ventral view for two intrinsic bite scenarios, with blue denoting the lowest magnitude of stress experienced and grey displaying the highest. The muscle-driven bite scenarios: (**A**) skull bilateral front bite; (**B**) skull bilateral back bite; (**C**) mandible bilateral front bite; (**D**) mandible bilateral back bite. Units for von Mises stress = MPa.

Contrary to the dorsal view of the skull (Fig. 10), the ventral view displayed almost identical stress distribution patterns for the two intrinsic bite scenarios (Fig. 11). The high von Mises stress was relatively homogenously distributed from the anterior to the posterior end of the ventral skull during both scenarios. The posterior ventral projections of the quadrate; basipterygoid; pterygoid (middle sections); and the anterior margin of the vomer and ectopterygoid displayed extreme stress hotspots (Fig. 11A, B). Both scenarios displayed very low stress magnitudes for the basisphenoid; and the ventral projections of the pterygoid, ectopterygoid, and palatine. One of the only differences between the two scenarios was observed in the pterygoid body. During the FBS (Fig. 11A), it displayed higher stresses experienced in the middle region of the anterior pterygoid compared to for the BBS (Fig. 11B). Another dissimilarity was observed in the regions around the teeth (premaxillary and maxillary), which remained relatively stress-free except for the area around the

premaxillary teeth (PM1) where the loads were applied (Fig. 11A). During the BBS, there were stresses experienced in the regions around the premaxillary as well as the maxillary teeth (M14) where the loads were applied (Fig. 11B). In the ventral view of the skull model, it was clear to see that the areas of maximum von Mises stress in the premaxilla and maxilla were isolated from each other. Therefore, during the FBS, the premaxillary teeth where the loads were applied indicated a stress hotspot and the maxillary teeth remain unstressed (Fig. 11A); as for the BBS, the maxillary teeth where the loads were applied showed a stress hotspot whereas the premaxillary teeth remained unstressed (Fig. 11B).

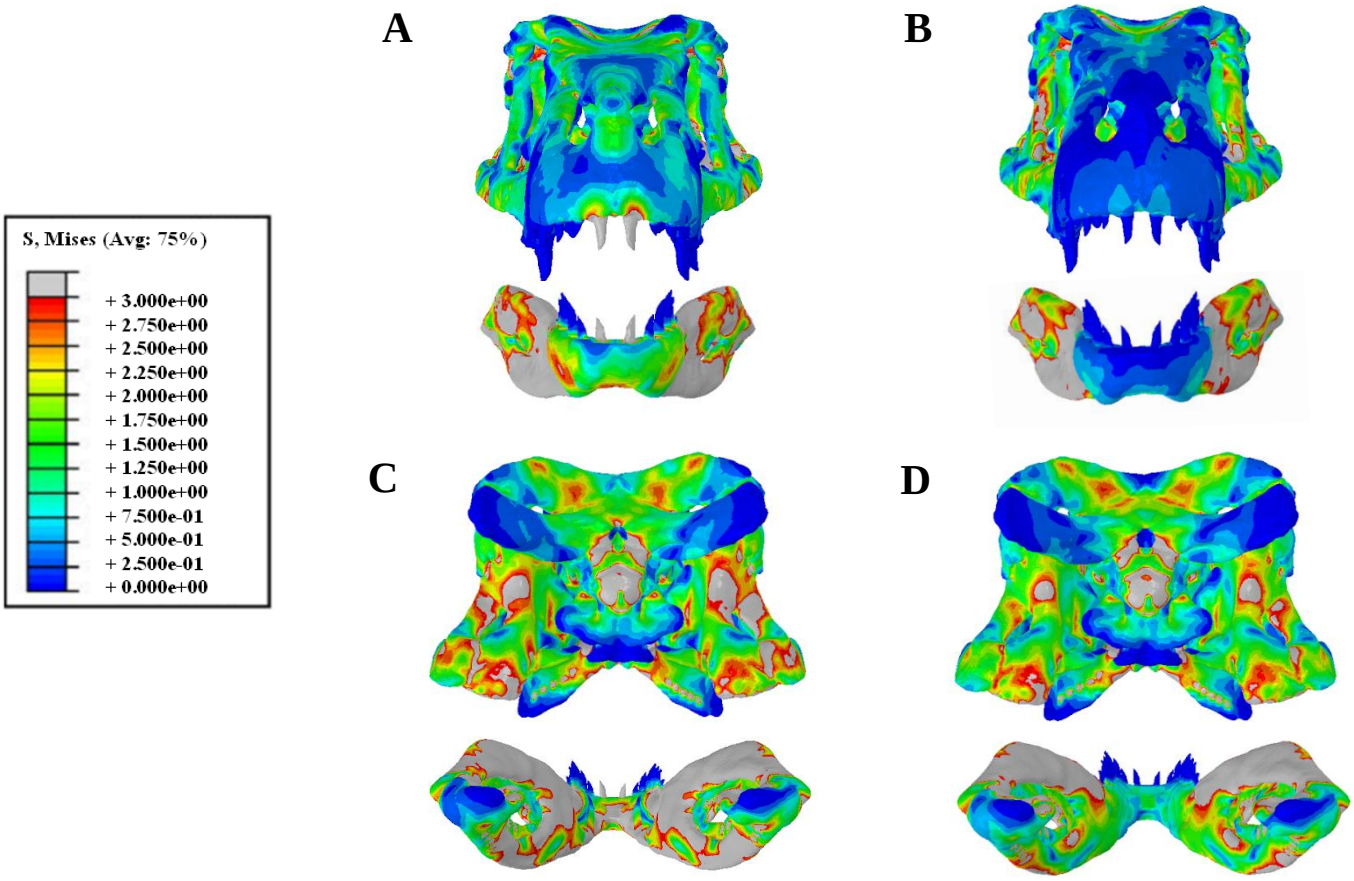

Fig. 12. Von Mises stress contour plots from finite elements analysis (FEA) of the *Saurosuchus galilei* digital model (PVSJ 32) for two intrinsic bite scenarios, with blue denoting the lowest magnitude of stress experienced and grey displaying the highest. The muscle-driven bite scenarios: (**A**) bilateral front bite for skull and mandible in anterior view; (**B**) bilateral back bite for skull and mandible in anterior view; (**C**) bilateral front bite for skull and mandible in posterior view; (**D**) bilateral back bite for skull and mandible in posterior view. Units for von Mises stress = MPa.

The anterior view of the skull further highlighted the differences in stress distribution for the two intrinsic bite scenarios, especially in the rostrum of the skull and anterior margin of the dentary (Fig. 12A, B). Both anterior sections of the skull and mandible during the BBS displayed low to no stresses experienced (Fig. 12B), whereas during the FBS, it displayed patches of moderate to high stresses in the anterior section of the skull and mandible (Fig. 12A). Interestingly, amongst the low to no stress experienced by the premaxilla during the BBS, there was increased stress indicated in the regions around the front two premaxillary teeth, even though the load was not applied to them in that scenario.

3.2 Measured Stress Magnitude

When the von Mises stress magnitudes were measured along the middle line of the skull in dorsal view (Fig. 10A, B; measurement point locations along the skull can be found in appendix 1), it produced a graph that clearly displayed the stress distribution pattern of the skull model for both intrinsic bite scenarios (Fig. 13). This gives further evidence to the von Mises contour plots that the main differences in stress distribution are located at the anterior section of the skull. Higher stress magnitudes were observed at the anterior end of the skull for the FBS compared to for the BBS. Albeit with variation, the graph further highlights the higher stresses experienced by the median section of the skull during the BBS compared to for the FBS. The highest stresses experienced by the skull model during the two bite simulations can be observed at the very most posterior end. The posterior section of the skull model displayed nearly identical stress pattern for the two bite scenarios (Fig. 13), this can be observed in the von Mises contour plot of the skull in posterior view (Fig. 12C, D). Although minimal, the stress magnitudes at the posterior section of the skull were higher during the FBS compared to for the BBS.

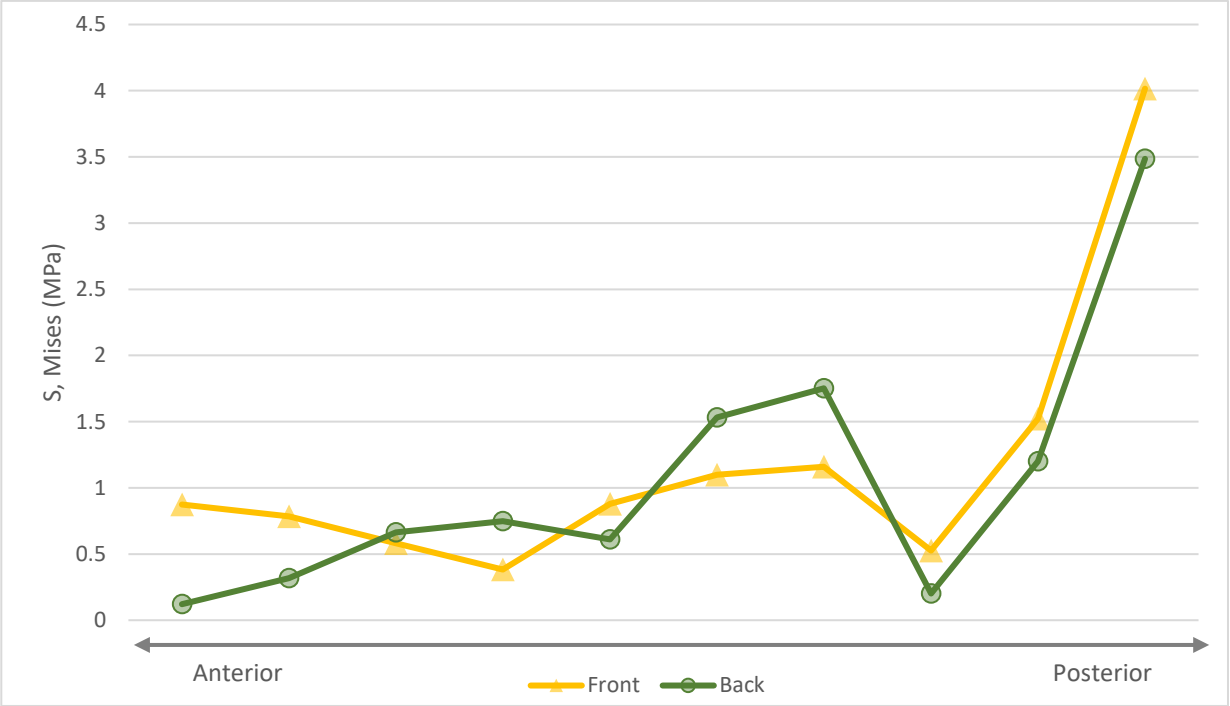

Fig. 13. Von Mises stress magnitudes (MPa) of the *Saurosuchus galilei* skull model (PVSJ 32) at 10 measurement locations along the dorsal surface for two intrinsic bite scenarios – bilateral front bite scenario (yellow triangles); bilateral back bite scenario (green circles). Same von Mises stress limits as for Fig. 10. Measurement point locations along the skull can be found in appendix 1.

When the von Mises stress values were measured along the middle line of the skull in ventral view (Fig. 11A, B; measurement point locations along the skull can be found in appendix 2), it produced a graph that clearly displayed the stress distribution pattern of the skull model for both intrinsic bite scenarios (Fig. 14). This gives further evidence from the von Mises contour plots that the main differences in stress patterns are located at the dorsal side of the skull. The stress distribution pattern for the two intrinsic scenarios in ventral view displayed nearly identical results along the whole skull, this also can be observed in the von Mises contour plot of the skull in ventral view (Fig. 11A, B). Although minimal, higher stress magnitudes in the ventral view of the skull were observed during the FBS compared to for the BBS. High stress magnitudes were observed for both the scenarios at the anterior and posterior ends of the skull. As shown in the stress distribution graph in dorsal view (Fig. 13), the highest stresses experienced by the skull model during both bite

simulations were observed at the very most posterior end (Fig. 14). However, the lowest stress magnitude during the two scenarios was also observed at the measurement point just before the posterior end point.

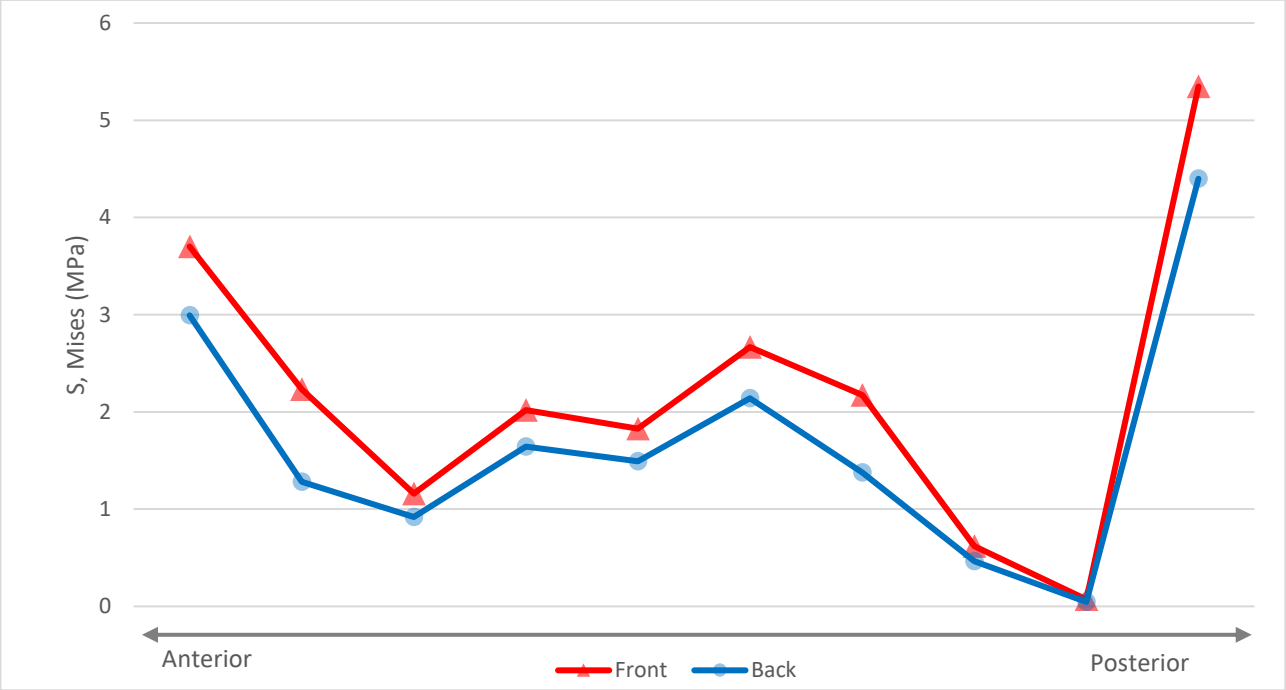

Fig. 14. Von Mises stress magnitudes (MPa) of the *Saurosuchus galilei* skull model (PVSJ 32) at 10 measurement locations along the ventral surface for two intrinsic bite scenarios – bilateral front bite scenario (red triangles); bilateral back bite scenario (blue circles). Same von Mises stress limits as for Fig. 12. Measurement point locations along the skull can be found in appendix 2.

3.3 Deformation

There were many similarities and differences for the deformation of the cranium during the two intrinsic bite scenarios (Fig. 15). Regardless of the bite scenario, the whole skull rotated dorsally with the centre of rotation being located at the median-posterior section of the skull, specifically at the frontal and parietal bones. This can be observed by the high levels of compressive, shear stresses and strains in this region of the skull model. Considerable deformation

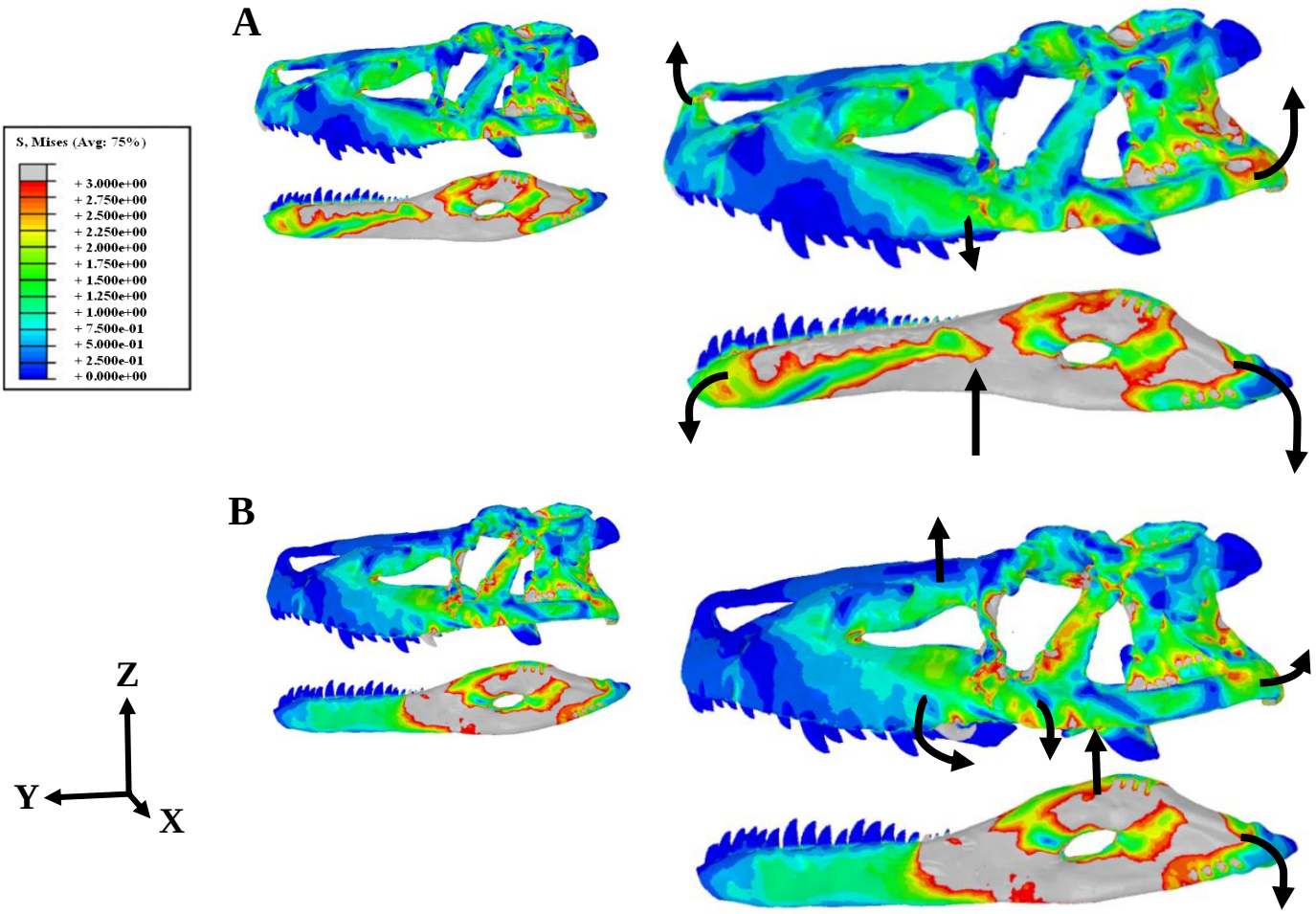

Fig. 15. Von Mises stress contour plots with the addition of the deformation plots from finite elements analysis (FEA) of the *Saurosuchus galilei* digital model (PVSJ 32) for two intrinsic bite scenarios in left lateral view, with blue denoting the lowest magnitude of stress experienced and grey displaying the highest. The muscle-driven bite scenarios: (**A**) bilateral front bite for skull and mandible, undeformed model on the left and deformed on the right; (**B**) bilateral back bite for skull and mandible, undeformed model on the left and deformed on the right. The thick black arrows on models indicate the direction of deformation, size of arrow indicates the magnitude of deformation. Units for von Mises stress plots = MPa.

was observed for the constrained teeth. However, no deformation was observed for all the other teeth in the jaw. For both bite simulations, there was deformation ventrally in the median section of the skull (especially on the pterygoid where the m. PTd attaches), this deformation was more noticeable during the BBS around the location of the maxillary tooth that the load was applied to (Fig. 15B). There was considerable deformation dorsally for the posterior section of the skull

(onwards from the posterior margin of the orbital fenestra). However, this deformation was noticeably more severe during the FBS (Fig. 15A) compared to for the BBS (Fig. 15B). During the FBS, the snout (defined here as the area from the anterior rostrum to the posterior margin of the antorbital fenestra) was deformed dorsally around the premaxilla-nasal suture and shifts caudally about a transverse axis, to be approximately level with the nasofrontal suture (Fig. 15A). Contrastingly, during the BBS the rostrum was deformed dorsally about the nasofrontal contact (Fig. 15B).

3.4 *Allosaurus* Comparison

For the *Saurosuchus* and *Allosaurus* comparisons, the pattern of stress distribution in the profile models indicated very similar results (Fig. 16). They both indicated the main differences in stress distribution at anterior section of the skull and mandible models for the two intrinsic bite scenarios. The shared stress hotspots include: the quadratojugal; quadrate; and the regions around the antorbital and orbital fenestra – posterior margin of the maxilla, lacrimal, jugal, and postorbital. The stress magnitudes were quite similar in most regions of the respective models but were slightly less for *Allosaurus*. For the *Saurosuchus* model, the estimate bite force was 1,015 N FBS and 1,885 N BBS for the skull and 1,087 N FBS and 1,920 N BBS for the mandible (Fig. 9). Whereas for the *Allosaurus* model, the estimated bite force was 1,796 N FBS and 3,472 N BBS for the skull and 3,230 N FBS and 4,036 N BBS for the mandible. The stress distribution was more homogenously displayed for *Saurosuchus* compared to *Allosaurus,* where the high stresses were more concentrated in certain regions. The majority of differences were observed in the median section of the skulls of

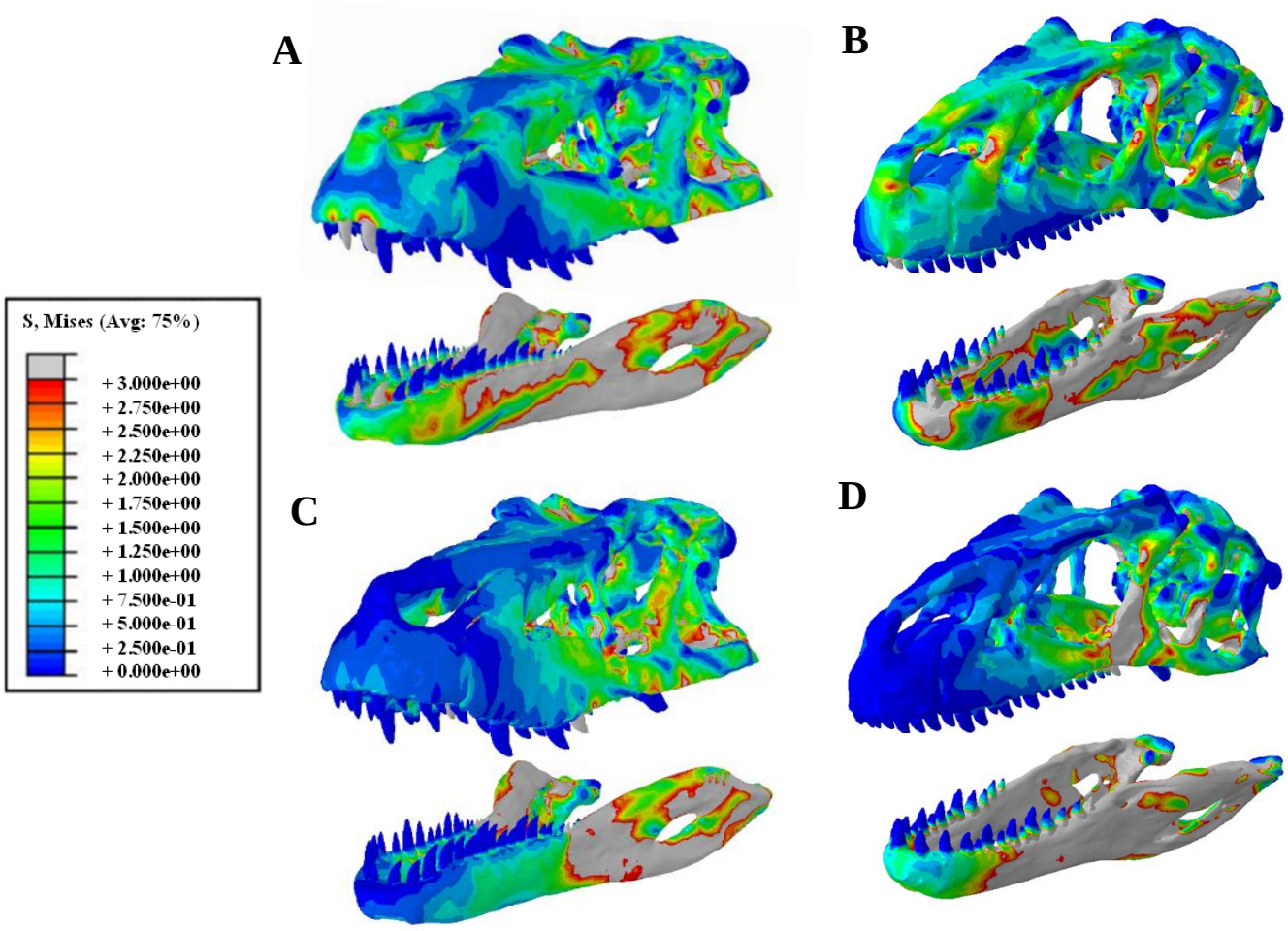

Fig. 16. Von Mises stress contour plots from finite element analysis (FEA), with blue denoting the lowest magnitude of stress experienced and grey displaying the highest. The comparison of scaled models of *Saurosuchus galilei* and *Allosaurus fragilis* during two muscle-driven bite scenarios: (**A**) bilateral front bite scenario for *Saurosuchus*; (**B**) unilateral front bite scenario for *Allosaurus*; (**C**) bilateral back bite scenario for *Saurosuchus*; (**D**) unilateral back bite scenario for *Allosaurus*. Units for von Mises stress = MPa.

Saurosuchus and *Allosaurus*. For example, the postorbital and the quadratojugal indicated higher stresses for *Saurosuchus* during both bite scenarios (Fig 16A, C). Another contrast was observed in the dorsal view of the frontoparietal, which displayed significantly higher stresses for *Saurosuchus*. Albeit with these two observations, the general pattern of stress distribution indicated similar stress magnitudes and patterns at the most anterior and posterior ends of the two skulls, and higher stresses experienced in the median region of the skull for *Allosaurus*. However, the *Allosaurus* model indicated large stress hotspots during the FBS in the anterior section of the skull (Fig. 16A,

B) compared to the *Saurosuchus* model. The *Allosaurus* model displayed a stress hotspot on the anterior margin of the premaxilla and on the posterior premaxillary notch connecting to the nasal body (Fig. 16B). This was also the case in the anterior section of the nasal and posterior margin of the maxilla touching the antorbital fenestra for the *Allosaurus* model during the FBS. A very large stress hotspot was observed for the jugal-lacrimal and jugal-postorbital articular connection with the *Allosaurus* model during the BBS (Fig. 16D). *Saurosuchus* experienced considerably less stress in this region during the BBS compared to *Allosaurus* (Fig. 16C). The stress pattern for the teeth displayed almost identical results for both *Saurosuchus* and *Allosaurus*. For the mandible, *Allosaurus* indicated a similar pattern during both bite scenarios. However, it displayed slightly higher stress magnitudes in the mandible compared to *Saurosuchus*, especially in the anterior region during the BBS .

CHAPTER IV
DISCUSSION

The *Saurosuchus galilei* digital reconstruction (see Fig. 6 for digital reconstruction) presented here indicates a mechanically strong and relatively high stress resistant skull, which was well adapted for the killing of prey. The reconstructed model highlights many characters as morphological convergences between hypercarnivorous pseudosuchians (in this case: a rauisuchian) and theropod dinosaurs. For example, a large cranium; dorsoventrally high skull; mediolaterally narrow, structured skull roof; enlarged orbits; shorter preorbital skull length; and large robust ziphodont dentition (Sill, 1974; Alcober, 2000). When comparing *Saurosuchus* with some hypercarnivorous theropod dinosaurs (e.g., *Allosaurus fragilis, Tyrannosaurus rex, Teratophoneus curriei,* etc.) there are many similarities in the morphological structure of the cranium, and in the von Mises stress distribution patterns of the skull (Fig. 16). However, I also identified some major differences which lie closer to extant crocodilians (e.g., *Alligator mississippiensis*), especially when further exploring the feeding behaviours from the analysis of the stress and deformation of the skull during the two intrinsic bite simulations. Among all the extant tetrapods, pseudosuchians, in the form of the extant crocodilians, exhibit the largest bite forces observed (Erickson *et al.*, 2003, 2012). Consistent with previous biomechanical studies (McHenry *et al.*, 2006; Walmsley *et al.*, 2013; Montefeltro *et al.*, 2020; Bestwick *et al.*, 2021), the results shown here indicate that hypercarnivorous pseudosuchian skulls, *Saurosuchus* in this case, are well adapted to resist high feeding-generated forces, particularly when biting at the posterior end of the jaw. These advanced cranial adaptations that grant this capacity enabled many pseudosuchian reptiles to occupy apex predator niches in terrestrial and semi-aquatic ecosystems from the Mesozoic to modern times (Montefeltro *et al.*, 2020; Somaweera *et al.*, 2020; Bestwick *et al.*, 2021).

4.1 Possible Feeding Behaviours

As suggested in previous research, the morphological and functional evidence presented here indicates that *Saurosuchus* was most likely adapted for hypercarnivory (Sill, 1974; Alcober, 2000; Heckert *et al.*, 2002; Irmis, 2005; Weishampel *et al.*, 2007; Nesbitt, 2011; Trotteyn *et al.*, 2011; Martínez *et al.*, 2013; Nesbitt *et al.*, 2013; Wallace, 2018). One of these morphological adaptations for its hypercarnivorous diet is a large and highly competent skull. Many previous studies have stated that these large skulls exhibited by apex predators throughout the Mesozoic Era are deemed to be a convergent adaptation for a hypercarnivorous diet (Chatterjee, 1985; Nesbitt *et al.*, 2013; Butler *et al.*, 2019; Ezcurra *et al.*, 2021; Bestwick *et al.*, 2022). A recent study found similarities in the skull-femur ratio between rauisuchians and theropod dinosaurs, displaying a clear convergence between the two groups of distantly related archosauromorph carnivores (Bestwick *et al*., 2022). The relatively low stresses displayed indicate that *Saurosuchus* had a somewhat robust cranium that was adapted for handling struggling prey, which was possibly subdued by the infliction of a series of bites using large ziphodont posterior maxillary and dentary teeth, suggested to be very similar to theropod teeth (Renesto *et al.*, 2003), which could easily pierce the skin of their prey. Although there is a lack of direct evidence, *Saurosuchus* would have likely had similar hunting behaviour to what is observed in extant apex predators with the use of head movements to worsen wounds made with their teeth, ultimately allowing a quick death of the prey. The von Mises stress contour plots displayed very low stress magnitudes for the teeth, and the regions around the teeth, in both the skull and mandible model (with the exception of the teeth where the load was applied). It is known that ziphodont dentition (serrated, blade-shaped teeth) supports individual denticles and can dissipate the stresses associated with feeding when carrying out a biting behaviour. These serrations were previously thought to be unique to theropod dinosaurs, however, this adaptation has been

observed in many hypercarnivorous predators from modern times to the teeth of Permian gorgonopsian synapsids (Whitney *et al.*, 2020). The presence of large robust ziphodont dentition in *Saurosuchus* is a good indicator of its role as an apex predator of the Triassic (Riff and Kellner, 2011; Godoy *et al.*, 2014). These large labiolingually compressed, distally curved, serrated knife-like teeth observed are a dental adaptation optimal for defleshing vertebrate carcasses (D´Amore, 2009). Although varying in attributes among different taxa, this structure has independently evolved in a series of unrelated apex predators, including the majority of Pseudosuchia including basal forms (e.g., heterodont phytosaurs and rauisuchians), large monitor lizards, and theropod dinosaurs (D'Amore & Blumensehine, 2009; D'Amore *et al.*, 2011; Brink and Reisz, 2014; Torices *et al.*, 2018).

The estimated bite force and stress distribution indicated that it would have been more advantageous for *Saurosuchus* to bite at the posterior end of the jaw rather than the anterior end (Fig. 9-12). The dorsal margin of the frontal interestingly displayed low levels of stress for both bite scenarios, which could be the advantage of the unique frontal thickening present in *Saurosuchus*, allowing the lowering of stress and deformation (shear and compression) on the frontal where some of the main forces are applied in the skull when biting (Alcober, 2000). Some of the highest von Mises stress experienced on the *Saurosuchus* skull during both simulated bites were located in the posterior and median sections of the skull, especially the interfenestral bars and other regions around the openings in the skull (antorbital fenestra, orbit, and lower temporal fenestra), with the exception of the subnarial fenestra. The interfenestral bars in particular experience some of the highest magnitudes of stress. This high stress experienced in these regions has often been seen in theropod dinosaurs. For example, Rayfield (2005) indicated that the areas around the antorbital and orbital fenestra experienced high magnitudes of tensile stress for the theropod dinosaurs analysed

(e.g., *Tyrannosaurus rex*, *Allosaurus fragilis*, and *Coelophysis bauri*). These higher stresses observed in the median section of the skull are likely due to the larger orbital fenestra along with extreme forces induced from biting in Tyrannosaurids. It has been proposed that an elevated bite-force comes with an increase in the jaw adductor muscles volume, which originates immediately posterior to the orbit (Henderson, 2003). However, this stress in *Saurosuchus* is lower than most theropod dinosaurs due to the thicker interfenestral bars of bone reducing the width of the orbit creating a stronger skull, which has been indicated to link to less stress and deformation in the stronger-skulled apex predators e.g., *Tyrannosaurus rex* (Molnar, 1998). This similar orbital shape in *Saurosuchus* and other apex theropod dinosaurs with more robust skulls indicates that it has convergently been evolved to be dorsoventrally high and smaller in width in order to keep up with the requirements of the posterior half of the skull, so that it is able to resist the muscle forces generated with prey capture and dismemberment (Henderson, 2003).

The posterior section of the skull for *Saurosuchus* experiences the highest amounts of stress when biting, which is expected as this is where the cranial muscles attachment sites are located causing high forces when biting (Fig. 12C, D). However, the stress distribution indicates nearly identical results for both bite scenarios even with the increased bite force during a bite at the back of the jaw. This once again suggests the most advantageous area of the jaw to bite for *Saurosuchus* is towards the posterior end of the jaw. Large stress hotspots can also be observed in the jugal and quadratojugal body for both intrinsic bite scenarios of the *Saurosuchus* skull (Fig. 9). However, it is important to note that the connecting margins of the jugal and quadratojugal were missing from the skull specimen –PVSJ 32 (Fig. 4), so was therefore digitally reconstructed from a plastic substitute as a template. Furthermore, this substitute and reconstruction was only an estimate, and so whether

this section was thicker or thinner in width is unknown. This could slightly affect the amount of stress and strain that was experienced for the jugal and quadratojugal during the two bite simulations. This is likewise for the mandible and teeth in this digital reconstruction, which was reconstructed using an *Allosaurus fragilis* mandible model and a generic archosaur tooth as a basis, along with the template of the reconstructed *Saurosuchus galilei* cranium carried out by Alcober (2000). However, contrary to the reconstruction in Alcober (2000), the teeth here were reconstructed to have the larger, more robust teeth at the back of the jaw where, similar to extant crocodilians, *Saurosuchus* would have preferred to bite its prey. The presence of relatively stress-free regions around the teeth in both the skull and mandible model during both simulations indicates the highly structured craniomandibular architecture that could most likely perform in much higher stress conditions than what was imposed during the scenarios using only muscle-driven biting forces (Fig. 9-12). The presence of these highly structured overengineered regions has also been displayed in theropod dinosaurs, such as *Allosaurus*, (Fig. 16), and has been used as evidence that these taxa used mechanisms to enhance killing potential in their regular feeding strategy (Rayfield *et al.*, 2001). The high stresses experienced in the back of the skull again looks very similar to a that in many carnivorous theropod dinosaurs. Although *Saurosuchus* indicates a preference for a more posterior bite similar to that in extant crocodilians, it has been observed in previous biomechanical modelling research that extant crocodilians experience minimal stresses at the back of the skull when biting. (e.g., Sellers *et al.*, 2017; Bestwick *et al.*, 2021). This similarity of high stresses in the posterior region of the skull for *Saurosuchus* and theropods could be due to the similar convergently evolved morphological structure of their skulls, especially in the posterior most margin.

Although expected given the nature of vertical bite forces and the constraining points anchoring the rear of the skull, the *Saurosuchus* skull is bent so that it is ventrally tensed and dorsally compressed (Fig. 15). There is considerable deformation observed on the *Saurosuchus* model during the FBS (Fig. 15A), compared to the BBS (Fig. 15B). This further gives evidence for a more favoured posterior bite by *Saurosuchus* for an efficient feeding strategy. Although *Saurosuchus* shares many anatomical features to predatory theropod dinosaurs, they ultimately lie closer to extant crocodilians when it comes to the feeding behaviour. It is important to note that when reviewing these results, the fossilised specimen (PVSJ 32) used in this reconstruction shows indications of being a juvenile. This can be seen by the poor ossification of the quadrate, particularly in the articular end (Alcober, 2000). It has a subnarial fenestra between the premaxilla and maxilla, that has been observed in the skulls of previous pseudosuchian juveniles (Krebs, 1976). This immaturity is also indicated in the braincase; with the disarticulation from the skull, and the basioccipital and exoccipital showing an open suture between them (Alcober, 2000). The fact that the specimen used was a juvenile had mixed impacts on the FEA results. Low stresses and deformation were displayed in parts of the maxillae and premaxillae surrounding the subnarial fenestrae compared to the other parts of the bone. This indicates that the fenestrae had little impact on the biting behaviour during the FBS. In contrast, due to the constraints placed on the occipital condyle, the impact of the open suture in the braincase is difficult to determine. From previous research on the ontogenetic series of *Prestosuchus chiniquensis* (Fig. 3B), it is clear that these sutures would most likely reduce or close completely when skeletal maturity is reached by *Saurosuchus* (Alcober, 2000; Lacerda *et al.*, 2016). It would also be likely that parts of the cranium, such as the lacrimal and jugal, would thicken more. These slight changes would lower the stress and deformation in the cranium, and therefore would increase the bite force.

4.2 Biomechanical Modelling Comparisons

The bite force estimated for *Saurosuchus* (1,015 N during the FBS and 1,885 N during the BBS for the skull, and 1,087 N during the FBS and 1,920 N during the BBS for the mandible; Fig. 9) demonstrates a weak bite for an animal of its size, that is similar to and/or weaker than extant crocodilians. For example, *Alligator sinensis* can have a bite of up to 963 N (measured at the caniniform tooth) which is similar to *Saurosuchus* (Montefeltro *et al.*, 2020). However, this bite force is considerably weaker than apex theropod dinosaurs from the Jurassic and Cretaceous, which could potentially exceed 50,000 N (Gignac and Erickson, 2017). Previous research on extinct crocodylomorphs estimated bite forces from equations based on extant crocodilian regression data (e.g., Aureliano *et al.*, 2015). However, these equations do not consider the variation of cranial architecture that can be observed in more distantly related taxa, such as rauisuchians (Fig. 3), like *Saurosuchus* (Fig. 4). Here, the *Saurosuchus* bite force estimates were calculated from the FEA. These estimates vary when using the skull or the mandible, indicating higher bite force estimates for the mandible models (Fig. 9). However, this is not surprising since the skull has increased constraints compared to the mandible due to a more complex architecture and geometry (Montefeltro *et al.*, 2020). Furthermore, previous studies have shown realistic mandible bite force estimates using this technique (Porro *et al.*, 2011; Montefeltro *et al.*, 2020; Bestwick *et al.*, 2021). Porro *et al.* (2011), found that although including sutures in finite element models affected the stress and strain distributions in the mandible (*Alligator*), reaction forces including bite force were not considerably affected. Therefore, the bite forces estimated for the *Saurosuchus* model were likely not affected although the sutures were not included.

As previously stated, the *Saurosuchus* specimen modelled was a juvenile and means that the stress and strain magnitudes are likely to be lower than if it were an adult specimen, this is shown in a ontogenetic-based study on tyrannosaurids by Rowe and Snively (2022). Both the *T. rex* and the *Alligator mississippiensis* have been shown to undergo considerable transformations in morphology that creates substantial differences in cranial stresses and strains (Gignac, 2010; Johnson-Ransom *et al.*, 2021; Rowe & Snively, 2022). Juveniles most likely fed on smaller prey compared to the adults, fulfilling different predatory ecological roles. Due to dietary changes, an animal's size may increase, this increase causes dramatic morphological ontogeny transitions, affecting their prey size, bite force and therefore the cranium stress distribution. For example, an adult *Tyrannosaurus* can have an average bite force of 16,352–31,284 N (LACM 23844; Gignac & Erickson, 2017) during a front bite, whereas the bite force in a juvenile has been observed to be around 1,430–3,850 N (BMRP 2002.4.1; Bates & Falkingham, 2012; Johnson-Ransom *et al.*, 2021). This highlights the considerable differences between an adult and a juvenile cranium. The bite force of the juvenile *Tyrannosaurus* is very similar to the bite force estimate during the FBS discovered for the juvenile *Saurosuchus* in the results displayed here (1,051 N). Since the juvenile *Saurosuchus* bite force estimated is similar to that of a *Tyrannosaurus* juvenile, this suggests that an adult *Saurosuchus* could possibly have a significantly higher bite force. However, histological examinations of PVSJ 32 have inferred that the *Saurosuchus* specimen did not have much more to grow (Cerda *et al.*, 2013). Therefore, representative inferences on the functional behaviours of both *Saurosuchus* and rauisuchians can be made from the specimen PVSJ 32 used in this study.

Table 2. Specimens for FEA, for including mandibular ramus lengths in cm, and calculated muscle force in N. *Tyrannosaurus rex, Albertosaurus sarcophagus, Allosaurus fragilis, Sinraptor dongi, Yangchuanosaurus shangyouensis, Ceratosaurus nasicornis, Gorgosaurus libratus,* and *Dilophosaurus wetherelli* from Rowe and Snively, (2022); *Alligator mississippiensis* from Sellers *et al.*, (2017); *Baurusuchus pachecoi* from Montefeltro *et al.*, (2020).

Taxon	Specimen	Length (cm)	F_{muscle} (N)
Adult *Tyrannosaurus rex*	LACM 23845	88.0	32,625.8
Albertosaurus sarcophagus	TMP 81.10.1	92.2	29,387.6
Juvenile *Tyrannosaurus rex*	BMRP 2002.4.1	72.0	14,065.1
Allosaurus fragilis	UUVP 6000	88.3	8,322.6
Sinraptor dongi	IVPP 10600	87.6	8,024.5
Saurosuchus galilei	**PVSJ 32**	**72.0**	**7,172.9**
Yangchuanosaurus shangyouensis	CV 00215	81.0	7,004.6
Ceratosaurus nasicornis	USNM 4735	59.6	6,343.2
Gorgosaurus libratus	TMP 91.36.500	70.6	4,711.8
Alligator mississippiensis	AL 008	45.4	3,520.0
Dilophosaurus wetherelli	UCMP 37302	59.7	3,306.7
Baurusuchus pachecoi	LPRP/USP 0697	30.2	3,193.8

When comparing the total muscle force (F_{muscle}) produced by *Saurosuchus* to other similarly sized carnivorous archosaurs, it indicates its place as one of the apex predators. Respectively to its cranium length, it has a very high total muscle force estimated. However, it is still quite small in comparison to the top theropod dinosaur predators such as *Tyrannosaurus rex* and *Albertosaurus sarcophagus* (Table 2). On the other hand, *Saurosuchus* has a total muscle force similar to that of many theropod dinosaur predators such as *Allosaurus fragilis*, *Sinraptor dongi*, *Yangchuanosaurus shangyouensis*, and *Ceratosaurus nasicornis*. *Saurosuchus* (PVSJ 32) has a bite force to muscle force ratio of 14.7% which is similar again to the juvenile *T. rex* (BMRP 2002.4.1) that has a ratio of ~17%, whereas an adult *T. rex* (LACM 23844) has a much larger ratio of ~50%. An adult *Allosaurus* has a ratio of ~25% (MOR 693; Therrien *et al.*, 2005), this suggests that an adult

Saurosuchus may have had a higher percentage ratio of bite force to muscle force than many of the carnivorous theropod dinosaurs that are similar in size to *Allosaurus*. Furthermore, *Baurusuchus pachecoi* a large, terrestrial crocodyliform displays a much lower ratio of 7.9% (LPRP/USP 0697; Montefeltro *et al*., 2020), and the extant *Alligator mississippiensis* (AL 008; Sellers *et al*., 2017) displays a ratio of ~6.1%.

The von Mises stress distribution comparison indicates that *Saurosuchus* could have had a similar functional behaviour to that of *Allosaurus fragilis* (Fig, 16). *Allosaurus* is one of the most well-known theropods from North America of the Jurassic Period (Chure & Loewen, 2020). *Allosaurus* was chosen as the theropod comparison for *Saurosuchus* in this thesis due to the availability of high-quality, three-dimensional scans, but also *Allosaurus* is generally a stereotypical large theropod, so the comparisons will be very similar to many other post-Triassic theropods. A contemporaneous theropod from the Triassic would have been the most ideal for comparison, however, their fossils are poorly preserved, and no digital models currently exist at the time of writing. The complete MOR 693 *Allosaurus fragilis* skull was also modelled due to its similar size to the PVSJ 32 *Saurosuchus galilei* (61 cm and 72 cm respectively). The many similarities when comparing the von Mises stress distribution contour plots of *Saurosuchus* and *Allosaurus* indicates the morphological convergence in predatory archosaurs that share similar niches (Fig. 16). Although the comparison between the *Saurosuchus* and *Allosaurus* models was using different bite scenarios (bilateral and unilateral respectively), *Allosaurus* has previously indicated a similar von Mises stress values when carrying out both a bilateral and unilateral bite (Rayfield, 2005). The similar stress distributions displayed by *Saurosuchus* and *Allosaurus* indicates that there is a certain degree of convergence in functional behaviour. This suggests that *Saurosuchus* had a somewhat strong cranium which could handle strong magnitudes of loads applied to the skull. When exploring

the deformation of the *Allosaurus* model it displays shifting of the snout dorsally during the FBS and shifting of the snout ventrally during the BBS, suggesting that there is a region in the tooth row somewhere between these two bite scenarios where a vertical bite produces neither dorsal nor ventral deformation at the snout. These results are supported in previous studies, and therefore this region, instead of the front of the jaw, would have been the most advantageous place to bite for *Allosaurus* (Rayfield, 2005). This preference in a more central bite for *Allosaurus* is also similar to *Saurosuchus*. However, *Saurosuchus* experiences slightly more deformation than *Allosaurus*, which indicates that Saurosuchus may have had a mechanically weaker cranium. Overall *Saurosuchus* experiences slightly more stress in the skull compared to *Allosaurus*, particularly in the anterior section. These differences in stress and distribution could be due to *Saurosuchus* having a rectangular shaped cranium when observed in lateral view (Sill, 1974, Alcober, 2000). Whereas, Allosaurus has the ventral maxillae being more concave, with the cranium having rounded anterior and posterior ends (Snively *et al.*, 2013). This could explain the increased stress and deformation in the anterior section of *Saurosuchus* during the FBS. On the other hand, very large stress hotspot can be observed for the jugal-lacrimal and jugal-postorbital interfenestral bars on the *Allosaurus* model during the BBS (Fig. 16D). Interestingly, the *Allosaurus* model indicates some high stress magnitudes in the dorsal rostrum of the skull during the FBS, compared to the *Saurosuchus* model which lacks these stress hotspots (Fig. 16). This is unexpected since all evidence so far has pointed towards theropod dinosaurs having the adaptations for a high stress-resistant front bite. These unexpectedly high stress hotpots in the anterior section of the skull could be the result of the unilateral bite, indicating a bilateral bite would be preferable for *Allosaurus* to spread out the high loads applied to the skull during a strong front bite.

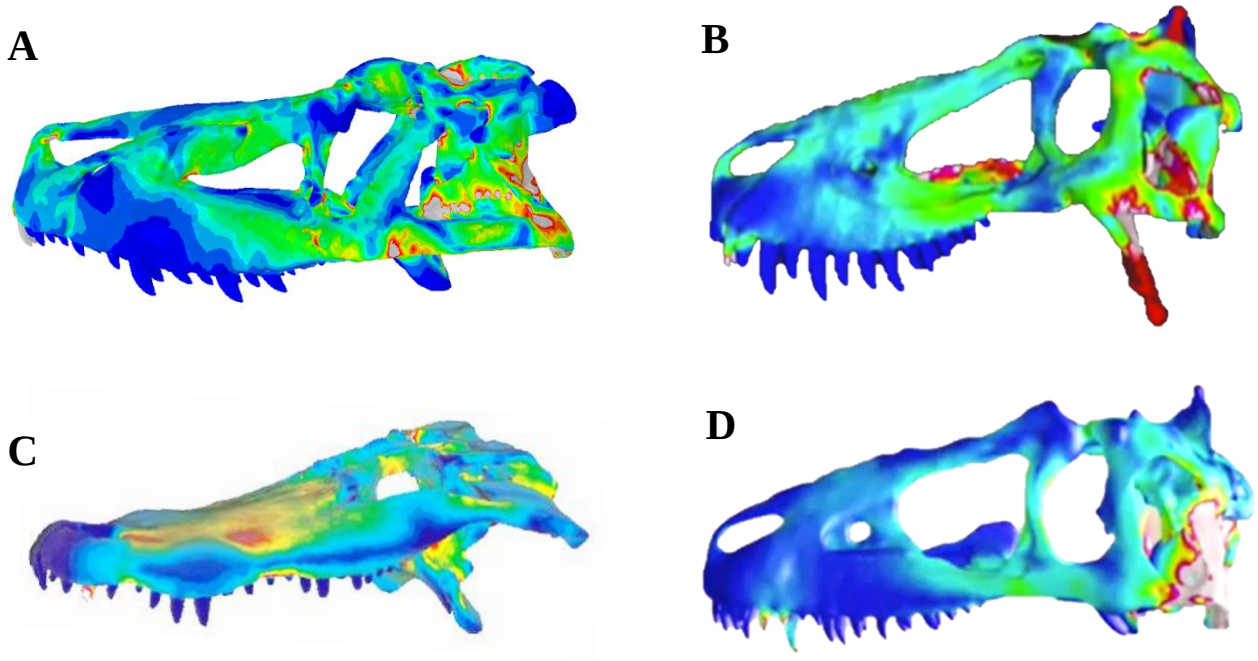

Fig. 17. Von Mises contour stress contour plots from finite element analysis (FEA), with blue denoting the lowest magnitude of stress experienced and grey displaying the highest. The comparison of scaled models during the intrinsic front bite scenario: (**A**) juvenile *Saurosuchus galilei* (PVSJ 32); (**B**) juvenile *Tyrannosaurus rex* (BMRP 2002.4 from Johnson-Ransom *et al.*, 2021); (**C**) adult *Alligator mississippiensis* (AL 008 from Sellers *et al.*, 2017); (**D**) subadult *Teratophoneus curriei* (BYU 8120/9402 from Johnson-Ransom *et al.*, 2021). Models are scaled to maximum stress, but the actual magnitude is not available. Units for von Mises stress = MPa.

The comparison of the mechanical function of taxonomically disparate archosaurs, *Saurosuchus*, *Tyrannosaurus*, and *Teratophoneus*, reveals that all of them distribute biting stresses in a similar but different manner. The similar structure of the lacrimal in *Saurosuchus* and the theropod dinosaurs indicates counteracting properties to high magnitude stresses. Interestingly, when comparing the *Saurosuchus* model to an adult *Tyrannosaurus rex* FEA model (USNM 555000 from Johnson-Ransom *et al.*, 2021) the stress distribution differs greatly. The *Tyrannosaurus* model indicates relatively low von Mises stress around the whole skull, with the areas of higher stresses being located at the posterior end of the skull (particularly the parietal, quadrate, and the ventral projection of pterygoid and ectopterygoid). However, like with the bite force, when comparing the stress distribution of *Saurosuchus* model with the juvenile

Tyrannosaurus, it displays extremely similar results (Fig. 17A & B). The similarities in the stress distribution are likely due to the similar skull structure. For example, similar to *Tyrannosaurus, Saurosuchus* possesses an extremely robust, transversely expanded cranium with stout interfenestral bars that encroach into the orbit (Rayfield, 2005). Nearly identical stress magnitudes in the median section of the skull – e.g., maxilla, lacrimal and jugal, are likely due to the triangular-shaped antorbital fenestra that *Saurosuchus* and *Tyrannosaurus* share. This suggests that this shape of antorbital fenestra is advantageous for a terrestrial, hypercarnivorous predator that needs to withstand strong feeding-generated forces on the skull when tearing through flesh and bone. Compared to extant crocodilians, such as *Alligator mississippiensis* (Fig. 17C), *Saurosuchus* experiences fairly high stresses at the posterior end of the skull when biting both from the front and back of the jaw. Although not as extreme, this is similar to the theropod dinosaurs, indicating that *Saurosuchus* would have preferred to bite around the posterior end of the jaw, but may not have bitten as far back as observed in extant crocodilians.

Despite these stress distribution similarities, there are some major differences in how the skull contains stress in specific regions of the skull. The most obvious difference can be observed in the nasal body. The variation in stress and in the location of high compression and shear in the skulls may be due to this differing nasal morphology in extant crocodilians – *Alligator*, a rauisuchian – *Saurosuchus*, and the theropod dinosaurs – *Teratophoneus* and *Tyrannosaurus* (Fig. 17). During the FBS, the theropod dinosaurs indicate lower von Mises stress magnitudes in the anterior region (snout) compared to *Saurosuchus* and *Alligator*, with *Alligator* having very high stresses in the dorsal margin of the nasal and *Saurosuchus* having moderately high stresses in the premaxilla and nasal. Bestwick *et al.* (2021) conducted FEA contour plot comparisons between a rauisuchian (*Effigia*) and an extant crocodilian (*Alligator*), with clear morphological and functional

similarities/differences indicated. Although not as significant in *Saurosuchus* since it has a skull morphologically convergent to those of theropod dinosaurs, the anterior bite simulation highlights the nasal bridge as mechanically weak, which can also be observed in *Alligator* and other rauisuchians (e.g., *Effigia* in Bestwick *et al.*, 2021). However, it has been suggested in previous research that many crocodilians mitigated the stresses in this area by using unilateral bites instead of the classic bilateral bite (Erickson *et al.*, 2012; Montefeltro *et al.*, 2020). *Saurosuchus* could have also carried out this behaviour, along with only biting the softer parts of its prey. The higher von Mises stress is concentrated at the posterior region of the skull for the two theropod dinosaurs during a front bite, whereas it is more homogenously spread around the skull in *Saurosuchus* and the extant crocodilians (Fig. 17). These stress distribution patterns observed between *Saurosuchus* and the extant crocodilians along with the similar location of large robust teeth, and bite force estimates, further indicates that the feeding behaviour of biting prey nearer to the back of the jaw is very similar, although morphologically dissimilar and distantly related. The exact feeding behaviour of all these archosaur carnivores seems to differ although all occupying similar apex predatory niches. Extant crocodilians have been indicated by past biomechanical modelling results to prefer biting at the posterior end of the jaw, whereas theropod dinosaurs prefer biting at the anterior end of the jaw The deviations in the stress distribution for the theropod dinosaurs compared to *Saurosuchus* and the extant crocodilians could be attributed to proportional changes and shortenings of certain bones in the skull. For example, the reduction of the prefrontal in theropod dinosaurs could be linked to the strengthening of the skull when biting (Rayfield, 2005). Another adaptation is the shortening of the preorbital skull length, which leads to the shifting of the peak shear to the antorbital fenestra from the frontoparietal. This shortening is stated to be greater in the *Tyrannosaurus* compared to the other theropod dinosaurs analysed (e.g., *Coelophysis bauri* and *Allosaurus fragilis*), which could link to its lower cranium stresses and extreme bite force, and

therefore success as the apex predator in the Cretaceous Period (Rayfield, 2005). This shortening of the preorbital length is greater in *Saurosuchus* compared to the *Alligator*, but less than in the theropod dinosaurs, with high strains still being observed around the frontoparietal region for *Saurosuchus* (Fig. 15) and not around the antorbital fenestra like theropod dinosaurs.

Overall, *Saurosuchus* seems to indicate having both similarities to the extant crocodilians (e.g., *Alligator*; Fig. 17C) and the theropod dinosaurs (e.g., *Allosaurus*, Fig. 16; *Tyrannosaurus* and *Teratophoneus*; Fig. 17B, D), displaying both a partial intermediate for the morphological structures in the cranium and in the stress distribution (Fig. 17A). This suggests that the stress flows do not opportunistically expand into all bony tissue that is available, and therefore the morphology of the cranium dictates the stress distribution only to a certain extent. These similarities and differences in cranial morphology are most likely concomitant with the similar/differing ecological and dietary pressures affecting these distantly related taxa.

4.3 Ecological Convergence

The results successfully characterise the exceptional suite of biomechanical properties displayed by the rauisuchian *Saurosuchus,* which combine novel morphological adaptations as well as features similar to theropod dinosaurs and others seen in extant crocodilians. Selective pressures from extrinsic environmental factors are suggested by many to exert an important influence during the amniote functional and biomechanical evolution (Sakamoto *et al.*, 2019). In the case of *Saurosuchus*, the palaeoenvironment of the Ischigualasto Formation of Argentina was a volcanically active floodplain covered with forests and often subject to strong seasonal rainfalls (Tucker & Benton, 1982). It is commonly suggested that the climate was moist and warm during the majority of the Triassic, permitting life to flourish (Tucker & Benton, 1982). These landmasses witnessed an extraordinary diversity of archosaurian reptiles which resulted in a diverse array of potential prey for *Saurosuchus* among terrestrial tetrapods, including non-dinosaurian dinosauromorphs, sauropodomorphs, theropods, herbivorous therapsids, rhynchosaurs, and dicynodonts (Zerfass *et al.*, 2004; Langer *et al.*, 2007; Tolchard *et al.*, 2019). This indicates that prey selection could have played an important role in the evolution of the *Saurosuchus* craniomandibular apparatus. For example, *Saurosuchus* has been found to be sympatric with herbivorous therapsids, rhynchosaurs, dinosauromorphs and dicynodonts (Zerfass *et al.*, 2004; Langer *et al.*, 2007). Most of these archosaurian taxa that *Saurosuchus* preyed upon had short, strong, barrel-shaped bodies with strong limbs, and could sometimes reach up to sizes equivalent to modern elephants. This would require *Saurosuchus* to adapt a large, highly robust skull with ziphodont dentition in order to easily slice through flesh and bone, and resist the stresses produced from the feeding-generated forces produced from biting into their prey. Many of these preyed upon taxa have morphology that suggests slower locomotion, this would of allowed Saurosuchus to

"strike and slash" them in order for a quick death. It is also likely due to the mechanical weaker anterior region of the *Saurosuchus* cranium, that it would have only consumed the soft fleshy parts of the carcass, similar to allosaurids and differing to tyrannosaurids who carried out osteophagy (consumption of bones). Many of these archosaurian reptile taxa survived the end-Triassic mass extinction event and carried on radiating into the Jurassic. This indicates a possible explanation for the morphological similarities that *Saurosuchus* and the Jurassic and Cretaceous theropod dinosaurs share although being from distantly related groups. In the past, several rauisuchians have been misidentified at first as being theropod dinosaurs because of some remarkable convergences between the two distantly related groups (e.g., Colbert, 1961; Chatterjee, 1985, 1993; Benton, 1986a; Nesbitt & Norell, 2006; Nesbitt, 2007; Brusatte *et al.*, 2009; Bates & Schachner, 2012). Therefore, it seems likely that rauisuchians occupied many ecological niches that were subsequently filled by theropod dinosaurs during the Jurassic and Cretaceous Period (Brusatte *et al.*, 2008). The anatomical features that are displayed on the cranium of *Saurosuchus* are very similar to many hypercarnivorous theropod dinosaurs (e.g., *Tyrannosaurus rex*; Fig. 17B) that emerged during the Jurassic and Cretaceous Period, due to the lack of large hypercarnivorous predators (rauisuchians) following the mass extinction event. This indicates the key characteristics that apex predators convergently evolve due to the dietary and ecological pressures, especially when exploring the craniomandibular architecture.

Many distantly related archosaurs throughout the Mesozoic Era have indicated hypercarnivorous niches (a diet comprising > 70% meat) (Holliday & Steppan, 2004). During the Early Triassic, this niche is suggested to have been occupied by the quadrupedal erythrosuchids, which are characterised by the large subrectangular profile of their skulls (Butler *et al*., 2019; Ezcurra *et al*., 2020, 2021; Maidment *et al.*, 2020). However, by the Middle-Late Triassic, the rauisuchians replaced the erythrosuchids as the apex predators. Into the Jurassic Period, multiple groups of

theropod dinosaurs are suggested to take this position as the apex predator, and their reign continued into the Cretaceous Period (Therrien & Henderson, 2007; Brusatte *et al.*, 2012; Novas *et al.*, 2013; Hendrickx & Mateus, 2014). For example, the megalosaurids were the apex predators at the start of the Cretaceous and eventually they were later replaced with the abelisaurids and tyrannosaurids (seen in Table 2) (Therrien & Henderson, 2007; Brusatte *et al*., 2012; Novas *et al*., 2013; Hendrickx & Mateus, 2014).

Although most archosaurian apex predators share similar morphological features in their cranium, their feeding behaviour/strategy has been indicated to greatly differ (Rayfield, 2005; Porro *et al.*, 2011; Sellers *et al.*, 2017; Montefeltro *et al.*, 2020; Bestwick *et al.*, 2021; Rowe & Snively, 2022). The FEA stress contour plots investigated in this study demonstrate that *Saurosuchus*, although morphologically similar to theropod dinosaurs, has a preferred biting point located around the posterior end of the jaw, differing from the usual front bite that the apex theropod dinosaurs such as *Tyrannosaurus rex* utilised. Interestingly, although morphologically very different in appearance, this certain feeding strategy is instead seen in extant crocodilians. Extant crocodilians have evolved dorsoventrally flattened skulls, this adaptation is widely regarded to have occurred due to the change to a semi-aquatic lifestyle (McHenry *et al.*, 2006; Grigg & Kirshner, 2015). The extension of the pterygoid flanges provides the adductor muscles larger attachment sites (Holliday *et al.*, 2013, 2015; Sellers *et al.*, 2017). Like extant crocodilians, many extinct archosaurs, such as the semiaquatic rauisuchian *Qianosuchus mixtus* (Li *et al.*, 2006), have evolved an elongated, narrow rostrum which is associated with having a diet that comprises of a higher proportion of fish (Cuff & Rayfield, 2013). *Saurosuchus* on the other hand, has a mediolaterally wide and dorsoventrally high snout similar to that of terrestrial theropod dinosaurs, indicating that *Saurosuchus* would have had a diet of similarly larger prey. However, since extant crocodilians

have evolved semi-aquatic morphology including the post-cranial adaptations, such as reduced limbs and a stream-line cylindrical body, this allowed them to acquire an advantageous twisting-feeding behaviour, often called the "death roll" (Fish *et al.*, 2007). This behaviour where the spinning causes large/tough prey to become manageable pieces, allows extant crocodilians to consume much larger prey (Cuff & Rayfield, 2013). This behaviour imparts a shear force which causes the rostrum to be subject to large torsional loading, however, previous research has shown that the cranium of extant crocodilians, such as *Alligator mississippiensis*, are resistance to such loads (Erickson *et al.*, 2003; Fish *et al.*, 2007; Cuff & Rayfield, 2013). Differing to crocodilians, theropod dinosaur fossils have displayed S-shaped necks that allow them to carry their heads high, this characteristic is observed in extant birds which allows them to efficiently strike down and forwards, and then quickly pull up and backwards (Snively *et al.*, 2013). This indicates that theropod dinosaurs may have been able to also carry out this feeding behaviour, although it has been indicated that some apex theropods, like *Tyrannosaurus rex*, could also use rapid sideways movements of the head to dismember its prey (Snively & Russell, 2007; Witmer & Ridgely, 2009). *Saurosuchus* on the other hand, although indicated to have a morphologically similar cranial structure to theropod dinosaurs and a similar feeding strategy to extant crocodilians where they bit prey in the posterior region of the jaw before swallowing (Cleuren & De Vree, 2000; Labarre *et al.*, 2017), has been suggested to be a terrestrial species with a postcranium morphology closer to that of extant large mammals, with the adaption of an erect quadrupedal gait (Bonaparte, 1984). Therefore, they would have more likely had a shaking-feeding behaviour similar to large carnivorous mammals; based on their erect quadrupedal gait, relatively short robust skulls, and serrated, jagged canines. This dentition would allow the individual to hold onto prey once biting them, and also allows for the efficient tearing of the flesh, tendon and bone. Another possible feeding behaviour that *Saurosuchus* may have employed could be the clamp-and-hold behaviour

often seen in both extant crocodilians and large mammal predators such as lions (*Panthera leo*; Figueiredo *et al.*, 2018). *Saurosuchus* is highly likely to have been able to carry out this feeding behaviour, since it demonstrates the mechanical properties needed with the ziphodont dentition, strong cranial muscles (strong bite force), and high stress-resistant skull.

Rauisuchians were convergent with dinosaurs throughout the whole of the Triassic (Brusatte *et al.*, 2008). *Saurosuchus* inhabited South America alongside many early dinosaurs including *Eoraptor, Herrerasaurus, Chromogisaurus, Panphagia*, and *Sanjuansaurus*, as well as other predators such as *Venaticosuchus* and the chiniquodontids (Weishampel *et al.*, 2007; Martínez *et al.*, 2013). Much more abundant than the carnivorous reptiles were the herbivorous ones, which included rhynchosaurs such as *Hyperodapedon*, aetosaurs, kannemeyeriid dicynodonts such as *Ischigualastia*, and therapsid traversodontids such as *Exaeretodon* (Weishampel *et al.*, 2007; Martínez *et al*., 2013). The diversity of rauisuchian cranial morphology allowed them to prey on wide range of Triassic reptiles, become more diverse and abundant, and subsequently occupy a larger morphospace compared to the early dinosaurs (Brusatte *et al.*, 2008). The two explanations for the eventual success of dinosaurs are that the rauisuchians died out by chance (despite their high abundance and larger morphospace) or dinosaurs acquired one or several key adaptations that aided in their survival of end Triassic mass extinction event (Brusatte *et al*., 2008). However, many palaeontologists agree that this second suggestion is hard to entertain since they lived side by side with the rauisuchians for 30 million years and rauisuchians were the more dominant group for the entirety of that time (Brusatte *et al.*, 2008). Therefore, it is more likely that the theropod dinosaurs became dominant not because they were the better adapted group but were merely beneficiaries of mass extinction events. Due to the end-Triassic mass extinction, the apex predators, rauisuchians

(including *Saurosuchus*), were wiped off the Earth, allowing the theropod dinosaurs to fill these now empty niches, and therefore become more abundant and diverse.

4.4 Future Directions

The FEA model of the *Saurosuchus* cranium presented here incorporates detailed geometry and comprehensive information on muscle architecture and contractile properties. Digital reconstructions and biomechanical modelling methodologies are exponentially increasing in popularity amongst the palaeontology community (Rayfield, 2001, 2005, 2007; Porro *et al.*, 2011; Sellers *et al.*, 2017; Montefeltro *et al.*, 2020; Bestwick *et al.*, 2021; Rowe & Snively, 2022). Analysing fossil specimens with these new advanced technological methodologies is allowing a better understanding of many extinct taxa. The digital approach not only allows the reconstruction/restoration of hard-tissue structures of fossil organisms (plus allowing the visualisation of fragile fossils embedded in hard rock such as limestone e.g, *Qianosuchus mixtus*; Li *et al.*, 2006), but recently also offers the huge potential of soft-tissue reconstructions as well. However, the accuracy of these soft-tissue reconstructions considerably depends on the presence and quality of the preserved hard-tissues of the fossil organism. There are many challenges that one must face when digitally reconstructing a fossilised specimen, such as taphonomic artifacts, pathologies, ontogeny, and intraspecific variation (Lautenschlager, 2017). In addition, the method and quality (e.g., model size, digital artifacts, scan resolution, etc.) of the digital models affects the ability to identify osteological correlates and other necessary information that is required for soft-tissue reconstructions (Lautenschlager, 2017). Therefore, it is recommended for future reconstructions of rauisuchians and other morphologically varied archosaur groups to include the use of both the physical specimen and the corresponding digital representation when carrying out these soft-tissue digital reconstructions. With the ability to physically observe the specimen, it would allow for more reliable location of the muscle attachment sites and therefore a more reliable muscle reconstruction and subsequently more reliable FEA results. Although we now better

understand the *Saurosuchus* cranial anatomy and feeding behaviours, along with morphological convergence with apex hypercarnivorous pseudosuchian reptiles and other distantly related apex archosaurs such as the theropod dinosaurs, there are a lot of questions still yet to be answered. The *Saurosuchus* specimen used in this study was one of the most well-preserved and complete specimens found, however, hopefully future specimens that are found will be even more complete and better preserved. Since the reconstruction of the *Saurosuchus* cranium was done using a prototype tooth and a mandible of an *Allosaurus* specimen, plus with reference to the reconstruction made by Alcober (2000), this means it was open to some interpretation when carrying out the digital reconstruction. If a complete *Saurosuchus* mandible is found, it will allow for a more reliable reconstruction of the mandible, furthermore it will help solidify the results that were produced in this study. Also, carrying out FEA on a fully mature specimen would allow us to explore and compare the maximum bite force and von Mises stress distribution within an adult *Saurosuchus* skull, as shown for *Tyrannosaurus rex* (Johnson-Ramson *et al*., 2021; Rowe & Snively, 2022). Together with the digital cranial endocast of *Prestosuchus chiniquensis* by Mastrantônio *et al.* (2019) and FEA of *Effigia okeeffeae* by Bestwick *et al.* (2021), this is one of the first digital reconstructions and FEA of a rauisuchian cranium. Future digital reconstruction and biomechanical modelling (FEA) on other rauisuchians and archosaurs should be investigated in future research, particularly the ones found near the end-Triassic mass extinction. The end-Triassic mass extinction event was a very important change in the evolutionary history since it was after this event that the theropod dinosaurs became the dominant group in the Jurassic Period. Previous research on the end-Triassic extinction concluded rauisuchians to extend to the end of the Triassic (Benton, 1986b, 1994; Olsen & Sues, 1986). However, there were some notable limitations to these analyses, which include: changes to the stratigraphic intervals for the Triassic Period have occurred (Muttoni *et al.*, 2004; Furin *et al.*, 2006; Mundil *et al.*, 2010); the use of non-monophyletic rauisuchians in the

analyses; and a poor global fossil record for the Late Triassic (Sues & Fraser, 2010). The discovery and study of the latest Triassic rauisuchians is currently a pressing area of future research (Nesbitt *et al.*, 2013). The results found in this study will allow for further comparisons of archosaurian cranial kinesis and feeding behaviours.

A lot of assumptions remain within the interpretation of the results derived from the *Saurosuchus* digital model are dependent on. For example, the model presented only tests the mechanical behaviour of the skull and mandible during a simple bilateral bite from two points in the jaw, front (FBS) and back (BBS). However, as observed in many extant animals, they utilise multiple feeding behaviours. It would be beneficial to test from the FEA using more biting points (e.g., a central bite), unilateral bites, and other bending scenarios (as seen in previous studies such as Rayfield, 2005; Montefeltro *et al.*, 2020; Bestwick *et al.*, 2021). Furthermore, as demonstrated by Porro *et al.* (2011), extant crocodilians have several ways to load their craniums, such as lifting prey, throwing prey, head shaking, and twist feeding. Many recent studies have used FEA to enable the modelling of a wider range of feeding behaviours, such as twisting, shaking and pecking (Rayfield, 2011; Walmsley *et al.*, 2013; McCurry *et al.*, 2015; Bestwick *et al.*, 2021; Taborda *et al.*, 2021). It is possible with the variable cranial morphology seen in rauisuchians that they might have carried out some of these different feeding strategies. However, although *Effigia* is beaked, similar to that of extant avian species, it was concluded that the pecking feeding behaviour in *Effigia* would not have been possible, due to the evidence of high stresses experienced during the pecking simulation (Bestwick *et al.*, 2021). On the other hand, this does makes sense, since crocodilian skulls are akinetic (Sellers *et al.*, 2017), and therefore possess no morphological adaptations to dissipate these stresses when carrying out a pecking behaviour (Bestwick *et al.*, 2021). All these different feeding behaviours induce different forces (orientation and magnitude) on both the skull

and mandible, and therefore produce different stress distribution patterns. The loading regimes applied to the *Saurosuchus* model assumes that all muscles, and all portions of individual muscles, fire simultaneously at maximal strength. However, although incomplete, previous data has shown that extant crocodilian jaw muscles do not behave in this manner (Busbey, 1989; Cleuren *et al*., 1995). Therefore, in future research on *Saurosuchus*, it would be interesting to carry out some of these more complicated loading regimes, to allow for a better understanding of the range of possible feeding behaviours that *Saurosuchus* could have performed. Further on this, here, the gape size was not considered during the bite simulations, however, future analyses could investigate changes in mechanical behaviour with changes in the gape angle for *Saurosuchus.* Previous research on the investigation of the different gape size preferences of theropod dinosaurs (e.g., *Tyrannosaurus rex*, *Allosaurus fragilis* and *Erlikosaurus andrewsi*) has been carried out, which confirmed many prior dietary and ecological assumptions (Lautenschlager, 2015). It indicated that the carnivorous taxa *T. rex* and *A. fragilis* were capable of sustained muscle force and a wide gape, whereas the herbivorous therizinosaurian *E. andrewsi* was constrained to only small gape angles (Lautenschlager, 2015). Given that the results observed in this thesis highlights the hypercarnivory in *Saurosuchus*, the exploration of the gape size could further confirm these findings. Lastly, with the development of multibody dynamics analysis (MDA), post-cranial material can be used as a numerical modelling tool in order to reconstruct the function and palaeobiology of *Saurosuchus* (Lautenschlager, 2020). With comparison to Triassic and Jurassic theropod dinosaurs we can further understand the advantage of a more bipedal locomotion as an apex predator when hunting prey.

CHAPTER V
CONCLUSIONS

This thesis concentrated on the digital reconstruction of the cranium of a juvenile *Saurosuchus* specimen (PVSJ 32). The stress and strain were investigated as the *Saurosuchus* digital model carried out a muscle-driven bite at two points in the jaw – front (FBS) and back (BBS). Constraints simulate the contact points for the teeth as it bites down and faces resistance from the flesh and bone (Rowe & Snively, 2022). Despite all the morphological similarities between the crania of *Saurosuchus galilei* and post-Triassic theropod dinosaurs, several key functional differences were observed between the studied representatives. For an animal of its size *Saurosuchus* had an estimated bite force that was quite weak (1015–1885 N), especially when compared to post-Triassic apex predators (e.g., *Tyrannosaurus rex*). Possessing features such as vomers and pterygoids causes the cranium to be mechanically weak, due to disproportionately influencing the functional behaviours of *Saurosuchus.* It was clear to see that the *Saurosuchus* cranium faces higher levels of stress when biting at the front of the jaw (FBS) compared to when it bit at the back (BBS), this validated the necessity of large, robust posterior teeth, similar to that of extant crocodilians, for the purpose of efficient feeding for *Saurosuchus*. Their large size, ziphodont dentition, and relatively low stress when biting indicates that *Saurosuchus* was indeed a carnivorous apex predator in the Late Triassic. However, their feeding behaviour would have differed greatly to that of apex theropod dinosaurs (e.g., *Teratophoneus curriei*, and *Tyrannosaurus rex*) which predominantly have a strong front bite carrying out osteophagy (Rayfield, 2001, 2004, 2005, 2007; Rowe & Snively, 2022). *Saurosuchus*, in contrast, perhaps fed by defleshing carcasses with its posteriorly-positioned its teeth, while minimising tooth-bone interactions, with osteophagy deemed very unlikely. This showcases previously unappreciated functional disparity between hypothesised Triassic and post-Triassic carnivores.

Overall, here I carried out the first analysis of a digital cranium and biomechanical modelling (FEA) of a juvenile *Saurosuchus galilei*, with the results contrasting with the inferred feeding behaviours of theropods and other rauisuchians. This provides novel insight into the functional diversity of this pseudosuchian group and gives useful information for future research, contributing to the poor knowledge of the cranial biomechanics and feeding behaviours of pseudosuchians. Future FEA comparisons will be informative about the cranium function in rauisuchians with varying cranial morphology. Comparisons in particular with the carnivorous rauisuchians and early dinosaurs found in Argentina during the Triassic, that would be competing for the same prey as *Saurosuchus*, would be useful to carry out in order to explore the effect of ecological and dietary pressures on morphological and functional adaptations of the cranial apparatus. For example, the Argentinian carnivorous rauisuchians include: *Sillosuchus longicervix*, *Fasolasuchus tenax*, *Luperosuchus fractus*; and the carnivorous Triassic dinosaurs include: *Eodromaeus murphy*, and *Herrerasaurus ischigualastensis*. Moreover, further analysis of the hypercarnivorous, apex rauisuchians and theropods, will also inform hypotheses of the degree of convergence and niche fulfilment within the diverse predatory guild. The inferred functional morphology of *Saurosuchus* indicates it was perhaps rather wasteful at carcasses and was therefore a keystone species of the Late Triassic ecosystem in which it lived, regulating the populations of both herbivores and mesopredators through direct predation and carrion production respectively.

LITERATURE CITED

Adams, L. A. (1918) A memoir on the phylogeny of the jaw muscles in recent and fossil vertebrates. *Annals of the New York Academy of Sciences*, 28(1), pp. 51–166

Alcober, O. (2000) Redescription of the skull of *Saurosuchus galilei* (Archosauria: Rauisuchidae). *Journal of Vertebrate Paleontology*. 20(2), pp. 302-316.

Anderson H. T. (1936) The jaw musculature of the phytosaur *Machaeroprosopus*. *J Morphol,* 59, pp. 549–587.

Arcucci, A. B., Marsicano, C. A., Caselli, A. T. (2004) Tetrapod association and palaeoenvironment of the Los Colorados Formation (Argentina): a significant sample from western Gondwana at the end of the Triassic. *Geobios,* 37, pp. 557–568.

Aureliano, T., Ghilardi, A. M., Guilherme, E., Souza-Filho, J. P., Cavalcanti, M., Riff, D. (2015) Morphometry, bite-force, and paleobiology of the Late Miocene Caiman *Purussaurus brasiliensis*. *PloS one*, *10*(2), p.e0117944.

Barghusen, H. R. (1973) The adductor jaw musculature of Dimetrodon (Reptilia, Pelycosauria): Journal of Paleontology, v. 47, p. 823–834.

Bates, K. T., Falkingham, P. L. (2012) Estimating maximum bite performance in *Tyrannosaurus rex* using multi-body dynamics. *Biology Letters*, *8*(4), pp. 660-664.

Bates, K.T., Schachner, E. R. (2012) Disparity and convergence in bipedal archosaur locomotion. *Journal of the Royal Society Interface*, 9(71), pp. 1339-1353.

Benton, M. J. (1984) Rauisuchians and the success of dinosaurs. *Nature*. 310(5973), p.101.

Benton, M. J. (1986a) The Late Triassic reptile *Teratosaurus*: a rauisuchian not a dinosaur. *Palaeontology*, 29, pp. 293–301.

Benton, M. J. (1986b) More than one event in the late Triassic mass extinction. *Nature*, 321(6073), pp. 857-861.

Benton, M. J. (1994) Late Triassic to Middle Jurassic extinctions among continental tetrapods: testing the pattern. In: Fraser, N. C. & Sues, H.-D. (eds) In the Shadow of the Dinosaurs. *Cambridge University Press,* Cambridge, pp. 366–397

Benton, M. J. (2004) Origin and relationships of Dinosauria. *The dinosauria*, 2, pp. 7-19.

Benton, M. J. (2021) The origin of endothermy in synapsids and archosaurs and arms races in the Triassic. *Gondwana Research*, 100, pp. 261-289.

Benton, M. J. & Clark, J. M. (1988) Archosaur phylogeny and the relationships of the Crocodylia. In: Benton, M. J. (ed.) The Phylogeny and Classification of the Tetrapods. Vol 1: Amphibians and Reptiles. *Clarendon Press*, Oxford, pp. 295–338.

Bestwick, J., Jones, A. S., Nesbitt, S. J., Lautenschlager, S., Rayfield, E. J., Cuff, A. R., Button, D. J., Barrett, P. M., Porro, L. B. and Butler, R. J. (2021) Cranial functional morphology of the pseudosuchian *Effigia* and implications for its ecological role in the Triassic. *The Anatomical Record*.

Bestwick, J., Godoy, P. L., Maidment, S. C., Ezcurra, M. D., Wroe, M., Raven, T. J., Bonsor, J. A. and Butler, R. J. (2022) Relative skull size evolution in Mesozoic archosauromorphs: potential drivers and morphological uniqueness of erythrosuchid archosauriforms. *Palaeontology*, *65*(3), p. e12599.

Blackburn, T. J., Olsen, P. E., Bowring, S. A., McLean, N. M., Kent, D. V., Puffer, J., McHone, G., Rasbury, T., Et-Touhami, M. (2013) Zircon U-Pb Geochronology Links the End-Triassic Extinction with the Central Atlantic Magmatic Province. *Science*. 340(6135), pp. 941–945.

Bonaparte, J. F. (1967) Dos nuevas 'faunas' de reptiles Triasicos de Argentina. In: Gondwana Stratigraphy. I.U.G.S. Symposium. Pris, UNESCO, pp. 283–306.
Bonaparte, J. F. (1982) Classification of the Thecodontia. *Geobios*, 15, pp. 99-112.
Bonaparte, J. F. (1984) Locomotion in rauisuchid thecodonts. *Journal of Vertebrate Paleontology*, 3 (4), pp. 210–218.
Brink, K. S., Reisz, R. R. (2014) Hidden dental diversity in the oldest terrestrial apex predator Dimetrodon. *Nature Communications*, *5*(1), pp. 1-9.
Brusatte, S. L. (2010) Representing supraspecific taxa in higher-level phylogenetic analyses: guidelines for palaeontologists. *Palaeontology*, 53, pp. 1–9.
Brusatte, S. L., Benton, M. J., Ruta, M. & Lloyd, G. T. (2008) Superiority, competition, and opportunism in the evolutionary radiation of dinosaurs. *Science*, 321, pp. 1485–1488.
Brusatte, S. L., Butler, R. J., Sulej, T. and Niedźwiedzki, G. (2009) The taxonomy and anatomy of rauisuchian archosaurs from the Late Triassic of Germany and Poland. *Acta Palaeontologica Polonica*, *54*(2), pp. 221-230.
Brusatte, S. L., Benton, M. J., Desojo, J. B., Langer, M. C. (2010) The higher-level phylogeny of Archosauria (tetrapoda: diapsida). *J. Syst. Palaeontol*. 8, pp. 3-47.
Brusatte, S. L., Sakamoto, M., Montanari, S. and Harcourt Smith, W. E. H. (2012) The evolution of cranial form and function in theropod dinosaurs: insights from geometric morphometrics. *Journal of Evolutionary Biology*, *25*(2), pp. 365-377.
Busbey III, A.B. (1989) Form and function of the feeding apparatus of *Alligator mississippiensis*. *Journal of Morphology*, *202*(1), pp. 99-127.
Busbey III, A. B. (1995) in *Functional Morphology in Vertebrate Paleontology*,, Thomason J. J., Ed. (Cambridge Univ. Press, Cambridge), pp. 173-192.
Butler, R. J., Barrett, P. M., Abel, R. L. & Gower, D. J. (2009) A possible ctenosauriscid archosaur from the Middle Triassic Manda beds of Tanzania. Journal of Vertebrate Paleontology, 29, pp. 1022–1031.
Butler, R. J., Brusatte, S. L., Reich, M., Nesbitt, S. J., Schoch, R. R. and Hornung, J. J. (2011) The sail-backed reptile Ctenosauriscus from the latest Early Triassic of Germany and the timing and biogeography of the early archosaur radiation. *PloS one*, *6*(10), p.e25693.
Butler, R. J., Sullivan, C., Ezcurra, M. D., Liu, J., Lecuona, A. and Sookias, R. B. (2014) New clade of enigmatic early archosaurs yields insights into early pseudosuchian phylogeny and the biogeography of the archosaur radiation. *BMC Evolutionary Biology*, *14*(1), pp. 1-16.
Butler, R. J., Nesbitt, S. J., Charig, A. J., Gower, D. J., Barrett, P. M. (2017) *Mandasuchus tanyauchen*, gen. et sp. nov., a pseudosuchian archosaur from the Manda Beds (?Middle Triassic) of Tanzania. *J. Vertebr. Paleontol.* 37(sup. 1), pp. 96-121.
Butler, R. J., Sennikov, A. G., Dunne, E. M., Ezcurra, M. D., Hedrick, B. P., Maidment, S. C., Meade, L. E., Raven, T. J., Gower, D. J. (2019) Cranial anatomy and taxonomy of the erythrosuchid archosauriform '*Vjushkovia triplicostata'* Huene, 1960, from the Early Triassic of European Russia. *Royal Society open science*, *6*(11), p.191289.
Butler, R. J., Fernandez, V., Nesbitt, N. J., Leite, J. V., Gower, D. J. (2022) A new pseudosuchian archosaur, *Mambawakale ruhuhu* gen. et sp. nov., from the Middle Triassic Manda Beds of Tanzania. *The Royal Society*. 9 (2).
Cerda, I. A., Desojo, J. B., Scheyer, T. M. and Schultz, C. L. (2013) Osteoderm microstructure of "rauisuchian" archosaurs from South America. *Geobios*, *46*(4), pp. 273-283.
Charig, A. J. (1956) New Triassic archosaurs from Tanganyika including Mandasuchus and Teleocrater. *University of Cambridge*, Cambridge.
Charig, A. (1967) Subclass Archosauria. In: Hartland, W. B., Holland, C. H., House, M. R., Hughes, N. F., Reynolds, A. B., Rudwick, M. J. S., Satterthwaite, G. E., Tarlo, L. B. H. & Willey, E. C. (eds) The Fossil Record. *Geological Society of London*, London, pp. 708–718.

Chatterjee, S. (1985) *Postosuchus*, a new thecodontian reptile from the Triassic of Texas and the origin of tyrannosaurs. *Philosophical Transactions of the Royal Society of London B*, 309, pp. 395–460.
Chatterjee, S. (1986) *Malerisaurus langstoni*, a new diapsid reptile from the Triassic of Texas. *Journal of vertebrate Paleontology*, *6*(4), pp. 297-312.
Chatterjee, S. (1993) Shuvosaurus, a new theropod. *National Geographic Research and Exploration*, 9, pp. 274–285.
Chure, D. J., Loewen, M. A. (2020) Cranial anatomy of *Allosaurus jimmadseni*, a new species from the lower part of the Morrison Formation (Upper Jurassic) of Western North America. *PeerJ*, *8*, p.e7803.
Cleuren, J. O. H. A. N., De Vree, F. (2000) Feeding in crocodilians. *Feeding: form, function, and evolution in tetrapod vertebrates*, pp. 337-358.
Cleuren, J., Aerts, P., Vree, F. D. (1995) Bite and joint force analysis in Caiman *crocodilius*. *Belgian Journal of Zoology (Belgium)*.
Colbert, E. H. (1961) The Triassic reptile *Poposaurus*. *Fieldiana Geology*, 14, pp. 59–78.
Cuff, A. R., Rayfield, E. J. (2013) Feeding mechanics in spinosaurid theropods and extant crocodilians. *PLoS One*, *8*(5), p.e65295.
Cunningham, J. A., Donoghue, P. C., Bengtson, S. (2014) Distinguishing biology from geology in soft-tissue preservation. *The Paleontological Society Papers*, *20*, pp. 275-288.
Currie, B. S., Colombi, C. E., Tabor, N. J., Shipman, T. C. & Montanez, I. P. (2008) Stratigraphy and architecture of the Upper Triassic Ischigualasto Formation, Ischigualasto Provincial Park, San Juan, Argentina. *Journal of South American Earth Sciences*, 27, pp. 74–87.
Curtis, N. (2011) Craniofacial biomechanics: an overview of recent multibody modelling studies. *Journal of anatomy*, *218*(1), pp. 16-25.
D'Amore, D. C. (2009) A functional explanation for denticulation in theropod dinosaur teeth. *Anatomical Record*, 292, pp. 1297–1314.
D'Amore, D. C. and Blumensehine, R. J. (2009) Komodo monitor (*Varanus komodoensis*) feeding behavior and dental function reflected through tooth marks on bone surfaces, and the application to ziphodont paleobiology. *Paleobiology*, *35*(4), pp. 525-552.
D´Amore, D. C., Moreno, K., McHenry, C. R. and Wroe, S. (2011) The effects of biting and pulling on the forces generated during feeding in the Komodo dragon (*Varanus komodoensis*). *PLoS ONE*, 6, p.e26226.
Damke, L. V. S., Pretto, F. A., Mastrantônio, B. M., Garcia, M. S., Da-Rosa, Á. A. S. (2022) New material of Loricata (Archosauria: Pseudosuchia) from the Late Triassic (Carnian, Hyperodapedon Assemblage Zone) of southern Brazil. *Journal of South American Earth Sciences*, *115*, p. 103754.
Damuth, J. D., DiMichele, W. A. and Potts, R. (1992) Terrestrial ecosystems through time: evolutionary paleoecology of terrestrial plants and animals.
Desojo, J. B., Arcucci, A. B. (2009) New material of *Luperosuchus fractus* (Archosauria: Crurotarsi) from the Middle Triassic of Argentina: the earliest known South American rauisuchian. *Journal of Vertebrate Paleontology*, 29, pp. 1311–1315.
Desojo, J. B., Rauhut, O. W. M. (2009) The taxonomic status and phylogenetic position of the Late Triassic Brazilian rauisuchian Prestosuchus. *Journal of Vertebrate Paleontology (suppl. 3)*, 29, pp. 87A.
Desojo, J. B., Vizcaíno, S. F. (2009) Jaw biomechanics in the South American aetosaur Neoaetosauroides engaeus. *Paläontologische Zeitschrift*, *83*(4), pp. 499-510.
Desojo, J. B., Fiorelli, L. E., Ezcurra, M. D., Martinelli, A. G., Ramezani, J., Da Rosa, Á., von Baczko, M. B., Trotteyn, M. J., Montefeltro, F. C., Ezpeleta, M. and Langer, M. C. (2020) The Late Triassic Ischigualasto Formation at Cerro Las Lajas (La Rioja, Argentina): fossil tetrapods, high-resolution chronostratigraphy, and faunal correlations. *Scientific reports*, *10*(1), pp.1-34.

Dilkes, D. W. (1999) Appendicular myology of the hadrosaurian dinosaur *Maiasaura peeblesorum* from the Late Cretaceous (Campanian) of Montana. *Earth and Environmental Science Transactions of the Royal Society of Edinburgh*, *90*(2), pp. 87-125.
Erickson, G. M.; Lappin, A. K.; Vliet, K. A. (2003) The ontogeny of bite-force performance in American alligator (*Alligator mississippiensis*). *Journal of Zoology.* 260 (3), pp. 317–327.
Erickson, G. M., Gignac, P. M., Steppan, S. J., Lappin, A. K., Vliet, K. A., Brueggen, J. D., Inouye, B. D., Kledzik, D. and Webb, G. J. (2012) Insights into the ecology and evolutionary success of crocodilians revealed through bite-force and tooth-pressure experimentation. *PLoS One*, *7*(3), p.e31781.
Ezcurra, M. D., Nesbitt, S. J., Bronzati, M., Dalla Vecchia, F. M., Agnolin, F. L., Benson, R. B., Brissón Egli, F., Cabreira, S. F., Evers, S. W., Gentil, A. R., Irmis, R. B. (2020) Enigmatic dinosaur precursors bridge the gap to the origin of Pterosauria. *Nature*, *588*(7838), pp. 445-449.
Ezcurra, M. D., Bandyopadhyay, S., Gower, D. J. (2021) A new erythrosuchid archosauriform from the Middle Triassic Yerrapalli Formation of south-central India. *Ameghiniana*, *58*(2), pp. 132-168.
Figueirido, B., Lautenschlager, S., Pérez-Ramos, A., Valkenburgh, B. (2018) Distinct predatory behaviors in scimitar- and dirk-toothed sabertooth cats. *Current Biology*, 28, pp. 3260–3266.
Fish, F. E., Bostic, S. A., Nicastro, A. J., Beneski, J. T. (2007) Death roll of the alligator: mechanics of twist feeding in water. *Journal of experimental biology*, *210*(16), pp. 2811-2818.
Fowell, S. J., Olsen, P. E. (1995) Time calibration of Triassic/Jurassic microfloral turnover, eastern North America—Reply. *Tectonophysics*. 245(1–2), pp. 96–99.
França, M. A. G. (2011) Decrição osteológica de *Decuriasuchus quartacolonia* (Archosauria, Pseudosuchia) *e a evolução dos Rauissúquios*. Unpublished PhD dissertation, Faculdade de Filosofia, Ciências e Letras deRibeirão Preto, Universidade de São Paulo, p. 434.
França, M. A. G., Ferigolo, J. & Langer, M. C. (2011) Associated skeletons of a new middle Triassic 'Rauisuchia' from Brazil. *Naturwissenschaften*, 98, pp. 389–395.
Furin, S., Preto, N., Rigo, M., Roghi, G., Gianolla, P., Crowley, J. L., Bowring, S. A. (2006) High-precision U-Pb zircon age from the Triassic of Italy: Implications for the Triassic time scale and the Carnian origin of calcareous nannoplankton and dinosaurs. *Geology*, *34*(12), pp. 1009-1012.
Galton, P. M. (1985) The poposaurid thecodontian Teratosaurus suevicus v. Meyer plus referred specimens mostly based on prosauropod dinosaurs from the Middle Stubensandstein Upper Triassic of Nordwuerttemberg West Germany. *Stuttgarter Beitraege zur Naturkunde Serie B (Geologie und Palaeontologie)*, 116, pp. 1–29.
Garwood, R., Dunlop, J. (2014) The walking dead: Blender as a tool for paleontologists with a case study on extinct arachnids. *Journal of Paleontology*, *88*(4), pp. 735-746.
Garwood, R. J., Sutton, M. D. (2010) X-ray micro-tomography of Carboniferous stem-Dictyoptera: new insights into early insects. *Biology Letters*, *6*(5), pp. 699-702.
Garwood, R. J., Sutton, M. D. (2012) The enigmatic arthropod Camptophyllia. *Palaeontologia Electronica*, *15*(2), p.12.
Garwood, R. J., Dunlop, J. A., Giribet, G., Sutton, M. D. (2011) Anatomically modern Carboniferous harvestmen demonstrate early cladogenesis and stasis in Opiliones. *Nature Communications*, *2*(1), pp. 1-7.
Garwood, R. J., Ross, A., Sotty, D., Chabard, D., Charbonnier, S., Sutton, M. D., Withers, P. J. (2012) Tomographic reconstruction of neopterous Carboniferous insect nymphs.
Gauthier, J. A., Padian, K., (1985) Phylogenetic, functional, and aerodynamic analyses of the origin of birds and their flight. In: Hecht, M.K., Ostrom, J.H., Viohl, G., Wellnhofer, P. (Eds.), The Beginings of Birds. *Freunde des Jura-Musems, Eichst¨ att*, pp. 185–197.
Gauthier, J. A., Nesbitt, S. J., Schachner, E. R., Bever, G. S., Joyce, W. G. (2011) The bipedal stem crocodilian Poposaurus gracilis: inferring function in fossils and innovation in archosaur locomotion. Bull. - *Peabody Mus. Nat. Hist.* 52 (1), pp. 107–126.

Gignac, P. M. (2010) *Biomechanics and the ontogeny of feeding in the American alligator (Alligator mississippiensis): reconciling factors contributing to intraspecific niche differentiation in a large-bodied vertebrate* (Doctoral dissertation, The Florida State University).
Gignac, P. M. and Erickson, G. M. (2017) The biomechanics behind extreme osteophagy in Tyrannosaurus rex. *Scientific Reports*, *7*(1), pp. 1-10.
Giles, S., Friedman, M. (2013) Virtual reconstruction of brain anatomy in early ray-finned fishes (Osteichthyes: Actinopterygii). *Journal of Palaeontology*, 88, pp. 636–651.
Golonka, J. and Ford, D. (2000) Pangean (late Carboniferous–Middle Jurassic) paleoenvironment and lithofacies. *Palaeogeography, Palaeoclimatology, Palaeoecology*, *161*(1-2), pp. 1-34.
Gower, D. J. (1999) The cranial and mandibular osteology of a new rauisuchian archosaur from the Middle Triassic of southern Germany. *Stuttgarter Beitraege zur Naturkunde Serie B (Geologie und Palaeontologie)*, 280, pp. 1–49.
Gower, D. J. (2000) Rauisuchian archosaurs (reptillia, diapsida): an overview. *Neues Jahrb. Geol. Palaontol. Abh.* 218, pp. 447–488.
Gower, D. J., Sennikov, A. G., Benton, M. J., Shishkin, M. A., Unwin, D. M. and Kurochkin, E. N., (2000) Early archosaurs from Russia. *The age of dinosaurs in Russia and Mongolia*, pp. 140-159.
Gower, D. J., Sennikov, A. G., Benton, M. J., Shishkin, M. A., Unwin, D. M., Kurochkin, E. N. (2000) Early archosaurs from Russia. The age of dinosaurs in Russia and Mongolia, pp. 140-159.
Gower, D. J., Nesbitt, S. J. (2006) The braincase of *Arizonasaurus babbitti*—further evidence for the non-monophyly of 'rauisuchian' archosaurs. *Journal of Vertebrate Paleontology*, *26*(1), pp. 79-87.
Godoy, P. L., Montefeltro, F. C., Norell, M. A., Langer, M. C. (2014) An Additional Baurusuchid from the Cretaceous of Brazil with Evidence of Interspecific Predation among Crocodyliformes. *PLoS ONE*, 9, p.e97138.
Griffin, C. T. and Nesbitt, S. J. (2020) Does the maximum body size of theropods increase across the Triassic–Jurassic boundary? Integrating ontogeny, phylogeny, and body size. *The Anatomical Record*, 303(4), pp. 1158-1169.
Grigg, G., Kirshner, D. (2015). Biology and Evolution of Crocodylians. *Cornell University Press: New York*.
Haas, G. (1955) The jaw musculature in *Protoceratops* and in other ceratopsians. *Am Mus Novit*, 1729, pp. 1–24.
Haas, G. (1963) A proposed reconstruction of the jaw musculature of *Diplodocus*. *Ann Carnegie Mus*, 36, pp. 139–157.
Haas, G. (1969) On the jaw muscles of ankylosaurs. *Am Mus Novit*, 2399, pp. 1–12.
Hagdorn, H., Mutter, R. J. (2011) The vertebrate fauna of the Lower Keuper Albertibank (Erfurt Formation, Middle Triassic) in the vicinity of Schwa¨bisch Hall (Baden-Württemberg, Germany). *Palaeodiversity*, 4, pp. 223–243.
Haug, J. T., Haug C. (2012) An unusual fossil larva, the ontogeny of achelatan lobsters, and the evolution of metamorphosis. *Bulletin of Geosciences*, 88, pp. 195–206.
Haug, J. T., Maas, A., Haug, C., Waloszek, D. (2011) *Sarotrocercus oblitus*–small arthropod with great impact on the understanding of arthropod evolution? *Bulletin of Geosciences*, 86, pp. 725–736.
Haug, J. T., Waloszek, D., Maas, A, Liu, Y., Haug, C. (2012) Functional morphology, ontogeny and evolution of mantis shrimp-like predators in the Cambrian. *Palaeontology*, 55, pp. 369–399
Heckert, A.B. (2004) *Late Triassic microvertebrates from the lower Chinle Group (Otischalkian-Adamanian: Carnian), southwestern USA: Bulletin 27* (Vol. 27). New Mexico Museum of Natural History and Science.
Heckert, A. B., Lucas, S. G., Krzyzanowski, S. E. (2002) The rauisuchian archosaur *Saurosuchus* from the Upper Triassic Chinle Group, Southwestern U.S.A., and its biochronological significance. In Heckert, A. B., Lucas, S. G. (eds.). Upper Triassic Stratigraphy and Paleontology. Vol. 21. *New Mexico Museum of Natural History and Science Bulletin*. pp. 241–247.

Heckert, A. B., Mitchell, J. S., Schneider, V. P., Olsen, P. E. (2012) Diverse new microvertebrate assemblage from the Upper Triassic Cumnock Formation, Sanford Subbasin, North Carolina, USA. *Journal of Paleontology*, *86*(2), pp. 368-390.
Henderson, D. M. (2003) The eyes have it: the sizes, shapes, and orientations of theropod orbits as indicators of skull strength and bite force. *Journal of Vertebrate Paleontology*, *22*(4), pp. 766-778.
Hendrickx, C., Mateus, O. (2014) Abelisauridae (Dinosauria: Theropoda) from the Late Jurassic of Portugal and dentition-based phylogeny as a contribution for the identification of isolated theropod teeth. *Zootaxa*, *3759*.
Herring, S. W., Teng, S. (2000) Strain in the braincase and its sutures during function. *American Journal of Physical Anthropology: The Official Publication of the American Association of Physical Anthropologists*, *112*(4), pp. 575-593.
Holliday C. M. (2009) New insights into dinosaur jaw muscle anatomy. *Anat Rec*, 292, pp. 1246–1265.
Holliday, J. A., Steppan, S. J. (2004) Evolution of hypercarnivory: the effect of specialization on morphological and taxonomic diversity. *Paleobiology*, 30(1), pp. 108-128.
Holliday, C. M., Tsai, H. P., Skiljan, R. J., George, I. D., Pathan, S. (2013) A 3D interactive model and atlas of the jaw musculature of *Alligator mississippiensis. PLoS One*, 8(6), p.e62806.
Holliday, C. M., Sellers, K. C., Vickaryous, M. K., Ross, C. F., Porro, L. B., Witmer, L. M., Davis, J. L. (2015). The functional and evolutionary significance of the crocodyliform pterygomandibular joint. Integr. *Comp. Bio*l. 55(1), p.e81.
Holtz Jr, T.R. (1998) Spinosaurs as crocodile mimics. *Science*, *282*(5392), pp.1276-1277.
Huang, C., Tong, J., Hinnov, L. and Chen, Z. Q. (2011) Did the great dying of life take 700 ky? Evidence from global astronomical correlation of the Permian-Triassic boundary interval. *Geology*, 39(8), pp. 779-782.
Huene, F. V. (1938a) Die fossielen Reptilien des su¨damerikanischen Gondwanalandes. Neues Jahrbuch fu¨r Mineralogie, Geologie und Pala¨ontologie, Abteilung B, 1938, pp. 142–151.
Huene, F. V. (1938b) Ein grosser Stagonolepide aus derju¨ngeren Trias Ostafrikas. Neues Jahrbuch fu¨r Geologie und Pala¨eontologie, Beilage–Ba¨nde Abt. B, 80, pp. 264–278.
Huene, F. V. (1942) Die fossilen Reptilien des Sudamerikanischen Gondwanalandes. Ergebnisse der Sauriergrabungen in Sudbrasilien, 1928/1929. C. H. Beck'she, Munchen.
Hughes, B. (1963) The earliest archosaurian reptiles. *South African Journal of Science*, 59(5), pp. 221-241.
Irmis, R.B. (2005) The vertebrate fauna of the Upper Triassic Chinle Formation in Northern Arizona. In Nesbitt, S.J.; Parker, W.G.; Irmis, R.B. (eds.). Guidebook to the Triassic Formations of the Colorado Plateau in northern Arizona: Geology, Paleontology, and History. Vol. 9. *Mesa Southwestern Museum.*
Irmis, R. B., Nesbitt, S. J., Padian, K., Smith, N. D., Turner, A. H., Woody, D. & Downs, A. (2007) A Late Triassic dinosauromorph assemblage from New Mexico and the rise of dinosaurs. Science, 317, pp. 358–361.
Irmis, R. B., Martz, J. W., Parker, W. G. & Nesbitt, S. J. (2010) Re-evaluating the correlation between Late Triassic terrestrial vertebrate biostratigraphy and the GSSP-defined marine stages. Albertiana, 38, pp. 40–52.
Jalil, N.-E. & Peyer, K. (2007) A new rauisuchian (Archosauria, Suchia) from the Upper Triassic of the Argana Basin, Morocco. *Palaeontology*, 50, pp. 417–430.
Jaslow, C. R. (1990) Mechanical properties of cranial sutures. *Journal of biomechanics*, *23*(4), pp. 313-321.
Jaslow, C. R., Biewener, A. A. (1995) Strain patterns in the horncores, cranial bones and sutures of goats (Capra hircus) during impact loading. *Journal of Zoology*, *235*(2), pp. 193-210.

Jenkins, I., Thomason, J. J., Norman, D. B. (2002) Primates and engineering principles: applications to craniodental mechanisms in ancient terrestrial predators. *Senckenbergiana lethaea*, *82*(1), pp. 223-240.
Johnson-Ransom, E., Gignac, P., Erickson, G. M., Snively, E. (2021) February. Finite Element Analysis Indicates Juvenile *Tyrannosaurus rex* Crania Experienced High Strain Under Normalized High Forces, in Contrast to the Adult Condition. In *Oklahoma State University Center for Health Sciences Research Days 2021: Poster presentation*.
Juul, L. (1994) The phylogeny of basal archosaurs. *Palaeontologia Africana*, 31, pp. 1–38.
Kakuturu, S. P. (2017) MicroCT data: CT Analyser porosity, Avizo 3D individual objects.
Krebs, B. (1965) Die Triasfauna der Tessiner Kalkalpen. XIX. Ticinosuchus ferox, nov. gen. nov. sp. Ein neuer Pseudosuchier aus der Trias des Monte San Georgio. *Schweizersiche Palaontologische, Abhandlungen*, 81, pp. 1–140.
Krebs, B. (1976) Pseudosuchia. Handb. Paläoherpetol. 13, pp. 40-98.
Kuhn, O. (1964). Ungelöste Probleme der Stammesgeschichte der Amphibien und Reptilien. *Jahreshefte des Vereins für vaterländische Naturkunde in Württemberg*. 118-119, pp. 293-325.
Labarre, D., Charruau, P., Platt, S. G., Rainwater, T. R., Cedeño-Vázquez, J. R., González-Cortés, H. (2017) Morphological diversity of the American crocodile (*Crocodylus acutus*) in the Yucatán peninsula. *Zoomorphology*, *136*(3), pp. 387-401.
Lacerda, M. B., Schultz, C. L. and Bertoni-Machado, C. (2015) First 'Rauisuchian' archosaur (Pseudosuchia, Loricata) for the Middle Triassic Santacruzodon Assemblage Zone (Santa Maria Supersequence), Rio Grande do Sul State, Brazil. *Plos One*, *10*(2), p. e0118563.
Lacerda, M. B., Mastrantônio, B. M., Fortier, D. C. and Schultz, C. L. (2016) New insights on *Prestosuchus chiniquensis* Huene, 1942 (Pseudosuchia, Loricata) based on new specimens from the "Tree Sanga" Outcrop, Chiniquá Region, Rio Grande do Sul, Brazil. *PeerJ*, *4*, p. e1622.
Langer, M. C. (2005) Studies on continental Late Triassic tetrapod biochronology. II. The Ischigualastian and a Carnian global correlation. *Journal of South American Earth Sciences*, 19, pp. 219–239.
Langer, M. C., Ribeiro, A. M., Schultz, C. L. & Ferigolo, J. (2007) The continental tetrapod-bearing Triassic of South Brazil. In: Lucas, S. G. & Spielmann, J. A. (eds) The Global Triassic. *New Mexico Museum of Natural History and Science Bulletin, Albuquerque*, New Mexico, 41, pp. 201–218.
Lautenschlager, S. (2008) Revision of Rauisuchus tirdentes (Archosauria: Rauisuchia) from the Late Triassic (Carnian) Santa Maria Formation of Brazil and its implications for rauisuchian phylogeny. *Ludwig-Maximilians-Universität, Munich*
Lautenschlager, S. (2012) Paleontology 2.0—A comprehensive protocol for the reconstruction of hard- and soft tissue structures in fossils: *Geological Society of America Abstracts with Programs, v. 44*, no. 7, p. 372.
Lautenschlager, S. (2013) Cranial myology and bite force performance of *Erlikosaurus andrewsi*: a novel approach for digital muscle reconstructions. *Journal of Anatomy*, 222(2), pp. 260-272.
Lautenschlager, S. (2015) Estimating cranial musculoskeletal constraints in theropod dinosaurs: *Royal Society Open Science*, 2, art. 150495.
Lautenschlager, S. (2020) Multibody dynamics analysis (MDA) as a numerical modelling tool to reconstruct the function and palaeobiology of extinct organisms. *Palaeontology*, *63*(5), pp.703-715.
Lautenschlager, S., Desojo, J. B. (2011) Reassessment of the Middle Triassic rauisuchian archosaurs *Ticinosuchus ferox* and *Stagonosuchus nyassicus*. *Paläontologische Zeitschrift*, *85*(4), pp. 357-381.
Lautenschlager, S., Witmer, L. M., Altangerel, P., Zanno, L. E., and Rayfield, E. J. (2014) Cranial anatomy of *Erlikosaurus andrewsi* (Dinosauria, Therizinosauria): New insights based on digital reconstruction: *Journal of Vertebrate Paleontology*, 34, p. 1263–1291.

Lautenschlager, S. (2016*a*) Reconstructing the past: methods and techniques for the digital restoration of fossils. *Royal Society Open Science*, 3, 160342.
Lautenschlager, S. (2016*b*) Digital reconstruction of soft-tissue structures in fossils. *The Paleontological Society Papers*, *22*, pp. 101-117.
Lautenschlager, S. (2017) From bone to pixel—fossil restoration and reconstruction with digital techniques. *Geology Today*, 33, pp. 155–159.
Lautenschlager, S. & Desojo, J. B. (2011) Reassessment of the Middle Triassic 'rauisuchian' archosaurs *Ticinosuchus ferox* and *Stagonosuchus nyassicus. Pala¨ontologische Zeitschrift*, 85, pp. 357–381.
Lessner, E. J., Stocker, M. R., Smith, N. D., Turner, A. H., Irmis, R. B. and Nesbitt, S. J. (2016) A new rauisuchid (Archosauria, Pseudosuchia) from the Upper Triassic (Norian) of New Mexico increases the diversity and temporal range of the clade. *PeerJ*, *4*, p. e2336.
Li, C., Wu, X.-C., Cheng, Y.-N., Sato, T. & Wang, L. (2006) An unusual archosaurian from the marine Triassic of China. *Naturwissenschaften*, 93, pp. 200–206.
Long, R. A. and Padian, K. (1986) Vertebrate biostratigraphy of the Late Triassic Chinle Formation, Petrified Forest National Park, Arizona: preliminary results. In *The beginning of the age of Dinosaurs, faunal change across the Triassic-Jurassic boundary. Symposium. Society of vertebrate paleontology. Annual meeting. 44*, pp. 161-169.
Long, R. A. & Murry, P. A. (1995) Late Triassic (Carnian and Norian) tetrapods from the southwestern United States. *New Mexico Museum of Natural History and Science Bulletin*, 4, pp. 1–254.
Iordansky, N. N., Gans, C. (1973) The skull of the Crocodilia. *Biology of the Reptilia, 4*, pp. 201-262.
Lucas, S. G. (1998) Global Triassic tetrapod biostratigraphy and biochronology. *Palaeogeography, Palaeoclimatology, Palaeoecology*, *143*(4), pp. 347-384.
Maidment, S. C., Sennikov, A. G., Ezcurra, M. D., Dunne, E. M., Gower, D. J., Hedrick, B. P., Meade, L. E., Raven, T. J., Paschchenko, D. I., Butler, R. J. (2020) The postcranial skeleton of the erythrosuchid archosauriform Garjainia prima from the Early Triassic of European Russia. *Royal Society open science*, *7*(12), p.201089.
Martínez, R. N., Apaldetti, C., Alcober, O. A., Colombi, C. E., Sereno, P. C., Fernández, E., Malnis, P. S., Correa, G. A., Abelin, D. (2013) Vertebrate succession in the Ischigualasto Formation. *Journal of Vertebrate Paleontology.* 32, pp. 10–30.
Mastrantônio, B. M. (2010) *Descrição osteológica de materiais cranianos e pós–cranianos de Prestosuchus chiniquensis (Archosauria, Rauisuchia) do Meso– Triássico do RS (Biozona de Dinodontosaurus, Formação Santa Maria) e considerações filogenéticas sobre os rauissúquio.* Universidade Federal do Rio Grande do Sul, Porte Alegre, Brazil.
Mastrantônio, B. M., Schultz, C. L., Desojo, J. B., Garcia, J. B. (2013) The braincase of *Prestosuchus chiniquensis* (Archosauria: Suchia). In: S. Nesbitt, J. B. Desojo, and R. B. Irmis (eds.), Anatomy, Phylogeny and Palaeobiology of Early Archosaurs and their Kin. *Geological Society of London Special Publications*, 379, pp. 425–440.
Mastrantônio, B., Von Baczko, M. B., Desojo, J. B., & Schultz, C. L. (2019) The skull anatomy and cranial endocast of the pseudosuchid archosaur *Prestosuchus chiniquensis* from the Triassic of Brazil. *Acta Palaeontologica Polonica*, 64, pp. 171-198.
McCurry, M. R., Mahony, M., Clausen, P. D., Quayle, M. R., Walmsley, C. W., Jessop, T. S., Wroe, S., Richards, H., McHenry, C. R. (2015) The relationship between cranial structure, biomechanical performance and ecological diversity in varanoid lizards. *PloS one*, 10(6), p.e0130625.
McHenry, C. R., Clausen, P. D., Daniel, W. J., Meers, M. B., Pendharkar, A. (2006) Biomechanics of the rostrum in crocodilians: a comparative analysis using finite-element modeling. *The*

Anatomical Record Part A: Discoveries in Molecular, Cellular, and Evolutionary Biology: An Official Publication of the American Association of Anatomists, *288*(8), pp. 827-849.
Mehl, M. G. (1915) Poposaurus gracilis, a new reptile from the Triassic of Wyoming. *Journal of Geology*, 23, pp. 516–522.
Meyer, H. V. (1861) Reptilien aus dem Stubensandstein des obern Keupers. *Palaeontographica*, A, 6, pp. 253–346.
Molnar, R. E. (1998) Mechanical factors in the design of the skull of *Tyrannosaurus rex* (Osborn, 1905). *GAIA: revista de geociências*, (15), p.193.
Montefeltro, F. C., Lautenschlager, S., Godoy, P. L., Ferreira, G. S. and Butler, R. J. (2020) A unique predator in a unique ecosystem: modelling the apex predator within a Late Cretaceous crocodyliform-dominated fauna from Brazil. *Journal of Anatomy*, 237(2), pp. 323-333.
Mundil, R., Pálfy, J., Renne, P. R. and Brack, P. (2010) The Triassic timescale: new constraints and a review of geochronological data. *Geological Society, London, Special Publications*, *334*(1), pp. 41-60.
Muttoni, G., Kent, D. V., Olsen, P. E., Stefano, P. D., Lowrie, W., Bernasconi, S. M., Hernández, F.M. (2004) Tethyan magnetostratigraphy from Pizzo Mondello (Sicily) and correlation to the Late Triassic Newark astrochronological polarity time scale. *Geological Society of America Bulletin*, *116*(9-10), pp. 1043-1058.
Nesbitt, S. J. (2005a) The osteology of the Middle Triassic pseudosuchian archosaur Arizonasaurus babbitti. Historical Biology, 17, pp. 19–47.
Nesbitt, S. J. (2005b) A new archosaur from the upper Moenkopi Formation (Middle Triassic) of Arizona and its implications for rauisuchian phylogeny and diversification. Neues Jahrbuch für Geologie und Paläeontologie Monatshefte, 2005, pp. 332–346.
Nesbitt, S. (2007) The anatomy of *Effigia okeeffeae* (Archosauria, Suchia), theropod-like convergence, and the distribution of related taxa. *Bulletin of the American Museum of Natural History*, *2007*(302), pp. 1-84.
Nesbitt, S. J. (2011) The early evolution of archosaurs: relationships and the origin of major clades. *Bulletin of the American Museum of Natural History.* 352, pp. 1–292.
Nesbitt, S. J. & Norell, M. A. (2006) Extreme convergence in the body plans of an early suchian (Archosauria) and ornithomimid dinosaurs (Theropoda). *Proceedings of the Royal Society of London B*, 273, pp. 1045–1048.
Nesbitt, S. J., Sidor, C. A., Irmis, R. B., Angielczyk, K. D., Smith, R. M. H. & Tsuji, L. A. (2010) Ecologically distinct dinosaurian sister-group shows early diversification of Ornithodira. *Nature*, 464, pp. 95–98.
Nesbitt, S. J., Liu, J. & Li, C. (2011) A sail-backed suchian from the Heshanggou Formation (Early Triassic: Olenekian) of China. *Earth and Environmental Science Transactions of the Royal Society of Edinburgh*, 101, pp. 271–284.
Nesbitt, S. J., Brusatte, S. L., Desojo, J. B., Liparini, A., De França, M. A., Weinbaum, J. C., Gower, D. J. (2013) Rauisuchia. *Geological Society, London, Special Publications, 379*(1), pp.241-274.
Nesbitt, S. and Desojo, J.B. (2017) The osteology and phylogenetic position of Luperosuchus fractus (Archosauria: Loricata) from the latest Middle Triassic or earliest Late Triassic of Argentina. *Ameghiniana, 54*(3), pp. 261-282.
Novak, S.E. (2004) *A New Speciman of Postosuchus from the Late Triassic Whitaker (Coelophysis) Quarry, Siltstone Member, Chinle Formation, Ghost Ranch, New Mexico* (Doctoral dissertation, University of North Carolina at Chapel Hill).
Novas, F. E., Agnolín, F. L., Ezcurra, M. D., Porfiri, J., Canale, J. I. (2013) Evolution of the carnivorous dinosaurs during the Cretaceous: the evidence from Patagonia. *Cretaceous Research*, *45*, pp. 174-215.

Nützel, A., Joachimski, M., Correa, M. L. (2010) Seasonal climatic fluctuations in the Late Triassic tropics—High-resolution oxygen isotope records from aragonitic bivalve shells (Cassian Formation, Northern Italy). *Palaeogeography, Palaeoclimatology, Palaeoecology*, *285*(3-4), pp. 194-204.
Olsen, P. E., Sues, H. D. (1986) Correlation of continental Late Triassic and Early Jurassic sediments, and patterns of the Triassic-Jurassic tetrapod transition. In *The beginning of the age of Dinosaurs, faunal change across the Triassic-Jurassic boundary. Symposium. Society of vertebrate paleontology. Annual meeting. 44*, pp. 321-351.
Olsen, P. E., Kent, D. V., Sues, H.-D., Koeberl, C., Huber, H., Montanari, E. C., Rainforth, A., Fowell, S. J., Szajna, M. J., Hartline, B. W. (2002) Ascent of Dinosaurs Linked to an Iridium Anomaly at the Triassic-Jurassic Boundary. *Science*, 296, pp.1305–1307.
Parrish, J. M. (1993) Phylogeny of the Crocodylotarsi, with reference to archosaurian and crurotarsan monophyly. *Journal of Vertebrate Paleontology*, 13, pp. 287–308.
Parrish, J. M. and Carpenter, K. (1986) A new vertebrate fauna from the Dockum Formation (Late Triassic) of eastern New Mexico. In *The beginning of the age of Dinosaurs, faunal change across the Triassic-Jurassic boundary. Symposium. Society of vertebrate paleontology. Annual meeting. 44*, pp. 151-160.
Paul, G. S. (1984) The archosaurs: a phylogenetic study. In *Symposium on Mesozoic terrestrial ecosystems. 3*, pp. 175-180.
Peyer, K., Carter, J. G., Sues, H.-D., Novak, S. E., Olsen, P. E. (2008) A new suchian archosaur from the Upper Triassic of North Carolina. Journal of Vertebrate Paleontology, 28, pp. 363–381.
Pires, E. F., Sommer, M. G., dos Santos Scherer, C. M. (2005) Late Triassic climate in southernmost Parana Basin (Brazil): evidence from dendrochronological data. *Journal of South American Earth Sciences*, *18*(2), pp. 213-221.
Porro, L. B., Holliday, C. M., Anapol, F., Ontiveros, L. C., Ontiveros, L. T. and Ross, C. F. (2011) Free body analysis, beam mechanics, and finite element modeling of the mandible of *Alligator mississippiensis*. *J. Morphol*. 272, pp. 910-937
Rafferty, K. L., Herring, S. W. (1999) Craniofacial sutures: morphology, growth, and in vivo masticatory strains. *Journal of Morphology*, *242*(2), pp. 167-179.
Rafferty, K. L., Herring, S. W., Marshall, C. D. (2003) Biomechanics of the rostrum and the role of facial sutures. *Journal of Morphology*, *257*(1), pp. 33-44.
Rahman, I.A. and Lautenschlager, S. (2016) Applications of three-dimensional box modeling to paleontological functional analysis. *The Paleontological Society Papers*, 22, pp. 119-132.
Rahman, I. A., Belaústegui, Z., Zamora, S., Nebelsick, J. H., Doménech, R., Martinell, J. (2015) Miocene Clypeaster from Valencia (E Spain): Insights 454 into the taphonomy and ichnology of bioeroded echinoids using X-ray micro455 tomography. *Palaeogeography, Palaeoclimatology, Palaeoecology*, 438, pp. 168–179.
Rayfield, E.J. (2001) Cranial form and function in a large theropod dinosaur: a study using Finite Element Analysis. Unpublished PhD Thesis, Cambridge University.
Rayfield, E,J. (2004) Cranial mechanics and feeding in Tyrannosaurus rex. *Proceedings of the Royal Society of London B.* 271, pp. 1451-1459.
Rayfield, E.J. (2005) Aspects of comparative cranial mechanics in the theropod dinosaurs Coelophysis, Allosaurus and Tyrannosaurus. *Zoological Journal of the Linnean Society*, *144*(3), pp. 309-316.
Rayfield, E. J. (2007) Finite element analysis and understanding the biomechanics and evolution of living and fossil organisms. *Annual Review of Earth and Planetary Sciences*, 35, pp. 541–576.
Rayfield, E. J. (2011) Strain in the ostrich mandible during simulated pecking and validation of specimen-specific finite element models. *Journal of Anatomy*, 218(1), pp. 47-58.

Rayfield, E. J., Norman, D. B., Horner, C. C, Horner, J. R., May Smith, P, Thomason, J. J., Upchurch, P. (2001) Cranial design and function in a large theropod dinosaur. *Nature*. 409, pp. 1033-1037.
Reig, O. A. (1959) Primeros datos descriptivos sobre nuevos arcosaurios del Triásico de Ischigualasto (San Juan, Argentina). *Revista de la Asociación Geológica Argentina*. 13(4), pp. 257–27.
Reig, O. A. (1961) Acerca de la posición sistemática de la familia Rauisuchidae y del género *Saurosuchus* (Reptilia -Thecodontia). *Publicaciones del Museo Municipal de Ciencias Naturales y Tradicionales de Mar del Plata*, 3, pp. 73-114.
Renesto, S., Confortini, F., Gozzi, E., Malzanni, M. and Paganoni, A. (2003) A possible rauisuchid (Reptilia, Archosauria) tooth from the Carnian (Late Triassic) of Lombardy (Italy). *Rivista Museo Civico di Scienze Naturali "E. Caffi" Bergamo*, *22*, pp. 109-114.
Riff, D., Kellner, A. W. A. (2011) Baurusuchid crocodyliforms as theropod mimics: clues from the skull and appendicular morphology of *Stratiotosuchus maxhechti* (Upper Cretaceous of Brazil). *Zoological Journal of the Linnean Society*, *163*(suppl_1), pp. S37-S56.
Roberto-Da-Silva, L., Müller, R. T., de França, M. A. G., Cabreira, S. F., Dias-Da-Silva, S., 2018. An impressive skeleton of the giant top predator Prestosuchus chiniquensis (Pseudosuchia: Loricata) from the Triassic of Southern Brazil, with phylogenetic remarks. *Hist. Biol*. pp. 1–20.
Rogers, R.R., Swisher III, C.C., Sereno, P.C., Monetta, A.M., Forster, C.A. and Martínez, R.N., (1993) The Ischigualasto tetrapod assemblage (Late Triassic, Argentina) and 40Ar/39Ar dating of dinosaur origins. *Science*, *260*(5109), pp. 794-797.
Romer, A. S. (1966) *Vertebrate Paleontology*. University of Chicago Press, Chicago.
Romer, A. S. (1972) The Chanãres (Argentina) Triassic reptile fauna. XIII. An early ornithosuchid pseudosuchian, *Gracilisuchus stipanicicorum*, gen. et sp. nov. *Breviora*, 389, pp. 1–24.
Rowe, A. J., Snively, E. (2022) Biomechanics of juvenile tyrannosaurid mandibles and their implications for bite force: Evolutionary biology. *The Anatomical Record*, *305*(2), pp. 373-392.
Sakamoto, M., Ruta, M. and Venditti, C. (2019) Extreme and rapid bursts of functional adaptations shape bite force in amniotes. *Proceedings of the Royal Society B*, *286*(1894), p.20181932.
Santi Malnis, P., Colombi, C. E., Kent, D. V., Alcober, O. A., Martı´nez, R. (2011) Assesing [sic] the age of Los Colorados Formation, Ischigualasto – Villa Union Basin, Argentina. Temporal implications for Coloradian fauna. In: IV Congreso Latinoamericano de Paleontologia de Vertebrados, Abstracts and Program. San Juan, Argentina, Museo de Ciencias Naturales, Universidad Nacional de San Juan.
Schoch, R. R. (2002) Stratigraphie und Taphonomie wirbeltierreicher Schichten im Unteren Keuper von Vellberg. Stuttgarter Beitraege zur Naturkunde Serie B (Geologie und Palaeontologie), 218, pp. 1–29.
Schoch, R. R., Nesbitt, S., Müller, J., Lucas, S. G., Boy, J. A. (2010) The reptile assemblage from the Moenkopi formation (Middle Triassic) of New Mexico. *Neues Jahrbuch fur Geologie und Palaontologie-Abhandlungen*, *255*(3), p. 345.
Schultz, C. L., Scherer, C. M. S. & Barberena, M. C. (2000) Bioestratigraphy (sic) of Southern Brazilian Middle–Upper Triassic. *Revista Brasileira de Geocieˆncias*, 30, pp. 495–498.
Sellers, K. C., Middleton, K. M., Davis, J. L., Holliday, C. M. (2017) Ontogeny of bite force in a validated biomechanical model of the American alligator. *Journal of Experimental Biology*, *220*(11), pp. 2036-2046.
Sen, K. (2005) A new rauisuchian archosaur from the Middle Triassic of India. *Palaeontology*, 48, pp. 185–196.
Sereno, P. C. (1991) Basal archosaurs: phylogenetic relationships and functional implications. *Journal of Vertebrate Paleontology*, *11*(S4), pp. 1-53.

Sereno, P. C. (2007) Logical basis for morphological characters in phylogenetics. *Cladistics*, 23, pp. 565–587.
Sill, W. D. (1974) The anatomy of *Saurosuchus galilei* and the relationships of the rauisuchid thecodonts. *Bulletin of the Museum of Comparative Zoology*, 146, pp. 317-362.
Snively, E., Cotton, J. R., Ridgely, R., Witmer, L. M. (2013) Multibody dynamics model of head and neck function in *Allosaurus* (Dinosauria, Theropoda). *Palaeontologia Electronica*, *16*(2), p.11A.
Snively, E., Russell, A. R. (2007) Craniocervical feeding dynamics of *Tyrannosaurus rex*. *Paleobiology*. 33(4), pp. 610-638.
Somaweera, R., Nifong, J., Rosenblatt, A., Brien, M. L., Combrink, X., Elsey, R. M., Grigg, G., Magnusson, W. E., Mazzotti, F. J., Pearcy, A., Platt, S. G. (2020) The ecological importance of crocodylians: towards evidence-based justification for their conservation. *Biological Reviews*, *95*(4), pp. 936-959.
Spencer, A. R. T., Hilton J., Sutton, M. D. (2012) Combined methodologies for three-dimensional reconstruction of fossil plants preserved in siderite nodules: *Stephanospermum braidwoodensis* nov. sp. (Medullosales) from the Mazon Creek lagerstätte. *Review of Palaeobotany and Palynology*, 188, pp. 1–17.
Stein, M. (2010) A new arthropod from the early Cambrian of North Greenland, with a ‘‘great appendage’’-like antennula. *Zoological Journal of the Linnean Society*, 158, pp. 477–500.
Stein, M., Selden, P. A. (2012) A restudy of the Burgess Shale (Cambrian) arthropod *Emeraldella brocki* and reassessment of its affinities. *Journal of Systematic Palaeontology*, 10, pp. 361–383.
Stewart, J. H., Poole, F. G. & Wilson, R. F. (1972) Stratigraphy and origin of the Upper Triassic Chinle Formation and related strata in the Colorado Plateau region. *United States Geological Survey, Professional Paper*, 692, pp. 1–336.
Stocker, M. R., Nesbitt, S. J., Criswell, K. E., Parker, W. G., Witmer, L. M., Rowe, T. B., Ridgely, R., Brown, M. A. (2016) A dome-headed stem archosaur exemplifies convergence among dinosaurs and their distant relatives. *Current Biology*, *26*(19), pp. 2674-2680.
Sues, H. -D. & Fraser, N. C. (2010) Triassic Life on Land: The Great Transition. *Columbia University Press*, New York.
Sulej, T. (2005) A new rauisuchian reptile (Diapsida: Archosauria) from the Late Triassic of Poland. *Journal of Vertebrate Paleontology*, 25, pp. 78–86.
Sutton, M. D. (2008) Tomographic techniques for the study of exceptionally preserved fossils. *Proceedings of the Royal Society B: Biological Sciences*, *275*(1643), pp. 1587-1593.
Taborda, J. R., Desojo, J. B. and Dvorkin, E. N. (2021) Biomechanical skull study of the aetosaur *Neoaetosauroides engaeus* using Finite Element Analysis. *Ameghiniana*, *58*(5), pp. 401-415.
Therrien, F., Henderson, D. M. (2007) My theropod is bigger than yours… or not: estimating body size from skull length in theropods. *Journal of Vertebrate Paleontology*, *27*(1), pp. 108-115.
Therrien, F., Henderson, D. M., Ruff, C. B. (2005) Bite me: biomechanical models of theropod mandibles and implications for feeding behavior. The carnivorous dinosaurs, pp. 179-237.
Thomason, J. J., Russell, A. P. (1986) Mechanical factors in the evolution of the mammalian secondary palate: a theoretical analysis. *Journal of Morphology*, *189*(2), pp. 199-213.
Tolchard, F., Nesbitt, S. J., Desojo, J. B., Viglietti, P., Butler, R. J. and Choiniere, J. N. (2019) ‘Rauisuchian’ material from the lower Elliot Formation of South Africa and Lesotho: Implications for Late Triassic biogeography and biostratigraphy. *Journal of African Earth Sciences*, 160, p.103610.
Torices, A., Wilkinson, R., Arbour, V. M., Ruiz-Omeñaca, J. I., Currie, P. J. (2018) Puncture-and-pull biomechanics in the teeth of predatory coelurosaurian dinosaurs. *Current Biology*, *28*(9), pp. 1467-1474.

Trotteyn, M. J., Desojo, J., Alcober, O. (2011) Nuevo material postcraneano de Saurosuchus galilei (Archosauria: Crurotarsi) del Triásico Superior del centro-oeste de Argentina. *Ameghiniana*. 48(1), pp. 13–27.
Tucker, M. E., Benton, M. J. (1982) Triassic environments, climates and reptile evolution. *Palaeogeography, Palaeoclimatology, Palaeoecology*, *40*(4), pp. 361-379.
Von Baczko, M. B. (2018) Rediscovered cranial material of *Venaticosuchus rusconii* enables the first jaw biomechanics in Ornithosuchidae (Archosauria: Pseudosuchia). *Ameghiniana*, *55*(4), pp. 365-379.
Von Baczko, M. B., Desojo, J .B., Pol, D. (2014) Anatomy and phylogenetic position of *Venaticosuchus rusconii* Bonaparte, 1970 (Archosauria, Pseudosuchia), from the Ischigualasto Formation (Late Triassic), La Rioja, Argentina. *Journal of Vertebrate Paleontology*, *34*(6), pp. 1342-1356.
Wallace, R. V. S. (2018) A new close mammal relative and the origin and evolution of the mammalian central nervous system (PDF) (PhD thesis). The University of Texas at Austin.
Walmsley, C. W., Smits, P. D., Quayle, M. R., McCurry, M. R., Richards, H. S., Oldfield, C. C., Wroe, S., Clausen, P. D., McHenry, C. R. (2013) Why the long face? The mechanics of mandibular symphysis proportions in crocodiles. *PLoS One*, *8*(1), p.e53873.
Weinbaum, J. C. (2002) *Osteology and relationships of Postosuchus kirkpatricki (Archosauria: Crurotarsi)* (Doctoral dissertation, Texas Tech University).
Weinbaum, J. C., and A. Hungerbühler (2007) A revision of Poposaurus gracilis (Archosauria: Suchia) based on two new specimens from the Late Triassic of the southwestern U.S.A. *Palaontologische Zeitschrift* 81/2, pp. 131–145.
Weishampel, D. B., Dodson, P., Osmolska, H. (2007). Dinosaur Distribution. *The Dinosauria, Second Edition. University of California Press*. p. 528.
Werneburg, I. (2011) The cranial musculature of turtles. *Palaeontologia Electronica*, *14*(2), pp. 15A-99p.
Whitney, M. R., LeBlanc, A. R. H., Reynolds, A. R. and Brink, K. S. (2020) Convergent dental adaptations in the serrations of hypercarnivorous synapsids and dinosaurs. *Biology Letters*, *16*(12), p.20200750.
Witmer, L. M., Ridgely, R. C. (2009) New insights into the brain, braincase, and ear region of tyrannosaurs (Dinosauria, Theropoda), with implications for sensory organization and behavior. *The Anatomical Record: Advances in Integrative Anatomy and Evolutionary Biology: Advances in Integrative Anatomy and Evolutionary Biology*, *292*(9), pp. 1266-1296.
Wu, X. C. (1981) The discovery of a new thecodont from north east Shanxi. *Vertebrata PalAsiatica*, 19, pp. 122–32.
Zhang, F. K. (1975) A new thecodont Lotosaurus, from the Middle Triassic of Hunan. *Vertebrata Palasiatica*, 13, pp. 144–147.
Zamora, S., Rahman, I. A., Smith, A. B. (2012) Plated Cambrian bilaterians reveal the earliest stages of echinoderm evolution. *PLoS One*, *7*(6), p.e38296.
Zeigler, K. E., Geissman, J. W. (2011) Magnetostratigraphy of the Upper Triassic Chinle Group of New Mexico: Implications for regional and global correlations among Upper Triassic sequences. *Geosphere*, *7*(3), pp. 802-829.
Zerfass, H., Chemale, F., Schultz, C. L. & Lavina, E. L. (2004) Tectonics and sedimentation in southern South America during Triassic. *Sedimentary Geology*, 166, pp. 265–292.
Zhongming, Z., Linong, L., Xiaona, Y., Wangqiang, Z. and Wei, L. (2021) The 'Great Dying'.

APPENDICES

Appendix 1 – Table of the 10 measurements along the dorsal surface of the skull model for two intrinsic bite scenarios (FBS and BBS) with the Node ID from the finite element analysis (FEA).

Measurement	FBS	BBS	Node ID
1	0.874039	0.121247	432412
2	0.784931	0.318863	441138
3	0.581626	0.664764	206328
4	0.382798	0.747998	249787
5	0.878929	1.310366	248558
6	1.09854	1.5322	222849
7	1.15992	1.75075	228345
8	0.52602	0.200769	419784
9	1.52188	1.20042	208522
10	4.01536	3.48533	147964

Appendix 2 – Table of the 10 measurements along the ventral surface of the skull model for two intrinsic bite scenarios (FBS and BBS) with the Node ID from the finite element analysis (FEA).

Measurement	FBS	BBS	Node ID
1	3.70177	2.99385	254998
2	2.23223	1.28174	438490
3	1.15807	0.918726	357595
4	2.01909	1.64336	253631
5	1.82831	1.49343	245106
6	2.66789	2.14015	345171
7	2.1728	1.37647	47068
8	0.619723	0.463845	92099
9	0.071672	0.0451761	56923
10	5.34747	4.39836	142497